Passive Microwave Imaging using Reflected GPS Signals Processing based on Synthetic Aperture Radar (SAR) Technique

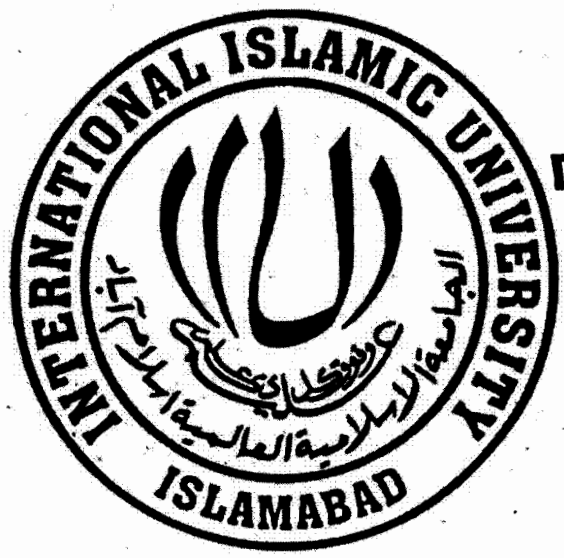

Muhammad Waqas Rehan
(93-FET/MSEE/F07)

MS Electronic Engineering

Department of Electronic Engineering

Faculty of Engineering and Technology

International Islamic University, Islamabad.

(2010)

1- Remote sensing.
2- Radar.

D.F
3.9.14

Passive Microwave Imaging using Reflected GPS Signals Processing based on Synthetic Aperture Radar (SAR) Technique

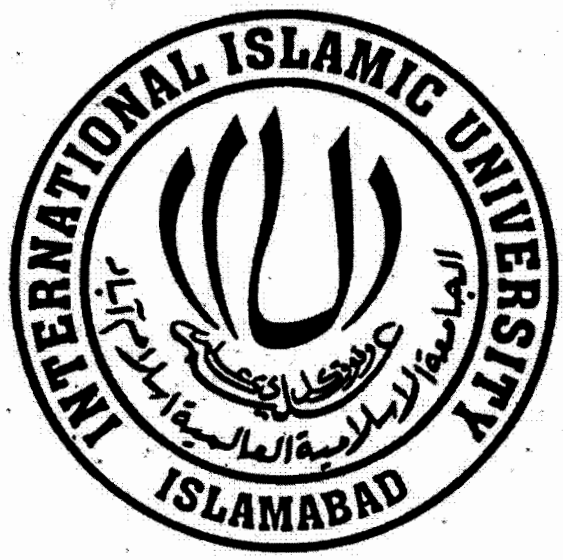

Muhammad Waqas Rehan
(93-FET/MSEE/F07)

This dissertation is submitted as partial fulfillment of degree

MS Electronic Engineering

Department of Electronic Engineering

Faculty of Engineering and Technology

International Islamic University, Islamabad.

(2010)

Certificate of Approval

Title of Thesis: Passive Microwave Imaging using Reflected GPS Signals Processing based on Synthetic Aperture Radar (SAR) Technique

Name of Student: Muhammad Waqas Rehan

Registration No: 93-FET/MSEE/F07

Accepted by the Faculty of Engineering and Technology, INTERNATIONAL ISLAMIC UNIVERSITY, ISLAMABAD, in partial fulfillment of the requirements for the Master of Philosophy Degree in Electronic Engineering.

External Examiner
Dr. Abdul Jalil
Associate Professor,
P.I.E.A.S.

Internal Examiner
Dr. Arbab Ali Khan
Associate Professor,
FET, IIU, Islamabad

Supervisor
Dr. Muhammad Usman
Visiting Professor,
FET, IIU, Islamabad

Declaration

I certify that except where due acknowledgments has been made, the work is that of my alone: the work has not been submitted previously, in whole or in the part, to qualify for any other academic award; the content of the thesis is the result of work which has been carried out since the official commencement date of the approved research program; and, any editorial work, paid or unpaid, carried out by a third party is acknowledged.

M. Waqas Rehan

Muhammad Waqas Rehan

93–FET/MSEE/F07

Acknowledgements

In the name of Allah, the Most Gracious and the Most Merciful.

All praise and glory goes to Almighty Allah (Subhanahu Wa Ta'ala) Who gave me the courage and patience to carry out this research work. Peace and blessings of Allah be upon His last Prophet Muhammad (Sallulaho-Alaihihe-Wassalam) and all his Sahaba (Razi-Allaho-Anhum) who devoted their lives for the prosperity and spread of Islam.

First and foremost gratitude is due to the esteemed university, the International Islamic University Islamabad for my admittance. My deepest appreciation goes to my supervisor **Dr. Muhammad Usman** for his guidance and providing me the relevant material regarding thesis. He always helped me more than he can in my whole thesis. I would also like to thank my respected teacher **Dr. Ihsan-ul-Haq** who has always been a source of inspiration during my MS studies. My inspiration also goes to **Dr. Arbab Ali Khan** and, the honorable dean of the faculty of engineering and technology, **Dr. Ahmed Shuja Syed** for all their support during my thesis.

I extend my gratitude to all my close friends and university fellows who helped me a lot during my thesis. I am also thankful to all my other friends for their materialistic support and prayers. I would like to thank my beloved parents and family members. Their prayers and encouragement has always helped me to take the right steps in life.

May Allah help us in following the true spirit & principles of Islam write down in the Holy Quran and Sunna! (Aameen)

Muhammad Waqas Rehan
93–FET/MSEE/F07

Abstract

The direct GPS signals are used to locate the position of a GPS receiver at nearly any place of the world. However, the indirect GPS signals can be used as the illuminator of opportunity by providing the location/imaging of object reflecting the GPS signals in the area of interest. The principle of bi-static radar is used to detect the targets or any movement or changes in the area of interest. In order to improve the system resolution, the signals processing is performed using matched filter processing technique. This simulation is carried out in MATLAB under different conditions with moving receiver and the two targets. The receiver position is calculated from the satellite ephemeris data by taking into consideration the receiver clock, ionospheric and tropospheric errors. Moreover, to simulate a more practical scenario noise and attenuation is also induced in the direct and reflected signals. The simulation results verify that by using the reflected GPS signals, it is possible to detect and image the targets by employing reflected GPS signals using the matched filter processing technique with acceptable spatial resolution.

TABLE OF CONTENTS

Declaration		**iii**
Acknowledgements		**iv**
Abstract		**v**
List of Figures		**ix**
List of Tables		**xiii**
Acronyms		**xiv**
1	**Introduction to Dissertation**	1
	1.1 Introduction	1
	1.2 Dissertation Purpose	4
	1.3 Advantages and Disadvantages of Remote Sensing	5
	1.4 Organization of Dissertation	6
2	**Satellite Navigation Essentials**	7
	2.1 Satellite Navigation Principles	7
	2.2 Understanding Worldwide Geodetic Coordinate System (WGS-84)	8
	2.2.1 Geoid	8
	2.2.2 Ellipsoid and Datum	9
	2.2.3 World Geodetic System (WGS-84)	10
	2.2.4 Satellite Technology Foundations	13
	2.2.4.1 Kepler's Laws of Orbital Motion	13
	2.2.4.2 Satellite Orbits	14
	2.2..5 Time System	15
3	**Brief Overview of GPS and SAR**	16
	3.1 The Global Positioning System	16
	3.1.1 The Space Segment	17
	3.1.1.1 Satellite Distribution and Movement	17
	3.1.1.2 GPS Services	18
	3.1.1.3 GPS Satellite Signals	19
	3.1.1.3.1 C/A Code	19
	3.1.1.3.2 P(Y) Code	23

		3.1.1.3.3 Navigation Message	23
	3.1.1.4	Satellite Signals Generation	23
3.1.2	The Control Segment		27
	3.1.2.1	Selective Availability and GPS improvements	28
3.1.3	The user Segment		29
3.1.4	The GPS Navigation Message		29
	3.1.4.1	Navigation Message Structure	29
	3.1.4.2	The Ephemeris Data	32
3.1.5	The GPS Signal Levels		35
3.1.6	GPS Errors		36
3.2	Auto Correlation Characteristics		36
4	**SAR and Passive Microwave Imaging**		39
4.1	Synthetic Aperture Radar (SAR)		39
4.1.1	SAR Imaging		44
4.2	Matched Filtering		45
4.3	FM Chirp Signal		48
4.4	Characteristics of Target		49
4.5	Passive Microwave Imaging (PMI)		50
4.5.1	Radiometric Brightness Temperature		51
4.5.2	Microwave emission and surface characteristics		52
4.5.3	PMI using GPS Signals		52
5	**The Modified GPS Receiver**		54
5.1	GPS Receiver		54
5.2	Position Measurement		57
5.2.1	GPS Receiver Position Measurement		57
5.2.2	GPS Errors Measurement		62
	5.2.2.1	Ionospheric Klobuchar Error Model	62
	5.2.2.2	Tropospheric Hopfield Error Model	65
	5.2.2.3	Satellite Clock Error	65
5.2.3	GPS Receiver Position Measurement Algorithm		67
5.3	Target Imaging System (TIS)		68
5.3.1	Display of Image		70
5.3.2	Image Reconstruction using Matched Filter		71

Processing

5.3.3 TIS Block Diagram 73
5.3.3.1 Simplified block Diagram of TIS 73
5.3.3.2 Detailed block Diagram of TIS 74

6 **Simulation and Results** 76
6.1 Overview of Simulation 76
6.2 Receiver Position Measurement 77
6.3 Target Imaging 79

7 **Conclusions and Recommendations** 101

8 **References** 104

Appendices 106
Appendix A: Geoid and Ellipsoid 107
Appendix B: Maximum Length Sequences and Gold codes 108
Appendix C: Diagrammatic Representation of the Ephemeris Data Parameters 110
Appendix D: Elevation and Azimuth Angles Calculation from ENU Coordinates 112

LIST OF FIGURES

Figure 1.1	Schematic representation of the scenario	4
Figure 2.1	Receiver position measurement using 4-satellites in XYZ Space	8
Figure 2.2	Geoid (Earth's surface approximation)	8
Figure 2.3	Ellipse showing Earth's structure	9
Figure 2.4	Ellipsoid (with local reference)	10
Figure 2.5	WGS-84 coordinate system (x,y,z)	11
Figure 2.6	WGS-84 coordinate system (φ, λ, h)	12
Figure 2.7	Kepler's 1st & 2nd Laws of orbital motion	14
Figure 2.8	Six orbital elements	15
Figure 3.1	The GPS segments	17
Figure 3.2	C/A code or Gold code generator	20
Figure 3.3	(a) BPSK signal spectrum without spreading (b) BPSK signal spectrum with spreading	24
Figure 3.4	Data structure of a GPS signal	26
Figure 3.5	Simplified block diagram of GPS signal generation	26
Figure 3.6	Detailed block diagram of a GPS signal generation	27
Figure 3.7	Structure of the entire Navigation Message	30
Figure 3.8	Auto-Correlation Characteristics of PN Sequence	37
Figure 4.1	The concept of SAR using platform/receiver motion	41
Figure 4.2	The platform/receiver radiating the point target	42

Figure 4.3	SAR imaging concept	45
Figure 4.4	Comparison between matched filter and correlator	46
Figure 4.5	Matched filter demodulator	47
Figure 4.6	FM chirp signal	49
Figure 5.1	GPS receiver channel block diagram	57
Figure 5.2	Measuring signal travel time	58
Figure 5.3	Taylor series conversion	59
Figure 5.4	Ionospheric Model	64
Figure 5.5	Receiver position measurement block diagram	67
Figure 5.6	Target Imaging System (TIS) block diagram	68
Figure 5.7	Candidate position for the target	71
Figure 5.8	TIS (Simplified block diagram)	73
Figure 5.9	TIS (Detailed block diagram)	74
Figure 6.1	(a) GPS receiver position error solution (b) Zoomed value of norm error (in meters) from iteration 4 to 5 (rightmost figure) (c) Norm error ($\sqrt{\Delta x^2 + \Delta y^2 + \Delta z^2}$) final value less than 0.1 (leftmost figure)	77
Figure 6.2	GPS receiver position measurement	78
Figure 6.3	GPS receiver covariance solution	78
Figure 6.4	GPS receiver final position	79
Figure 6.5	Integration time 0.1 seconds with no noise	80
Figure 6.6	Integration time 0.1 seconds with 16 db noise	81
Figure 6.7	Integration time 0.2 seconds with no noise	82

Figure 6.8	Integration time 0.2 seconds with 16 db noise	83
Figure 6.9	Integration time 0.1 seconds and target moving with 10 m/s	84
Figure 6.10	Integration time 0.1 seconds and target moving with 20 m/s	84
Figure 6.11	Integration time 0.1 seconds and target moving with 50 m/s	85
Figure 6.12	Integration time 0.1 seconds and target moving with 100 m/s	85
Figure 6.13	Integration time 0.1 seconds (with noise) & target moving with 100 m/s	86
Figure 6.14	Integration time 0.1 seconds and receiver moving with 600 m/sec	87
Figure 6.15	Integration time 0.1 seconds (with noise) and receiver moving with 600 m/sec	87
Figure 6.16	Integration time 0.1 seconds and receiver deviating from the planned route	88
Figure 6.17	Attenuation of 0.3 for reflected signal	90
Figure 6.18	Attenuation of 0.3 for reflected signal with 16 db noise	90
Figure 6.19	Attenuation of 0.1 for reflected signal	91
Figure 6.20	Attenuation of 0.1 for reflected signal with 16 db noise	91
Figure 6.21	Attenuation of 0.05 for reflected signals	92
Figure 6.22	Attenuation of 0.01 for reflected signals	92
Figure 6.23	Integration time 0.1 seconds with direct signals attenuation 0.5 and reflected signals attenuation 0.01 (no noise)	93
Figure 6.24	Integration time 0.1 seconds with direct signals attenuation 0.3 and reflected signals attenuation 0.01 (no noise)	94
Figure 6.25	Integration time 0.1 seconds with direct signals attenuation 0.1 and reflected signals attenuation 0.01 (no noise)	94

Figure 6.26	Integration time 0.1 seconds with direct signals attenuation 0.05 and reflected signals attenuation 0.01 (no noise)	95
Figure 6.27	Integration time 0.1 seconds with direct signals attenuation 0.03 and reflected signals attenuation 0.01 (no noise)	96
Figure 6.28	Integration time 0.1 seconds with direct signals attenuation 0.03 and reflected signals attenuation 0.01 (with noise)	96
Figure 6.29	Integration time 0.2 seconds with direct signals attenuation 0.03 and reflected signals attenuation 0.01(with noise)	97
Figure 6.30	Integration time 21600 seconds with no noise	98
Figure 6.31	Integration time 21600 seconds with 16 db noise	99
Figure 6.32	Integration time 21100 seconds with increased over sampling	100
Figure A.1	Relationship between geoid and ellipsoid	107
Figure B.1	Generation of MLS sequences	108
Figure B.2	Detailed diagram of Gold codes generator	109
Figure C.1	Diagrammatic representation of the orbital anomalies (E,M,V)	111
Figure C.2	Diagrammatic representation of ephemeris data parameters	111

LIST OF TABLES

Table 2.1	The WGS-84 ellipsoid parameters	11
Table 2.2	Conversion of ECEF (x,y,z) to ECEF (φ, λ, h)	11
Table 3.1	GPS code generator polynomials with initial states	20
Table 3.2	Code phase assignments and initial code sequences for c/a code	21
Table 3.3	GPS Ephemeris data definitions	33
Table 3.4	GPS Ephemeris Data calculations	34
Table 6.1	Set of parameters for case no. 1	80
Table 6.2	Set of parameters for case no. 2	82
Table 6.3	Set of parameters for case no. 6.1	89
Table 6.4	Set of parameters for case no. 6.2	93
Table 6.5	Set of parameters for case no. 7	98

Acronyms

GNSS	Global Navigation Satellite System
UTC	Universal Time Coordinates
NAVATAR	Navigation System with Timing and Ranging
DoD	Department of Defense
SPS	Standard Positioning Service
PPS	Precision Positioning Service
BSAR	Bistatic Synthetic Aperture Radar
MSAR	Multistatic Synthetic Aperture Radar
FM	Frequency Modulatation
WGS-84	Worldwide Geodetic system 84
ECEF	Earth Centered Earth Fixed
ECI	Earth Centered Inertial
TAI	Temps Atomique International
UTC	Universal Time Coordinate
GPS	Global Positioning System
C/A code	Coarse Acquisition Code
SA	Selective Availability
AS	Anti-Spoofing
DSSS	Direct Sequence Spread Spectrum
PRN	Pseudorandom Noise

CDMA	Code Division Multiple Access
RHCP	Right Hand Circular Polarized
LHCP	Left Hand Circular Polarized
P code	Precision code
EXOR	Exclusive-or Operation
BPSK	Binary-Phase-Shift-Keying
ADC	Analogue to Digital Converter
FAFB	Falcon Air Force Base
MCS	Master Control Station
GCS	Ground Control Stations
MS	Monitor Stations
SAR	Synthetic Aperture Radar
ISAR	Inverse Synthetic Aperture Radar
SNR	Signal to Noise ratio
RCS	Radar Cross Section
PMI	Passive Microwave Imaging
TIS	Target Imaging System
RSA	Radar Synthetic Aperture

CHAPTER 1

INTRODUCTION

1.1 Introduction

Satellite navigation employing the Global Navigation Satellite System (GNSS) is used to measure the position (longitude, latitude and altitude coordinates) and time (Universal Time Coordinates UTC) anywhere on the earth. The satellite navigation receivers are therefore utilized in positioning, navigating and surveying and measuring the exact time for the personal, leisure and commercial applications [1].

As of 2009, the only fully functional GNSS System is the **N**avigation **S**ystem with **T**iming and **R**anging **G**lobal **P**ositioning **S**ystem (NAVATAR-GPS) developed and operated by the United States Department of Defense (DoD). The first GPS Satellite was placed into the orbit, at an altitude of 20,180 km, on 22 February 1978. It was planned to have a total of 32 such satellites in the 6 orbital planes with an inclination of 55° with the equator. The satellite locations were set in a manner that at-least 4 satellites would be in radio communication with any location on the earth. Moreover, each satellite had four

atomic clocks and could orbit the earth in approximately 12 hours. The GNSS Systems by Russia i.e.; GLONASS is operational with 23 satellites but needs improvements whereas GALILEO by the European Union will be fully operational until 2014-2015 [1].

The GPS satellites emit two different types of signals for the civilian and military Usage. The civilian signals are sent on L1 frequency and termed as SPS (Standard Positioning Service). The military signals are sent on L2 frequency and termed as PPS (Precision Positioning Service). These signals arrive to the receiver, not only from the direct path from the satellites in the view, but, also from the indirect path by reflecting from some nearby surfaces. This phenomenon is termed as multi-path. Normally, these reflected signals, also termed as nuisance factor in navigation, interfere with the signals which are received directly from the satellites and in this way reduce the positioning accuracy [2]. Therefore, the reflected GPS signals can be categorized as the unwanted signals because they degrade the overall accuracy of our system [3]. But, fortunately, the researchers have discovered that these reflected signals can be proved as 'illuminators of opportunity' and therefore can be utilized for imaging the objects from which they are reflected [4][5]. Hence they are a resource for remote sensing applications.

In the radar technology, if the same antenna is used for transmitting and receiving the signals then such a system is known as mono-static radar system. But, if different antennas are used for transmitting and receiving the signals, the, such a system is known as bi-static radar system [6]. In case of GPS system, the signals are transmitted by the antennas of satellites and received by the antennas of the GPS receivers. So, that is why such a system forms a bi-static system. The motion of the receiver is the source of synthetic aperture for such a system; therefore, the GPS satellites and a modified GPS

receiver form the Bistatic Synthetic Aperture Radar (BSAR) system which is used to model the reflected GPS signals.

The movement of a visible GPS platform serves as a base for a synthetic aperture. As the GPS satellites and the GPS receiver are in motion during the integration time, therefore, the received GPS signals will be the frequency modulated (FM) signals with a constantly changing Doppler shift. These signals are also termed as chirp signals. The reflected chirp signals from the target(s) are acquired by the receiver, and are further processed by the matched filter, which is an optimum filter for signal detection in a white noise environment. Because the auto-correlation function of a linear FM signal exhibits a narrow pulse property, the output wave will become even narrower when it is passed through a matched filter and the system resolution is thus increased. Therefore the bi-static SAR system has the potential to develop high quality and low cost images of a localized area.

A SAR system differs from a normal radar system in such a way that a normal radar system simultaneously transmits and receives all the elements for target imaging, but, a SAR System achieves the same process by transmitting and receiving the first element, doing some processing on it, storing the processed information and repeating the process until all the elements are utilized. The long range propagation characteristics of the radar signals and the complex information processing capability of the modern digital electronics helped the SAR System in achieving high-resolution imagery [7]. The GPS system with its precise timing requirement has the ability to serve as the basis of a BSAR system.

1.2 Dissertation Purpose

In this research effort, a constellation of visible GPS satellite transmitters, a modified GPS receiver and multiple targets have been simulated and thus an effort is made to generate a Multistatic Synthetic Aperture Radar (MSAR) environment. The two targets monitored are airborne (may be some stationary reflective surfaces or moving aero planes as simulated in Chapter 6).

Initially, the modified GPS receiver calculates its position using the ephemeris data sent by satellites by keeping in view the ionospheric, tropospheric and satellite clock errors. The receiver is then moved on some ground based platform (e.g. railway track etc) with some speed towards the region of interest to be imaged (having the targets at specified location). The receiver then takes the images of the targets using the Synthetic Aperture Radar (SAR) technique. The simulation results given in Chapter 6 also validate the SAR technique.

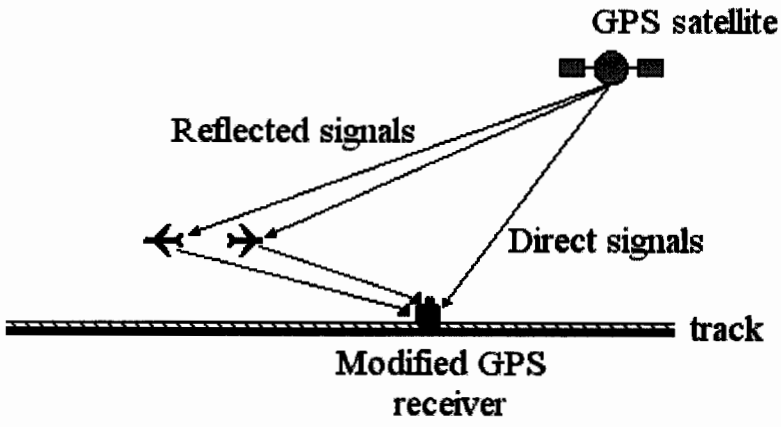

Figure 1.1: Schematic representation of the scenario

1.3 Advantages and Disadvantages of Remote Sensing

The remote sensing using the GPS Signals by utilizing SAR technique is very advantageous.

- Firstly, it doesn't require any dedicated signal transmitting source, so, power consumption is very low.
- Secondly, it is based on the frequency reuse concept of the GPS Signals which are available round-the clock at nearly all the locations in the world and there is no need to spend a huge sum of money for deploying any additional infrastructure for this purpose.
- Thirdly, it processes the GPS Signals whose structure is known and can draw the desired conclusions with less difficulty.
- Fourthly, it is much cost effective to build the GPS receivers which are very small like note book computer, a palm device or a mobile phone and can be built for a fraction of the cost spent on making the other equipments such as traditional radars, space-borne equipment and other sensors.
- Fifthly, the application areas includes:
    - Military applications
    - Atmospheric remote sensing for weather forecasting
    - Monitoring of landslides and their pattern
    - Astronomical applications
    - Long-term seismic studies
    - Oceanic solutions

There are also some disadvantages of using the GPS Signals for remote sensing. The main disadvantage is the low signal to noise ratio of the received reflected GPS Signals [5]. This problem can be coped with by utilizing the multiple receiving antennas having different gain and polarization sensitivities and longer observation times.

1.4 Organization of Dissertation

Chapter 2: Satellite Navigation Essentials: This chapter describes the basic principles of the satellite navigation. Satellite coordinate systems, Kepler laws, satellite basic orbital elements and time systems are major topics.

Chapter 3: Brief overview of GPS signals: This chapter describes a brief overview of GPS signals. Important topics discussed are the GPS segments, C/A code, navigation message, autocorrelation etc.

Chapter 4: SAR and Passive Microwave Imaging: This chapter describes in detail the concepts regarding SAR, Doppler frequency, match filter processing, FM chirp signal and passive microwave imaging etc.

Chapter 5: The Modified GPS Receiver: This chapter describes in detail the algorithms used to measure the position of the GPS receiver and reconstruction of the area of interest imaging the target position using SAR imaging technique.

Chapter 6: Simulation and Results: In this chapter, we will describe the simulation results based on the algorithms presented in the Chapter 5.

Chapter 7: Conclusions and Recommendations: In this chapter, we will summarized the results obtained in the Chapter 6 and elaborate the possible future scope of work.

Appendices: In this portion, we will put some light on those important topics of thesis that need some more explanation.

CHPTER 2

SATELLITE NAVIGATION ESSENTIALS

2.1. Satellite Navigation Principles

The GPS navigation data is used to measure the position of a receiver. These signals are transmitted with the speed of light (300,000 km/s) and reach the earth in approximately 67.3 msec. The accurate position of GPS receiver is measured through the principle of trilateration. In this method, when the receiver gets the signal of first satellite, then, the signal processing narrows its position on the surface of the earth. On getting the signals from the second satellite, the GPS receiver position is further narrows down on the region where the two spheres overlap. The signals from the third satellite narrows the position further which will be on the point of intersection of the three satellites. The fourth satellite provides more positional accuracy and helps to resolve the problem of altitude or elevation (especially in aero planes).

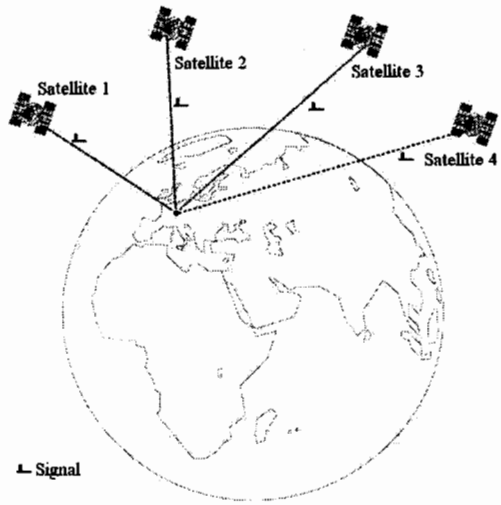

Figure 2.1: Receiver position measurement using 4-satellites in XYZ Space

2.2 Understanding Worldwide Geodetic Coordinate System (WGS-84)

The WGS-84 can be better understood by looking into geoid, ellipsoid and datum.

2.2.1 Geoid

The branch of science which deals with the surveying and mapping of the Earth's surface is termed as geodesy. The surface of the earth where the main sea level is zero comprises a shape known as geoid. The geometrical description of this shape is rather complex as it is defined by the gravity of the earth. A geoid is theoretical body whose surface intersects the gravitational field lines at the perpendicularly everywhere on the surface of the earth as shown in the figure 2.4 below [see also Appendix A].

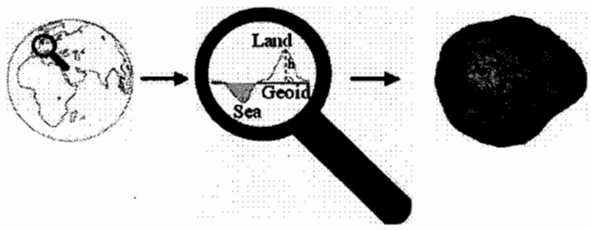

Figure 2.2: Geoid (Earth's surface approximation)

2.2.2 Ellipsoid and Datum

A geoid is a very complex shape and it is very difficult to perform the daily surveying calculations using this surface. Therefore, a simpler and more definable shape known as ellipsoid can be defined by the two parameters known as semi major axis 'a' (located on the equatorial plate) and semi minor axis 'b' (located on the north-south pole). Using 'a' and 'b', we can find out the flattening factor 'f' (the measure of amount by which the shape deviates from the ideal sphere) as

$$f = \frac{a-b}{a} \tag{2.1}$$

Moreover, in order to determine the positional coordinates of a GPS receiver on earth in terms of longitude and latitude, an ellipsoid is a very suitable shape. The information regarding the height is obtained from the reference ellipsoid or the geoid.

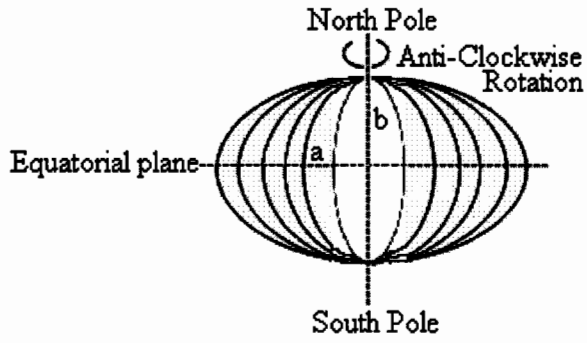

Figure 2.3: Ellipse showing Earth's structure

Datums are the national or international map reference systems used by the GNSS receivers for navigating and based on the different types of ellipsoids as shown in the figure 2.4. There are over 120 types of datums e.g. North American datum is NAD83, global standard datum is WGS-84 and CH-1903 datum is used for the Switzerland.

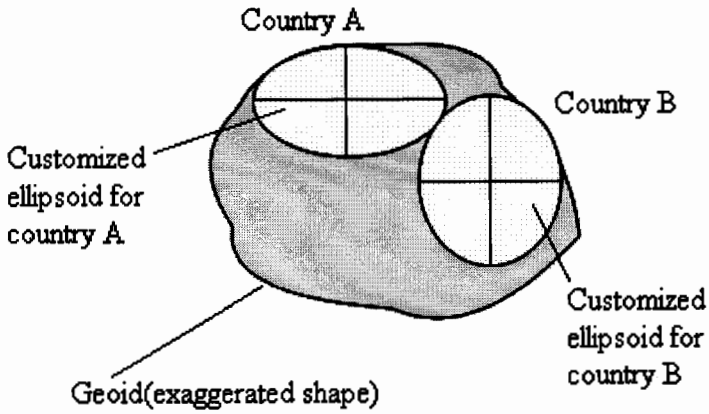

Figure 2.4: Ellipsoid (with local reference)

2.2.3 Worldwide Geodetic System (WGS-84)

The world geodetic system 1984 is a right handed, three dimensional coordinate system whose centre lies on the centre of mass (geocentric) of an ellipsoid which approximates to the total earth mass. Thus it is geocentrically positioned with respect to the earth's centre and is called Earth Centered Earth Fixed (ECEF) coordinate system.

The positive X-axis of the ellipsoid lies at the zero meridian which is present at the intersection of the equatorial plate and the line joining the north and South Pole after passing through the Greenwich meridian. The Y-axis also lies on the equatorial plane perpendicular to the X-axis. The Z-axis extends through the North Pole and lies perpendicular to the equatorial plane as shown in the figure 2.5. According to WGS-84, the earth's rotation rate is $\Omega e = 7.2921151467 \times 10^{-5}$ rad/sec.

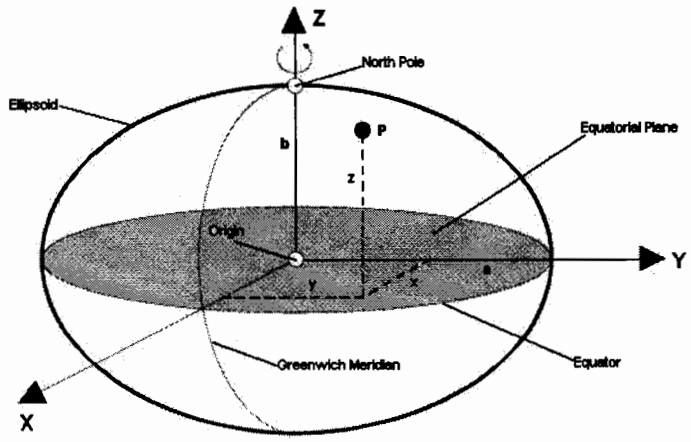

Figure 2.5: WGS-84 coordinate system(x,y,z)

Table 2.1: The WGS-84 ellipsoid parameters

Semi-Major axis (a) (m)	Semi-Minor axis (b) (m)	Inverse Flattening
6,378,137.00	6,356,752.31	298.257223563

For measuring the position of a receiver on earth, generally the Cartesian coordinates are converted into the ellipsoidal coordinates $(Latitude(\varphi), Longitude(\lambda), Height(h))$ by using the formulas shown in the table 2.2.

Table 2.2: Conversion of ECEF (x,y,z) to ECEF (φ, λ, h)

1.	$e^2 = \frac{a^2 - b^2}{a^2}$	Eccentricity

Table 2.2 (Continued)

2.	$e^{'} = \frac{a^2 - b^2}{b^2}$	Second Eccentricity
3.	$r^2 = x^2 + y^2$	Radius
4.	$\theta = \arctan 2\left(\frac{az}{bp}\right)$	Angle
5.	$N = \frac{a}{\sqrt{1 - e^2(\sin(\varphi))^2}}$	Radius of curvature
6.	$\varphi = \arctan\left(\frac{z + e^{'2} b(\sin(\theta))^3}{r - e^2 a(\cos(\theta))^3}\right)$	Latitude of position
7.	$\lambda = \arctan 2\left(\frac{y}{x}\right)$	Longitude of position
8.	$h = \frac{r}{\cos(\varphi)} - N$	Height of position

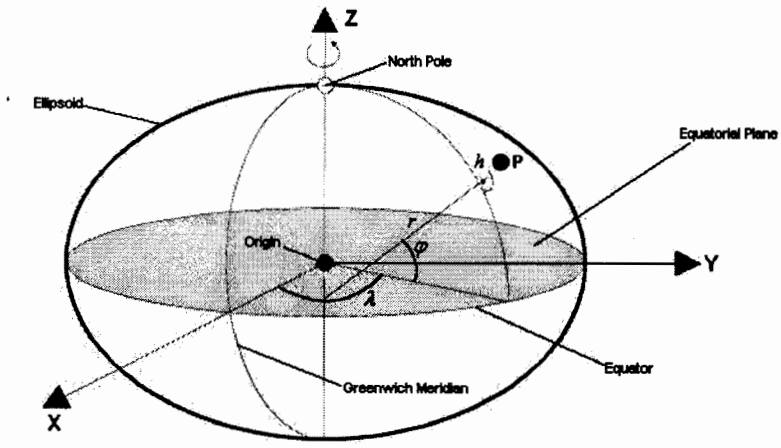

Figure 2.6: WGS-84 coordinate system (φ, λ, h)

In order to measure the position of the objects in space the Earth Centered Inertial (ECI) coordinate system is used having the origin at the center of mass of earth. But, for measuring the position of terrestrial objects the Earth Centered Earth Fixed (ECEF) coordinate system is used that rotates with the earth.

2.2.4 Satellite Technology Foundations

2.2.4.2 Kepler's Laws of Orbital Motion

The GPS ephemeris data contains the keplerian orbital elements along with the correction parameters for making possible the correct estimation of satellite positions in the time between the updates of the of the satellite's ephemeris message.

- **Kepler's 1st Law:** It states: "The planets revolve around the sun in the elliptic orbits with sun at one of the foci" as shown in the figure 2.9 (a).
- **Kepler's 2nd Law (Law of Equal Areas):** It states: "A line which joins the planet and the sun traverse equal distances in the equal internals of time" as shown in the figure 2.9 (b).
- **Kepler's 3rd Law** It states: "The squares of the orbital periods 'P' of the planets are directly proportional to the cubes of the semi major axis 'a' of their orbits".

$$P^2 \propto a^3 \tag{2.2}$$

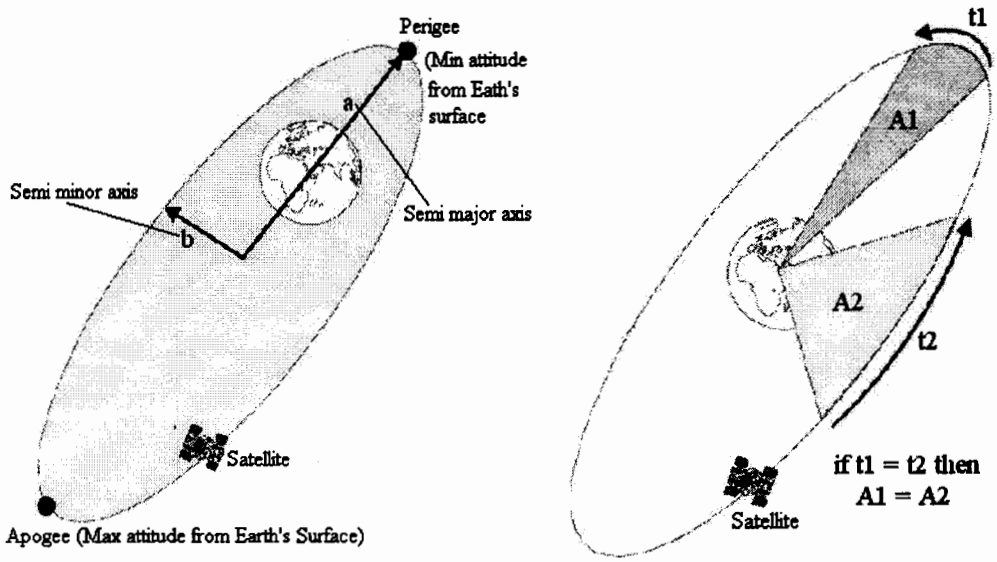

(a) (b)

Figure 2.9: (a) Kepler 1st Law of orbital motion
(b) Kepler 2nd Law of orbital motion

2.2.4.2 Satellite Orbits

The satellites move around the earth in the pre-defined orbits which may be elliptical or circular etc. Each orbit has six important parameters called orbital elements which are very helpful in describing orbit and the satellite position in the orbit [8] i.e.

- Semi-Major Axis 'a': It gives the size of the orbit.
- Eccentricity 'e': It gives the shape of the orbit.
- Inclination 'i': It shows the tilt of the orbit with respect to the equatorial plane
- Omega 'ω': Angle between the nodal line (on equatorial plane) and the perigee line.

- Right Ascension of the ascending node (RAAN) 'Ω ': Angle between X-axis (vernal equinox) and the nodal line. It tells about the about the ascending and the descending orbits.
- True anomaly 'v': Angle between the perigee line and the position vector of the satellite.

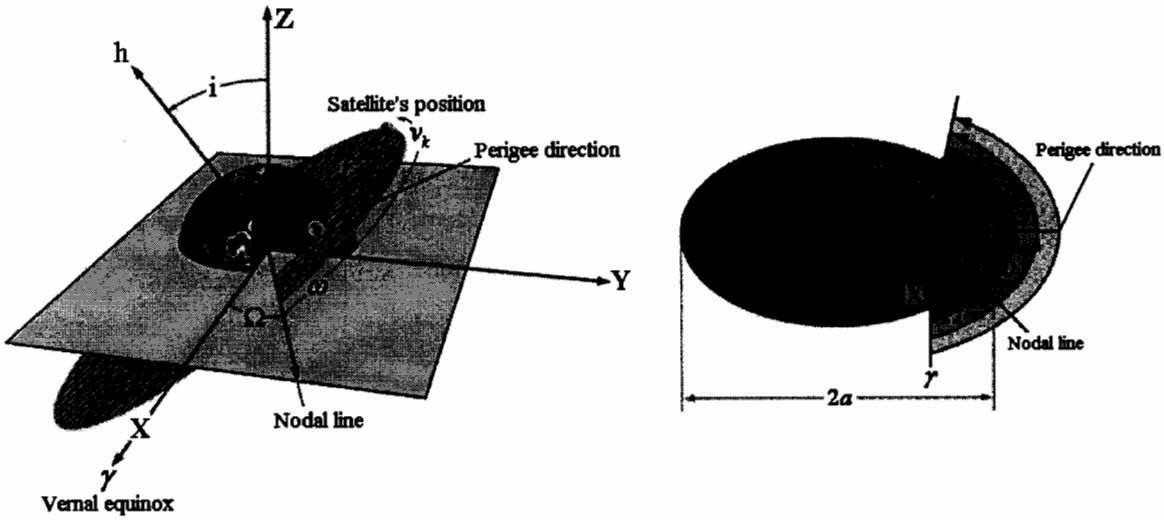

Figure 2.8: Six orbital elements

2.2.5 Time System

Global Positioning System Time Scale (GPS): It was started on Sunday 6th January, 1980 at 0:00h (UTC), and since then, maintained by the Master Control Station (MCS) along with the help of Ground Control Stations (GCS). Since 2009, the difference between the GPS and UTC is 15 seconds and is transmitted in the sub frame '4' of the navigation message. It has two parameters as week number and no of elapsed seconds in that week.

$$GPS - UTC = +15sec \tag{2.3}$$

CHAPTER 3

BRIEF OVERVIEW OF GPS SIGNALS

3.1 The Global Positioning System (GPS)

The GPS (Global Positioning Systems) has revolutionized navigation and position measurement for more than a decade [3]. It is the forerunner of the GNSS technology. I was originally called NAVSTAR-GPS and was developed by the United States Department of Defense and managed by the US Air Force 50th Space Wing. It was designed as a military navigating system for guiding missiles, ships and aircrafts towards their targets. It was researched in the 1960s and was officially established as a program in 1969. Since 1993, this system has become fully operational [9]. The GPS comprises of three major segments, which are explained below: -

The GPS is divided into three main segments as shown in the figure 3.1i.e.

- Space segment (consists all functional satellites)
- Control segment (consists MCS, GCS and MS (Monitor Stations))
- User segment (consists of civilian and military users)

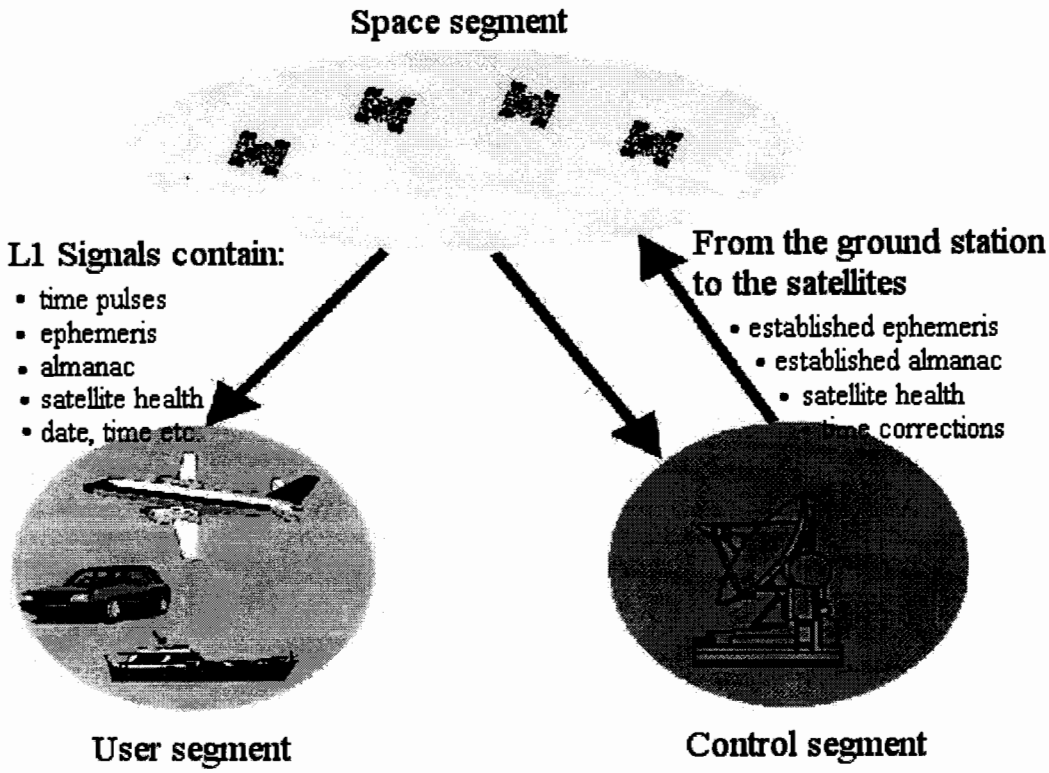

Figure 3.1: The GPS segments

3.1.1 The Space Segment

3.1.1.1 Satellite Distribution and Movement

The space segment consists of all the 34 operational GPS satellites in the space which are orbiting the earth in 6 orbital planes. There are 4 to 5 satellites in each orbital plane. The orbits are at a height of 20,180 km above the surface of earth with an inclination of 55 degrees to the equator. Each satellites orbit the earth in about 11 hours and 58 minutes. Due to the rotation of the earth about its axis, all the satellites are at their initial starting in 23 hours 56 minutes. The system is designed so that at least 4 to five

satellites are visible at any point on the earth's surface having a clear view of the sky. Moreover, the constellation is constantly been upgraded while some satellites are kept spared to be used for the emergency purpose. The initial operational capability was met with the help of 24 satellites in December, 1993 whereas the full operational capability achieved in April 1995. There is a unidirectional communication between the space and user segment and bi-directional communication between space and control segment. At present, about 32 satellites are orbiting the earth. [10].

3.1.1.2 GPS Services

The GPS provides two levels of services to the users i.e. Standard Positioning Service (SPS) and the Precise Positioning Service (PPS) [11].

- **Standard Positioning Service (SPS)** is a less accurate positioning and timing service that is provided to the civilian GPS users. This service is provided by using the Coarse Acquisition (C/A) code send on the L1 frequency (primary frequency at 1575.42 MHz). Before the discontinuation of selective availability (SA), the positional accuracy of SPS was 100 meter horizontal and 156 meter vertical [1].
- **Precise Positioning Service (PPS)** is an accurate positioning, velocity and timing service that is available to the authorized civilian/ military GPS users by introducing two cryptographic techniques i.e. Selective Availability (SA) and Anti-Spoofing (AS) on P code. It has the positional accuracy of 16 meter horizontal and 23 meter vertical [1].

3.1.1.3 GPS Satellite Signals

The GPS satellite signals are transmitted by the satellites on the two carrier frequencies i.e. L1 and L2 (secondary frequency at 1227.6 MHz). The signals are transmitted through the modulation technique known as Direct Sequence Spread Spectrum (DSSS). In this process the baseband signals are superimposed with a higher frequency signal which results in the spreading of the baseband frequency over the wider bandwidth.

As each satellite is assigned a unique pseudorandom noise (PRN) code which is uncorrelated with all the other satellite's codes, so, it is possible to separate and detect the satellite signals by a technique known as Code Division Multiple Access (CDMA).The signals transmitted by the satellite are RHCP (right hand circular polarized), but, the signals reflected from the ground or target are LHCP (Left Hand Circular Polarized). The complete GPS signal is comprised of:

3.1.1.3.1 C/A Code

The C/A (Coarse-Acquisition) code is a 1023 bit pseudorandom noise (PRN) code of length 1 millisecond and a clock rate of 1.023 MHz. Each GPS satellite is assigned a different PRN code signature with a length of $2^{10} - 1 = 1{,}023$ bits which is selected from a set of two Gold codes generated by using two 10 bit Linear Feedback Shift Registers (LFSR) as shown in the table 3.1and 3.2[3]. The Gold Codes are generated by linearly combining the two preferred pairs of the maximum length sequences (m-sequences or PRN sequences [see also Appendix B]) with the different offsets as shown in the figure 3.2 (see also Appendix B for the detailed diagram of C/A code or Gold Codes generator) [3]. The m-sequences have good auto correlation properties (poor cross correlation

properties) and have flat frequency spectrum like white noise, but, actually they are deterministic and repeatable with periods N ($N_{MLS} = 2^m - 1$, where m is length of shift registers). The Gold codes have very good cross correlation properties and are generated by two 10 bit LFSR registers with periodic cross correlation function having values as {-1, -t (m), t (m)-2}, where 't (m)' is cross correlation peak given by

$$t(m) = \begin{Bmatrix} 2^{(m+1/2)} + 1, & \text{for odd m} \\ 2^{(m+2/2)} + 1, & \text{for even m} \end{Bmatrix} \tag{3.1}$$

Table 3.1: GPS code generator polynomials with initial states

C/A Code G1	$1 + X^3 + X^{10}$	1111111111
C/A Code G2	$1 + X^2 + X^3 + X^6 + X^8 + X^9 + X^{10}$	1111111111

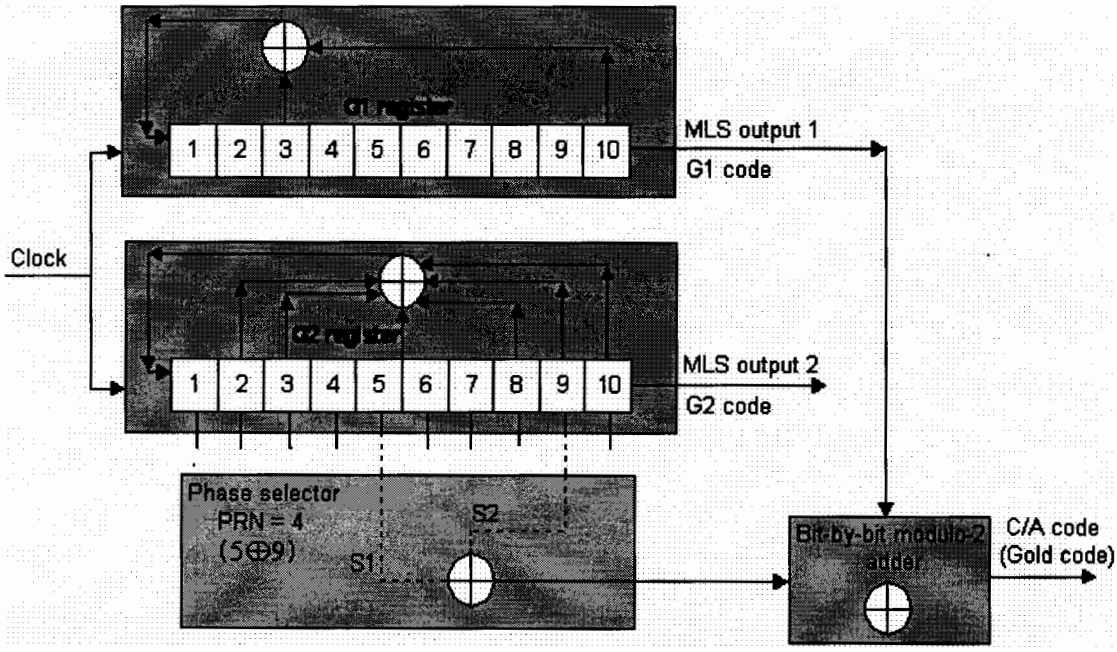

Figure 3.2: C/A code or Gold code generator

Table 3.2: Code phase assignments and initial code sequences for C/A code

[illegible]	[illegible]	[illegible]	[illegible]
1	2 ⊕ 6	5	1100100000
2	3 ⊕ 7	6	1110010000
3	4 ⊕ 8	7	1111001000
4	5 ⊕ 9	8	1111100100
5	1 ⊕ 9	17	1001011011
6	2 ⊕ 10	18	1100101101
7	1 ⊕ 8	139	1001011001
8	2 ⊕ 9	140	1100101100
9	3 ⊕ 10	141	1110010110
10	2 ⊕ 3	251	1101000100
11	3 ⊕4	252	1110100010
12	5 ⊕ 6	254	1111101000
13	6 ⊕ 7	255	1111110100
14	7 ⊕ 8	256	1111111010
15	8 ⊕ 9	257	1111111101
16	9 ⊕ 10	258	1111111110
17	1 ⊕ 4	469	1001101110
18	2 ⊕ 5	470	1100110111
19	2 ⊕ 6	471	1110011011

Table 3.2 (Continued)

[illegible]	[illegible]	[illegible]	[illegible]
20	4 ⊕ 7	472	1111001101
21	5 ⊕ 8	473	1111110011
22	6 ⊕ 9	474	1111110011
23	1 ⊕ 3	509	1000110110
24	4 ⊕ 6	512	1111000011
25	5 ⊕ 7	513	1111100011
26	6 ⊕ 8	514	1111110001
27	7 ⊕ 9	515	1111111000
28	8 ⊕ 10	516	1111111100
29	1 ⊕ 6	859	1001010111
30	2 ⊕ 7	860	1100101011
31	3 ⊕ 8	861	1110010101
32	4 ⊕ 9	862	1111001010
33	5 ⊕ 10	863	1111100101
34	4 ⊕ 10	950	1111001011
35	1 ⊕ 7	947	1001011100
36	2 ⊕ 8	948	1100101110
37	4 ⊕ 10	950	1111001011

3.1.1.3.2 P(Y) Code

The P code is a 10.23 MHz pseudorandom noise (PRN) code sequence. After applying cryptographic protection, P code is called P (Y)-code and is transmitted in 7 days on both the L1 and L2 Frequencies and repeated weekly after every Saturday/ Sunday midnight. The P code is normally encrypted and so only available to the authorized civilian/ military GPS users. However, it is beyond the scope of this project so it will not be discussed further.

3.1.1.3.3 Navigation Message

Each satellite transmits the navigation message with an information rate of 50 bits per second in 12.5 minutes [12]. It contains the following information:

- Satellite timing and synchronization pulses
- Precise orbital data of the satellite (ephemeris data)
- Time correction data for determining the exact time of the satellite
- Approximate orbital data for all the satellites (almanac data)
- Correction signals for measuring the transit time of the signal
- Data regarding the satellite health

With the help of navigation data, the receiver is able to determine the exact transmission time and exact position of each satellite at the time of data transmission.

3.1.1.4 Satellite Signals Generation

Each GPS satellite has 4 atomic clocks. One of the 4 clock's resonance frequency generates the following time pulses and frequencies which are required for the operations of the signal generation as shown in the figure 3.5 and 3.6.

- Data pulse containing the GPS navigation information i.e.

$$x_i(t) = \sum_{i=-\alpha}^{i=+\alpha} b_i \, p_b(t - iT_b) \tag{3.2}$$

Where:

$b_i \in \{+1, -1\}$ = Information bits having the duration of T_b

$p_b(t)$ = Information bits pulse shape (rectangular in this case)

- The Coarse Acquisition code i.e.

$$c_i(t) = \sum_{i=-\alpha}^{i=+\alpha} a_i \, p_c(t - iT_c) \tag{3.3}$$

Where:

$a_i \in \{+1, -1\}$ = Spreading sequence having chip rate of $1/T_c$

$p_c(t)$ = Spreading sequence pulse shape (rectangular in this case)

The C/A code modulates the data pulse of 50Hz through the exclusive-or operation (EXOR). As a result, the resultant data is spread over a 2 MHz bandwidth as shown in the figure 3.3 and given by:

$$y_i(t) = x_i(t) \bullet c_i(t) \tag{3.4}$$

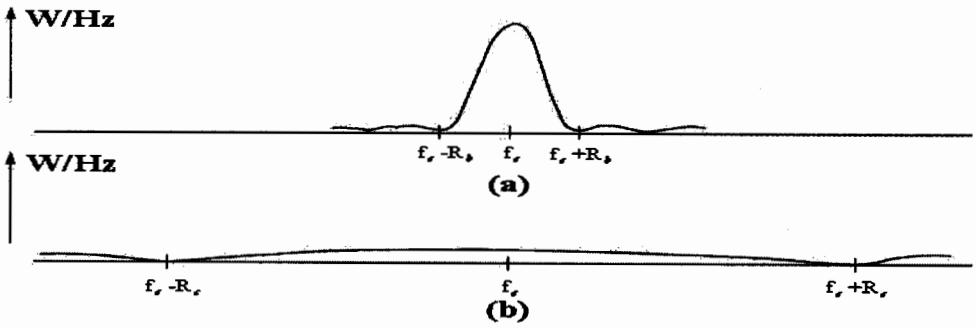

Figure 3.3: (a) BPSK signal spectrum without spreading
(b) BPSK signal spectrum with spreading

- The civil L1 carrier frequency of 1575.42 MHz which is used to modulate the spread sequence $y_i(t)$ using the Binary-Phase-Shift-Keying (BPSK) i.e.

$$s_i(t) = x_i(t) \bullet c_i(t) \bullet \sqrt{2P} \cos(2\pi \mathrm{f}_c t + \phi) \tag{3.5}$$

Where:

f_c = Carrier frequency

P = Signal power

ϕ = Data phase modulation

Each BPSK user uses the entire channel bandwidth given by:

$$B_w = 1/T_c \tag{3.6}$$

Moreover, the spreading ratio of the code modulation called Spreading/Processing gain 'N' gives the relation between bandwidth 'B_w' that must be spread and the bit rate 'R_b' for accommodating a given spreading code length is given by:

$$N = T_b / T_c = T_b B_w = B_w / R_b \tag{3.7}$$

Where:

R_b = Information bit rate

R_c = Spreading rate

Thus, due to BPSK, with every change in the modulated resultant of C/A code and 50Hz data pulses, the L1 carrier phase is changed by 180 degrees as shown in the figure 3.4.

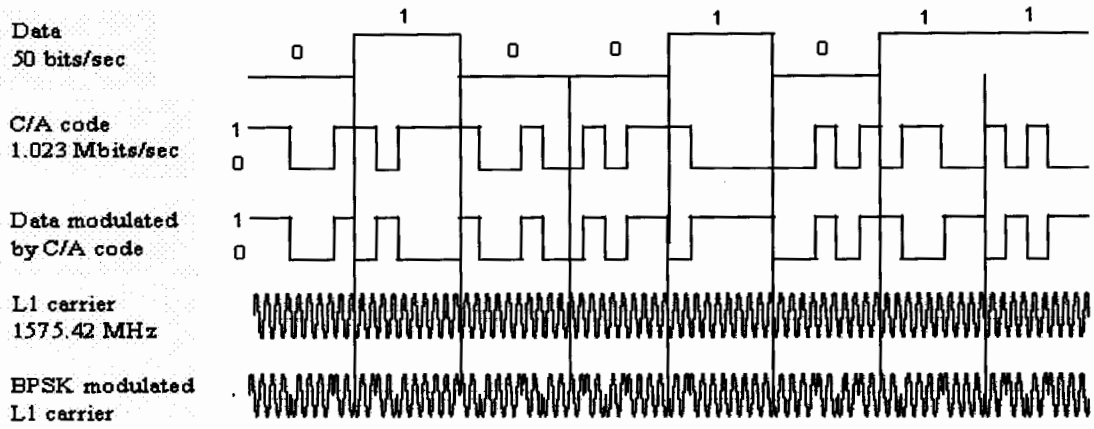

Figure 3.4: Data structure of a GPS signal

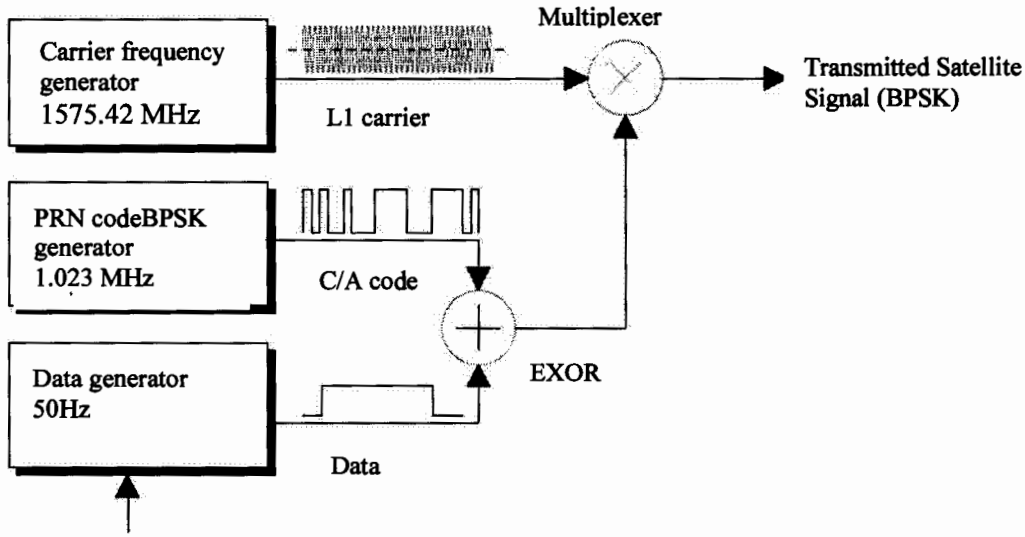

Figure 3.5: Simplified block diagram of GPS signal generation

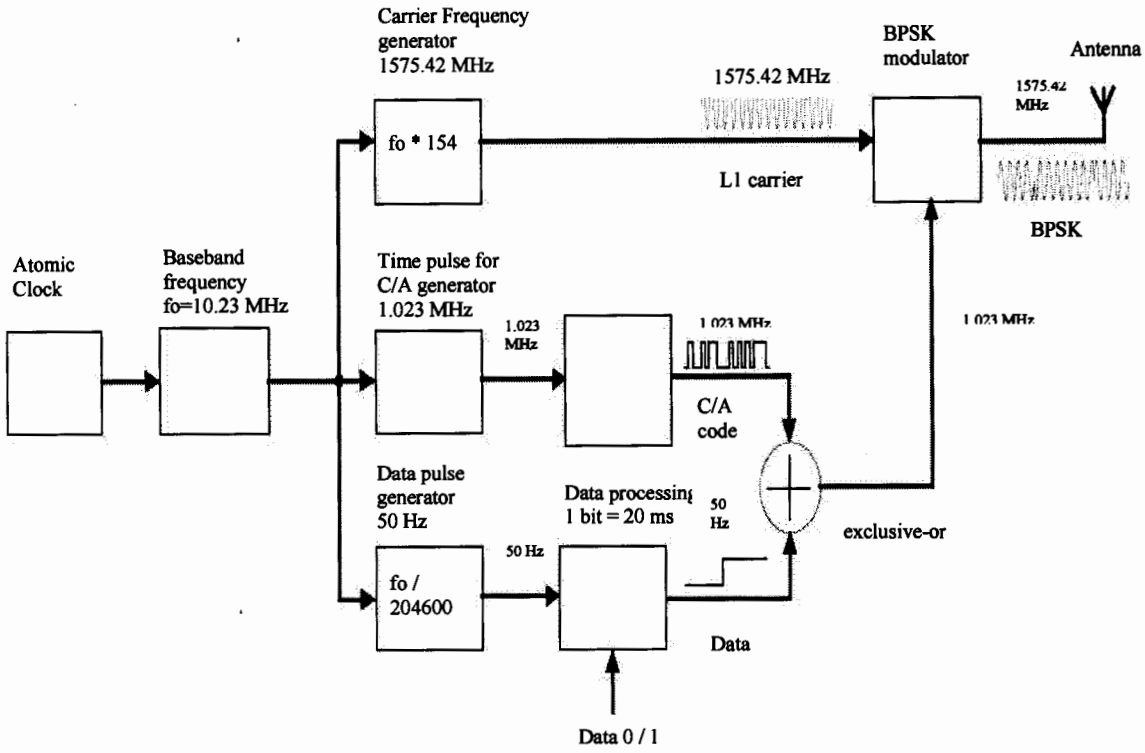

Figure 3.6: Detailed block diagram of a GPS signal generation

3.1.2 The Control Segment

The GPS control segment consists of one Master Control Station (MCS) at Falcon Air Force Base (FAFB) in the Colorado Springs USA, three Ground Control Stations (GCS) which transmit the information to the satellites and five Monitor Stations (MS) which are located at FAFB, Hawaii, Kwajalein, Diego Garcia and Ascension islands. The MS are equipped with the atomic clocks and are distributed around the globe in the vicinity of equator. They collect the ranging data from each satellite by passively tracking all the satellites. The MCS can be categorized as the central processing facility of the Control Segment.

It is performs the following tasks:

- Observes the movement of satellites, computes the orbital data (ephemeris data) and on the basis of it manages the satellite constellation. It predicts and estimates the ephemeris and the clock parameters on the basis of ranging data collected by MS.
- Uploads periodically, the navigation and clock data to each satellite, so that, they send the updated parameters to the GPS receivers for correct position measurement.
- Predicts the behavior of satellite clocks by constantly monitoring them
- Synchronization of the onboard satellite time
- Passes on (relays) the precise orbital data which is received from the satellites
- Passes on (relays) the approximate orbital data (almanac data) of all satellites
- Relays clock errors data and satellites health data etc
- Reconfigures the redundant satellite equipment

3.1.2.1 Selective Availability (SA) and GPS improvements

Before May 2000, the GPS Signals for the civilian use were degraded by either falsification of the ephemeris data or modulation of a random error signal with the time signals of the satellites. This artificial distortion is known as selective availability and it provides positional inaccuracy. On September 2007, it was declared on behalf of the U.S. DoD that in the next generation of GPS satellites system (GPS III), the technical possibility of signal distortion has been removed altogether. Moreover, the new GPS satellites are planned to transmit the C/A code at a third and a fourth L-band frequency with more power and provide improved accuracy.

3.1.3 The User Segment

The user segment consists of receivers which receive the GPS signals, decode and process them. The GPS signals travel with the speed of light and reach a ground based receiver in approximately 67 milliseconds. The travel time of these signals help us to determine the exact distance between the satellite and the receiver.

3.1.4 The GPS Navigation Message

The GPS navigation message of 50 Hz is superimposed on both the C/A code and P (Y) code and is extracted by a 50 bps BPSK demodulator in the GPS receiver. The navigation message having a narrow bandwidth ensures a high SNR ratio at the demodulator input and ensures a low bit errors probability (BER) in the navigation message [13].

3.1.4.1 Navigation Message Structure

The navigation data is very important for measuring the signal travel time and current position of the satellites. A complete navigation message also called complete almanac consists of 25 frames/ pages and takes about 12.5 minutes for transmission. Each frame contains 1500 bits and transmitted in 30 seconds. Each frame can be further divided into five sub frames. Each sub frame contains 300 bits and is transmitted in is 6 seconds. Each sub frame can be further divided into 10 words. Each word contains 30 bits and its transmission time is 0.6 seconds.

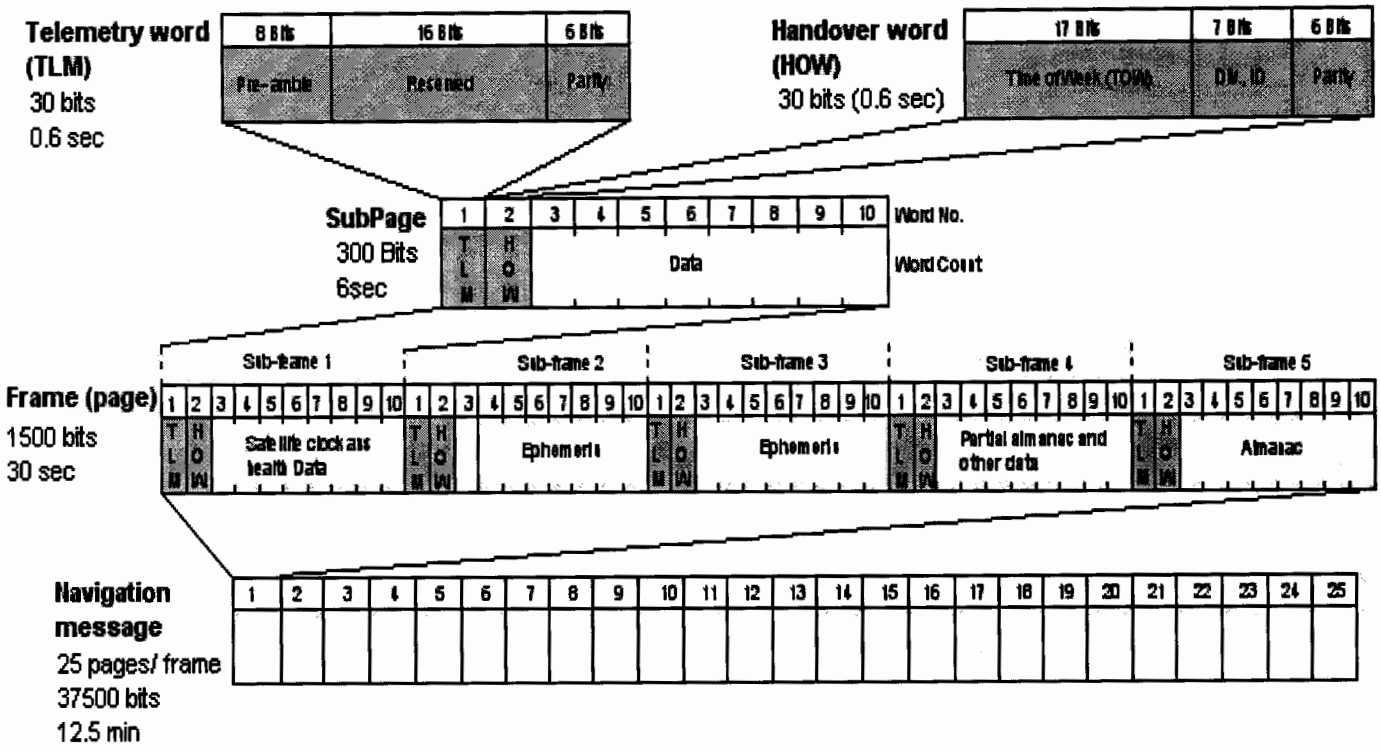

Figure 3.7: Structure of the entire navigation message

- **Sub-frames information**

Each frame is divided into 5 sub-frames which contain the following information as described below:

- The sub-frame 1 contains the time value of the satellites. It sends the correction parameters for satellite clock time and signal transit delay. It also provides an estimate of the satellite positional accuracy, a 10 bit week number whose value is from 0 to 1023 and information regarding the satellite health. The GPS time is started from the Sunday, 6th January 1980. The value of the week no parameter is incremented after every week and when it reaches a maximum of 1024 then value is reset to 0 through an event called "week rollover" (22 Aug 1999, week number made '0').

- The sub-frame 2 and 3 contain the ephemeris data and which provides the complete information about the satellite orbit.
- The sub-frame 4 contains the almanac data of the eight satellites numbered 25 to 32, the UTC offset (difference between UTC and GPS time) and information of ionospheric measurement errors.
- The sub-frame 5 contains the almanac data of the twenty four satellites numbered 1 to 24.

- **TLM and HOW**
  - The Telemetry word (TLM) has an 8 bits preamble for the synchronization purpose, 16 bits reserved data for the authorized users and remaining 6 parity bits.
  - The Handover word (HOW) has a 17 bits Time of week (TOW) data. It is used for transition from C/A-code to P (Y)-code tracking. It tells about the time of transmission of the next coming sub-frame of ephemeris. Its value is from 0 to 100,799. It gets the value of 0 on the starting of week (00:00:00) on each Sunday. Its value is incremented after every 6 seconds.
- **Frames/ Pages information**

The complete GPS navigation message consists of 25 frames and takes 12.5 minutes. Each frame can be divided into 5 sub-frames. The sub-frames 1 to 3 of all the 25 frames contain the same information. In the other words, for every 30 seconds, the sub-frames 1 to 3 contain the complete information of the ephemeris and clock data of transmitting satellite. But, the case of sub-frame 4 and 5 is different one i.e.

- Sub-frame 4: The sub-frame 4 of

- The frames 2,3,4,5,7,8,9 and 10 contain the almanac data of the satellites 25 to 32 respectively.
- The frames 18 contains UTC offset (difference between UTC and GPS time) and information of ionospheric measurement errors.
- The frame 25 contains the information regarding the health of the satellites 25 to 32 and configuration of all the 32 satellites.

- Sub-frame 5: The sub-frame 5 of
  - The frames 1 to 24 contain the almanac data of the satellites 1 to 24 respectively.
  - The frame 25 contains the information regarding the health of the satellites 1 to 24 and original almanac time.

3.1.4.2 The Ephemeris Data

It is a highly precise orbital data which is very important to calculate the exact position of a satellite at a given time. It includes not only the six basic orbital elements, but, also has some other parameters which tell about the time of their applicability and depict their change with time. With this information, the GPS receiver calculates position vector of a satellite (X, Y, Z) in the ECEF coordinate system and hence measures the corrected integral of motion for the space vehicles for solving the navigation problem. The parameters are given table 3.3 below [for better understanding, see also Appendix C having diagrammatic representation of the ephemeris data parameters].

Table 3.3: GPS Ephemeris data definitions

S/No	Symbol	Description
1.	t_{oe}	Reference time of ephemeris
2.	$\sqrt{a}$	Square root of semi-major axis
3.	e	Eccentricity
4.	i_0	Inclination angle (at time t_{oe})
5.	Ω_0	Longitude of the ascending node (at weekly epoch)
6.	ω	Argument of perigee. i.e. Point nearest to the orbited object (at time t_{oe})
7.	M_0	Mean anomaly (at time t_{oe})
8.	*di/dt (IDot)*	Rate of change of inclination angle
9.	$\dot{\Omega}$	Rate of change of longitude of the ascending node
10.	Δn	Mean motion difference from the computed value (Mean motion correction)
11.	C_{uc}	Amplitude of cosine harmonic correction to argument of latitude
12.	C_{us}	Amplitude of sine harmonic correction to argument of latitude
13.	C_{rc}	Amplitude of cosine harmonic correction to orbital radius
14.	C_{rs}	Amplitude of sine harmonic correction to orbital radius
15.	C_{ic}	Amplitude of cosine harmonic correction to inclination angle
16.	C_{is}	Amplitude of sine harmonic correction to inclination angle

Thus the satellite position can be calculated by demodulating and extracting the navigation data. The equations in the table 3.4 are helpful in finding the satellite position in the WGS-84 ECEF reference frame.

Table 3.4: GPS Ephemeris data calculations

Sl. No	Equation	Description
1.	$\alpha = (\sqrt{a})^2$	Semi major axis
2.	$n = \sqrt{\frac{\mu}{\alpha^3}} + \Delta n$	Corrected mean motion, where 'μ' is the earth's gravitational constant given by: $\mu = 3.986005 \bullet 10^{14} m^3 / \sec^2$
3.	$t_k = t - t_{oe}$	Time from ephemeris epoch. Where 't' is actual time of transmission and t_{oe} is the epoch time.
4.	$M_k = M_0 + n(t_k)$	Mean anomaly
5.	$M_k = E_k - e \sin E_k$	Eccentric anomaly (must be solved iteratively for E_k)
6.	$\sin v_k = \frac{\sqrt{1-e^2}\sin E_k}{1-e\cos E_k}$ $\cos v_k = \frac{\cos E_k - e}{1-e\cos E_k}$ $v_k = a\tan 2\left(\frac{\sin v_k}{\cos v_k}\right)$	True anomaly
7.	$\phi_k = v_k + \omega$	Argument of latitude

Table 3.4 (Continued)

8.	$\delta\phi_k = C_{us}\sin(2\phi_k) + C_{us}\cos(2\phi_k)$	Argument of latitude correction
9.	$\delta r_k = C_{rs}\sin(2\phi_k) + C_{rc}\cos(2\phi_k)$	Radius correction
10.	$\delta i_k = C_{is}\sin(2\phi_k) + C_{ic}\cos(2\phi_k)$	Inclination correction
11.	$\mu_k = \phi_k + \delta\phi_k$	Corrected argument of latitude
12.	$r_k = a(1 - e\cos E_k) + \delta r_k$	Corrected Radius
13.	$i_k = i_0 + (di/dt)t_k + \delta i_k$	Corrected inclination
14.	$\Omega_k = \Omega_0 + (\dot{\Omega} - \dot{\Omega}_e)(t_k) - \dot{\Omega}_e t_{0e}$	Corrected longitude of node
15.	$x_p = r_k \cos\mu_k$	In-plane x position
16.	$y_p = r_k \sin\mu_k$	In-plane y position
17.	$x_s = x_p\cos\Omega_k - y_p\cos i_k \sin\Omega_k$	ECEF x- coordinates
18.	$y_s = x_p\sin\Omega_k - y_p\cos i_k \cos\Omega_k$	ECEF y- coordinates
19.	$z_s = y_p \sin i_k$	ECEF z- coordinates

3.1.5 The GPS Signal Levels

It is apprized that the power spectral density of any given GPS C/A code signal is about 15 dB below the power spectral density of the noise.

3.1.6 GPS Errors

The major sources of error experienced by the GPS receiver are due to the atmospheric effect (Ionospheric & Tropospheric), satellite clock error, satellite orbits errors, ephemeris errors, selective availability (when switched on), measurement noise and multi-path effect [13]. These errors caused an overall position deviation of $\pm 50-100$ meters from the actual position of the GPS receiver. The satellite clock error and atmospheric error models (Klobuchar Ionospheric & Hopfield Tropospheric) are simulated in this project report.

3.2 Auto Correlations Characteristics

Correlation is the product integration of received signal with the replica of transmitted waveform and is very helpful in the optimum detection of the signal in white noise environment. That is why; it is used to detect the GPS signals buried in noise.

The GPS uses Gold codes that have auto-correlation and power spectrum properties like the random binary codes, but, they are deterministic, periodic, and predictable and are easily reproduced by suitably equipped receivers. The auto correlation function of a maximum length PN sequence is an infinite series of triangular functions, with the peaks depicting the value of maximum correlation given by mathematically as

$$RG(\tau) = \frac{1}{1023 T_{CA}} \int_{t=0}^{t=1023} Gi(t)\, Gi(t+\tau)dt \qquad (3.8)$$

Where:

Gi(t) = C/A code Gold code sequence as a function of time t for ith SV.

T_{CA} = C/A code chipping period (977.5 n sec) and,

τ = phase of the time shift in the autocorrelation function

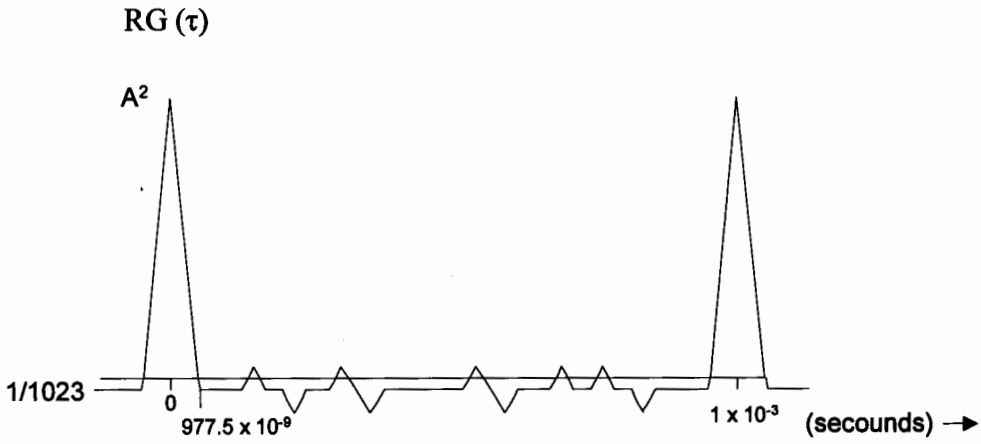

Figure 3.8: Auto-correlation characteristics of PN sequence

The signal received by the GPS receiver is:

$$r_i(t) = s_i(t) + n_i(t) \tag{3.9}$$

$$= x_i(t-\tau_d) \bullet c_i(t-\tau_d) \bullet \sqrt{2P}\cos(2\pi f_c (t-\tau_d) + \phi) + n_i(t) \tag{3.10}$$

Where $n_i(t)$ is the band pass AWGN. The GPS receiver correlates this signal with the delayed spreading waveform and this process is known as dispreading. In this way the maximum likelihood receiver calculates the decision station as follows:

$$Z(\tau_d) = \frac{1}{1023 \bullet T_c} \int_{t=0}^{t=1023} r_i(t) \bullet c_i(t-\hat{\tau}_d).dt \tag{3.11}$$

Where:

$\hat{\tau}_d$ = Receiver's best estimate of the transmission delay

$$Z(\tau_d) = \frac{1}{1023 \bullet T_c} \int_{t=0}^{t=1023} (x_i(t-\tau_d) \bullet c_i(t-\tau_d) \bullet \sqrt{2P}\cos(2\pi f_c (t-\tau_d) + \phi) + n_i(t)) \bullet c_i(t-\hat{\tau}_d).dt \tag{3.12}$$

$$Z(\tau_d)=\frac{1}{1023\bullet T_c}\int_{t=0}^{t=1023} x_i(t-\tau_d)\bullet c_i(t-\tau_d)\bullet c_i(t-\hat{\tau}_d)\bullet\sqrt{2P} \bullet\cos(2\pi f_c(t-\tau_d)+\phi).dt+\frac{1}{1023\bullet T_c}\int_{t=0}^{t=1023} n_i(t)\bullet c_i(t-\hat{\tau}_d).dt \tag{3.13}$$

$$Z(\tau_d)=\frac{1}{1023\bullet T_c}\int_{t=0}^{t=1023} x_i(t-\tau_d)\bullet c_i^2(t-\tau_d) \bullet\sqrt{2P}\cos(2\pi f_c(t-\tau_d)+\phi).dt+n \tag{3.14}$$

$$Z(\tau_d)=\frac{1}{1023\bullet T_c}\int_{t=0}^{t=1023} x_i(t-\tau_d)\bullet\sqrt{2P}\cos(2\pi f_c(t-\tau_d)+\phi).dt+n \tag{3.15}$$

Where n is the noise sample at the match filter output. As $\tau_d=\hat{\tau}_d$, therefore, the synchronization between the transmitter and receiver code is attained, so, $c_i^2(t-\tau_d)=1$. The remaining part $x_i(t-\tau_d)\bullet\sqrt{2P}\cos(2\pi f_c(t-\tau_d)+\phi)$, can be demodulated with the help of conventional coherent phase modulator. As a result, the decision statistics is given by:

$$Z=\frac{\sqrt{2P}}{2}x_\circ+n \tag{3.16}$$

Where $x_\circ$ is the original bit value corresponding to the interval of interest along with the noise term and shows the standard BPSK [14][15].

CHAPTER 4

SAR AND PASSIVE MICROWAVE IMAGING

4.1 Synthetic Aperture Radar (SAR)

Synthetic Aperture Radar is an echo mode, high resolution, array imaging system of the target area under observation which is used for remote sensing applications. Here, the synthetic aperture is provided by the moving receiver. With the help of SAR technique, an effective antenna of large aperture is created logically through signal processing by the moving receiver [15].

SAR can be of two types:

- Mono-static SAR, having the same antenna for transmission and reception
- Bi-static SAR, having the different antennas for transmission and reception with same or different moving platforms.

Inverse Synthetic Aperture Radar (ISAR) is used for target recognition in which the synthetic aperture is provided by the moving targets.

The conventional radar systems don't have good azimuth resolution (along-track resolution) due to their dependence on the slant range (thus platform altitude), Operating wavelength and position across the swath. Their azimuth resolution is given by

$$r_a = (\lambda / l_a) \bullet R_\circ \tag{4.1}$$

Where,

r_a = Azimuth resolution

λ = Wavelength of the transmitted pulses

l_a = Length of the antenna on the spacecraft

$R_\circ$ = Slant distance from platform to the ground

The SAR systems replaced the conventional radar systems because their azimuth resolution is independent of the slant range as given by

$$r_a = l_a / 2 \tag{4.2}$$

It shows that by reducing the antenna length of the spacecraft, the improvement in the azimuth resolution is possible. The length of the synthetic aperture radar is defined by the time instance during which the target is radiated by the transmitted radar signals as shown in the figure 4.1.

Let us consider that the slant range is ' $R(t)$ ', then, from the figure 4.2, we have

$$R(t) = \sqrt{R_\circ^2 + x^2} = R_\circ \left[1 + \left(\frac{x}{R_\circ} \right)^2 \right]^{\frac{1}{2}} \tag{4.3}$$

Considering ' $\frac{x}{R_\circ} << 1$ ', then the above equation can be written as

$$R(t) = R_\circ + \frac{x^2}{2R_\circ} \tag{4.4}$$

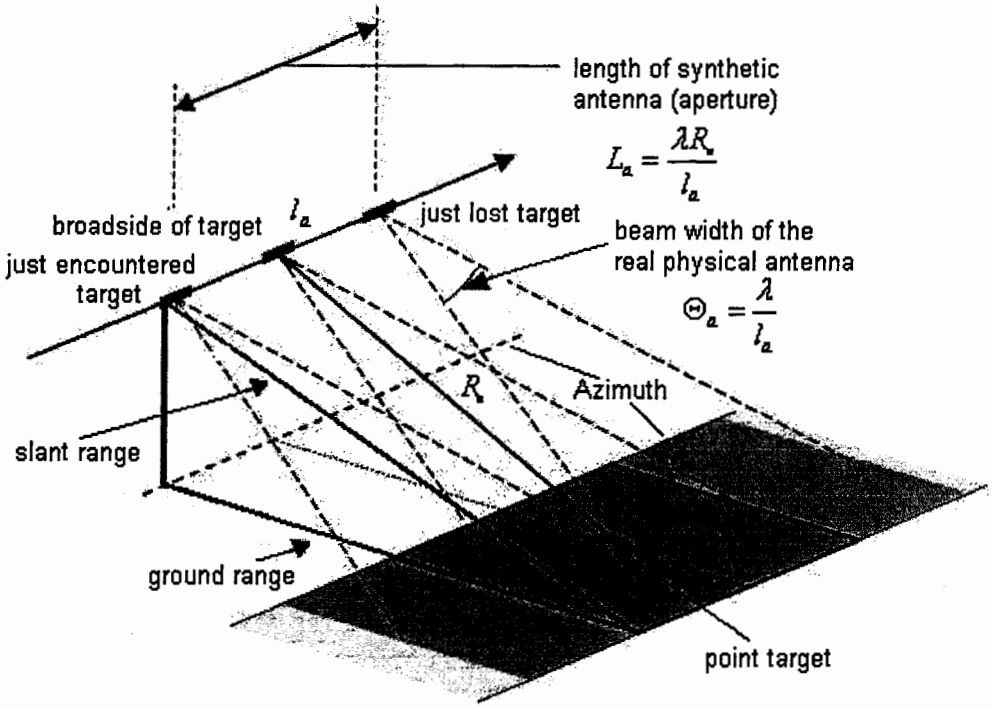

Figure 4.1: The concept of SAR using platform/receiver motion

If the transmitted signal by the moving platform is '$\cos\omega_\circ t$', then, the reflected signal from the target will be $\cos\omega_\circ(t+t_D)$. Here 't_D' is the time taken by the two way trip and is given by

$$t_D = \frac{2R(t)}{c} = \frac{2}{c}\left\{R_\circ + \frac{x^2}{2R_\circ}\right\} \tag{4.5}$$

Substituting $\omega_\circ / c = 2\pi f_\circ / c = 2\pi/\lambda\,(with\ \ c = f\lambda)$, then we have

$$\cos\omega_\circ(t+t_D) = \cos(\omega_\circ t + \omega_\circ t_D)$$

$$= \cos\left[\omega_\circ t + \omega_\circ\left\{\frac{2}{c}\left(R_\circ + \frac{x^2}{2R_\circ}\right)\right\}\right]$$

$$= \cos\left[\omega_o t + \frac{\omega_o}{c}\left\{2\left(R_o + \frac{x^2}{2R_o}\right)\right\}\right]$$

$$= \cos\left[\omega_o t + \frac{4\pi}{\lambda}\left(R_o + \frac{x^2}{2R_o}\right)\right]$$

$$= \cos\left[\omega_o t + \frac{4\pi R_o}{\lambda} + \frac{2\pi x^2}{\lambda R_o}\right]$$

$$= \cos[\omega_o t + \phi_R(t)] = \cos\phi_T(t) \qquad (4.6)$$

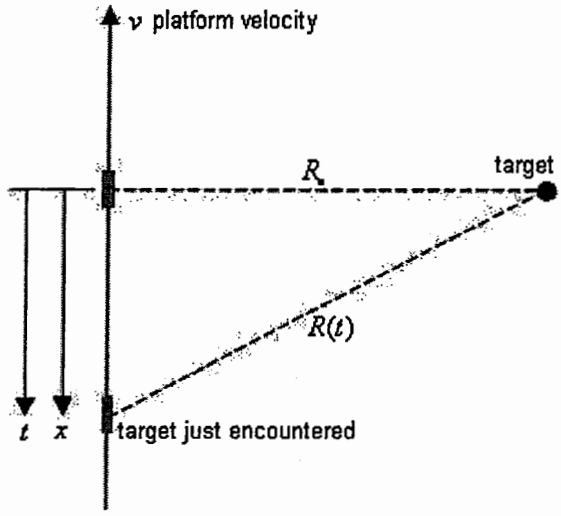

Figure 4.2: The platform/receiver radiating the point target

Where '$\phi_R(t)$' is the phase delay of the signal due to two way travel between the platform and the target while '$\phi_T(t)$' is the total phase angle of the received angle. The instantaneous frequency using total phase angle is given by

$$\omega = \frac{d(\phi_T(t))}{dt} = \frac{d}{dt}(\omega_o t + \phi_R(t)) = \omega_o + \frac{d}{dt}\phi_R(t)$$

$$= \omega_o + \frac{4\pi R_o}{\lambda} + \frac{2\pi v^2 t^2}{\lambda R_o} = \omega_o + 2 \bullet \frac{2\pi v^2 t}{\lambda R_o} \tag{4.7}$$

$$= \omega_o + \left(\frac{4\pi v^2}{\lambda R_o} \right) t = \omega_o + bt \tag{4.8}$$

The above equation shows a frequency variation in the form of 'bt'. This is known as Doppler shift and is caused by the moving platforms. It shows that the carrier frequency is up shifted, when the receiver is ahead of broadside (same as caused due to the siren of an approaching train) and the carrier frequency is down shifted, when the receiver is after the broadside (same as caused due to the siren of a receding train). The term 'b' in the above equation 4.8 is known as Doppler rate and is given by

$$b = \frac{4\pi v^2}{\lambda R_o} \; rad.s^{-1} \, s^{-1} \tag{4.9}$$

$$\beta = \frac{b}{2\pi} = \frac{2v^2}{\lambda R_o} \; Hzs^{-1} \tag{4.10}$$

The signal starts, when the receiver platform acquires the target, and ends, when the target is lost. Due to the Doppler affect, the signal is and called chirp. The distance traveled in the mean time is the real azimuth bandwidth on the ground. The chirp bandwidth is given by

$$\beta_c = \beta T_a = \frac{\beta L_a}{v} \tag{4.11}$$

Where, T_a is the time of visibility of point target (equal to existence of azimuth chirp) and 'L_a' is the antenna azimuth on the view. Therefore, the compressed azimuth chirp is given by

$$\tau_a = \frac{1}{\beta_c} = \frac{1}{\beta T_a} = \frac{v}{\beta L_a} = \frac{\lambda R_\circ}{2vL_a} \tag{4.12}$$

The spatial resolution in the azimuth direction is given by

$$r_a = v\tau_a = \frac{\lambda R_\circ}{2L_a} \tag{4.13}$$

Putting the value of 'r_a' from equation 4.2 in equation 4.13, we get

$$\frac{l_a}{2} = \frac{\lambda R_\circ}{2L_a}$$

$$L_a = \frac{\lambda R_\circ}{l_a} \tag{4.14}$$

Where, 'l_a' is the length of the physical antenna on the platform and 'L_a' shows the synthetic aperture radar length. The equation 4.13 shows that larger the length of synthetic aperture radar 'L_a', the finer will be the azimuth resolution 'r_a'.

4.1.1 SAR Imaging

SAR technique uses only one antenna in time multiplexing and works like the phased array. It creates a two-dimensional image [16].

- One dimension measures the "line-of-sight" distance from the radar to the target is termed as range (cross track). Range can be fond out by measuring the time from transmission of signal to the reception of the echo reflected from the target. The narrow the pulse, the more fine will be the range resolution [16].
- The other dimension which is perpendicular to range is called azimuth (or along track). The larger the antenna for producing the sharp beam through the focusing

of transmitted and received signals, the more fine will be the azimuth resolution [16].

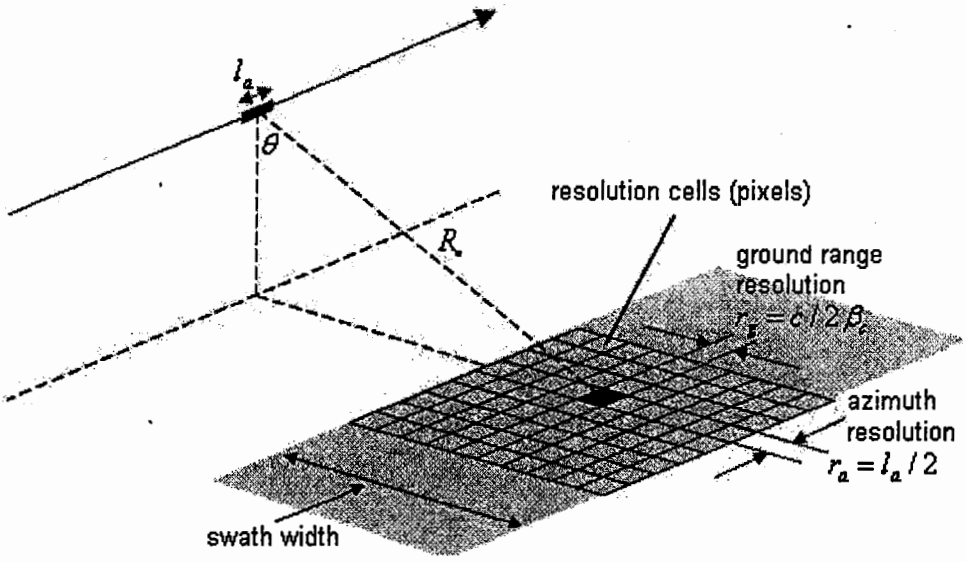

Figure 4.3: SAR Imaging concept

4.2 Matched Filtering

A matched filter (receiving network) maximizes the ratio of peak signal power to average noise power for an instant in time. If the signal changes the filter must change so it is matched to the signal being used [17][18]. Let '$s_I(t)$' is the indirect signal with time interval '$0 \le t \le T$' and $s_D(t)$ is the direct signal matched with $s_I(t)$, then, output of match filter having the impulse response '$h_I(t) = s_D(T-t)$' is given by

$$y_s(t) = \int_0 s_I(\tau) \bullet h_I(t-\tau) \bullet d\tau$$

$$= \int_0 s_I(\tau) \bullet s_D(T-t+\tau) \bullet d\tau \qquad (4.15)$$

Here, autocorrelation function '$y(t)$' is an even function of 't' and attains maximum value at '$t = T$', so

$$y_s(T) = \int_0^T s_I(\tau) \bullet s_D(T - T + \tau) \bullet d\tau$$

$$= \int_0^T s_I(\tau) \bullet s_I(\tau) \bullet d\tau = \int_0^T s_I^2(\tau) \bullet d\tau \qquad \text{as: } s_I(\tau) = s_D(\tau)$$

$$= \int_0^T \left(\sqrt{\varepsilon}\right)^2 \bullet d\tau = \varepsilon \qquad (4.16)$$

It is clear that the match filter flips the impulse response of the system and so it does auto correlation by using convolution [19]. It is important to know that the match filter's out put equals the correlator's output only a sampling instant(t = T) [18] as shown below in the figure 4.4.

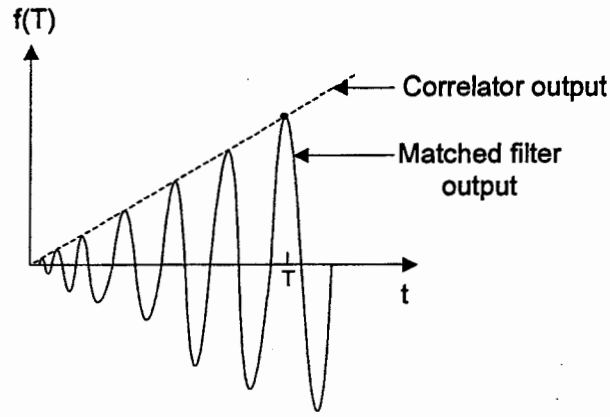

Figure 4.4: Comparison between matched filter and correlator

If '$r_I(t)$' is the indirect received signal from satellite, then

$$r_I(t) = s_I(t) + n(t) \qquad (4.17)$$

$$y(t) = \int_0^t r_I(\tau) \bullet h_I(t - \tau) \bullet d\tau$$

$$= \int_0^t s_1(\tau) \bullet h_1(t-\tau) \bullet d\tau + \int_0^t n(\tau) \bullet h_1(t-\tau) \bullet d\tau \tag{4.18}$$

By sampling at '$t = T$', we get

$$y(T) = \int_0^T s_1(\tau) \bullet h_1(T-\tau) \bullet d\tau + \int_0^T n(\tau) \bullet h_1(T-\tau) \bullet d\tau$$

$$= y_s(T) + y_n(T) \tag{4.19}$$

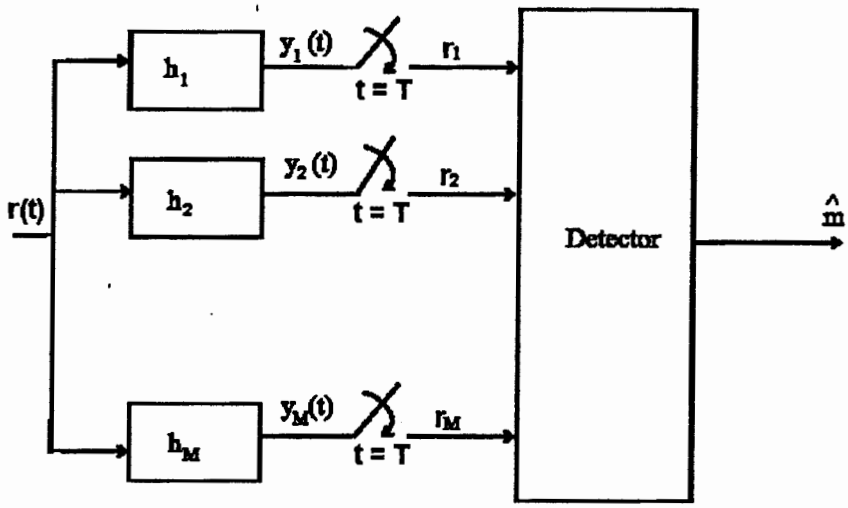

Figure 4.5: matched filter demodulator

The signal to noise ratio (SNR_0) is given by

$$\text{SNR}_0 = \frac{y_s^2(T)}{E[y_n^2(T)]} \tag{4.20}$$

Solving, we get

$$E[y_n^2(T)] = \int_0^T \int_0^T E\left[n(t) \bullet n(\tau)\right] \bullet h_1(T-t) \bullet h_1(T-\tau) \bullet dt.d\tau$$

$$= \frac{N_0}{2} \int_0^T \int_0^T \delta(t-\tau) \bullet h_1(T-t) \bullet h_1(T-\tau) \bullet dt.d\tau$$

$$= \frac{N_0}{2} \int_0^T h_I^2(T-t) \bullet dt \tag{4.21}$$

$$\text{SNR}_0 = \frac{y_s^2(T)}{E[y_n^2(T)]} = \left[\frac{\left(\int_0^T s_I(\tau) \bullet h_I(t-\tau) \bullet d\tau \right)^2}{\left(\frac{N_0}{2} \int_0^T h_I^2(T-t) \bullet dt \right)} \right] \tag{4.22}$$

Using the Cauchy-Schwarz inequality i.e.

$$\left[\int_{-\infty}^{+\infty} g_1(t) \bullet g_2(t).dt \right]^2 \leq \int_{-\infty}^{+\infty} g_1^2(t).dt \bullet \int_{-\infty}^{+\infty} g_2^2(t).dt \tag{4.23}$$

Where $g_1(t) = C \bullet g_2(t)$ with 'C' is constant, we get

$$\text{SNR}_0 = \frac{2}{N_0} \bullet \int_0^T s_I^2(t).dt$$

$$= \frac{2\varepsilon}{N_0} \tag{4.25}$$

4.3 FM Chirp Signal

For good working in the radar environment:

- The short duration pulses are required to improve the target resolution (target recognition).
- The long duration pulses are required to increase the signal energy.

With the help of Frequency Modulation (FM), it is possible to construct a waveform that has both the properties of the pulses of long duration and effective small duration (large bandwidth). When the received FM pulse is correlated with the transmitted pulse by match filter processing then the resultant Signal to Noise ratio (SNR) and the range resolution is increased. This signal processing technique is known is signal compression. The linear FM pulse called chirp signal is given by:

$$f(t) = \cos(\omega_o t + \pi F / T t^2) \quad for \quad -T/2 < t < T/2$$
$$F = f_2 - f_1 \tag{4.26}$$

Where, F is the sweep bandwidth and 'f_1' & 'f_2' are the initial and final instantaneous frequencies and 'T' is the time duration as shown in the figure 4.6.

Thus, the linear FM pulse signals are used to obtain wide frequency band within a relatively wide time width. The usage of chirp signals helps to reduce the complexity of the radar system through avoiding the high peak power of signals.

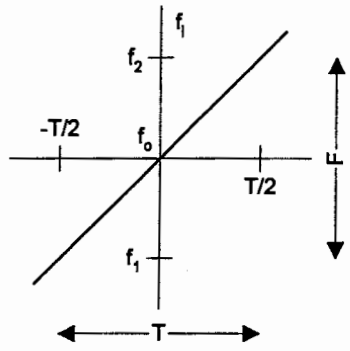

Figure 4.6: FM Chirp Signal

4.4 Characteristics of the Target

When a signal impinges upon a target it is reflected in various directions depending upon the characteristics and behavior of the target. Radar Cross Section is a term used to measure the ability of the target to reflect the radar signals in the direction of receiver and can be defined as,

"The ratio of PSD of the reflected signals from target towards receiver to the PSD of incident signals from the transmitter towards target is called Radar Cross Section (RCS)

of the reflecting object." The units of RCS are square meters m^2. The measurements of RCS of a target is made by comparing the signals reflected from the target's cross sectional area of one m^2 to the signals reflected from a perfectly smooth sphere of the same area..

In order to facilitate the simulation process the point target resolution theory is applied. The target is modeled as a set of point scatterers. A target can be resolved from another target if it falls into a different bin (or cell) and its return is not marked by self-clutter [20]. The theory for the resolution of point target states that the transmitted signal must have adequate bandwidth to achieve the desired small range resolution cell and it must be coherently integrated over a long enough time to achieve the small Doppler resolution cell.

4.5 Passive Microwave Imaging (PMI)

The conventional radar systems image the targets with the help of both the transmitters and receivers are therefore called as active imaging systems e.g. light detection and ranging system (LIDAR). But, if the system uses solar radiations, earthen radiations or any other source of energy such as reflected GPS signals for imaging purpose, then, such a system can be categorized as passive imaging system.

A microwave imaging system which has the ability to sense the naturally available energy is known as passive microwave imaging system. Such systems are used for remote sensing and measurement of soil moisture in agriculture, sea depth in oceanography and passive target detection etc. In addition to the microwave, visible light, near infrared, far infrared is also used for the remote sensing. In remote sensing, the large resolution cells are used in order to get the measurable power levels. In addition, the large

synthetic aperture is created by using an array of small antennas fore gathering the weak radiometric signals [16].

4.5.1 Radiometric Brightness Temperature

The passive microwave imaging system builds the images of the targets on the basis of the received power. The power spectral density (PSD) received by the radiometer is directly proportional to the temperature of the object being observer and is given by [16]

$$P = kT\beta \tag{4.27}$$

Where,

T = Surface temperature (°K) of the body

β = Bandwidth (in Hz) for microwave emission

k = Boltzmann's constant with value $1.38065 \bullet 10^{-23}\,\mathrm{JK}^{-1}$

The emissivity ' ε ' of a real scene is lower than a perfect black body and lies in the range $0 \le \varepsilon \le 1$. If ' P_r ' is the actual power received from a scene, then

$$P_r = \varepsilon kT\beta \tag{4.28}$$

$$P_r = k(\varepsilon T)\beta = kT_B\beta \tag{4.29}$$

$$T_B = \varepsilon T = P_r / k\beta \tag{4.30}$$

Where ' T_B ' is the radiometric brightness temperature in ' °K ' and it is used to characterized the imaging material.

4.5.2 Microwave emission and surface characteristics

The radiations incident on a surface are partly absorbed and partly reflected. If the reflectivity is 'Γ' then the absorptivity is '$1-\Gamma$'. In case of thermal equilibrium, the emissivity 'ε' is given by

$$\varepsilon_p = 1-\Gamma_p \tag{4.31}$$

Where, 'p' refers to polarization. The incidence radiations may hit a surface at some angle, so, the emissivity of the smoother surfaces is [16]

$$\varepsilon_p(\theta) = 1-\Gamma_p(\theta) = 1-\left|\rho_p(\theta)\right|^2 \tag{4.32}$$

Where, '$\rho_p(\theta)$' is the Fresnel reflection coefficient and depends on the incident angle. The emissivity of the rough surfaces is given by [16]

$$\varepsilon_p(\theta) = 1-\Gamma_p(\theta) = 1-(\sigma^\circ(0)/4) \tag{4.33}$$

Therefore, it is clear that in case of smoother surfaces, the emissivity depends upon the incident angle. As the surface increases in roughness, the emissivity and radiometric brightness temperature also increases and the incident angle dependence goes on weaker. Moreover, as the moisture content of a surface increase, the radiometric brightness temperature decreases.

4.5.3 PMI using GPS signals

The GPS signals can be sensed by the GPS receivers nearly at any location of the earth. The direct GPS signals are used for the navigation purpose and measure the distance from the receiver as,

$$D_{direct} = D_{sr} = \sqrt{(x_s - x_r)^2 + (y_s - y_r)^2 + (z_s - z_r)^2} \tag{4.34}$$

$$\text{Delay (direct)} = t_{direct} = D_{sr} / c \qquad (\text{sec}\,onds) \qquad (4.35)$$

Where 'c' is the velocity of light equals to 299,792,458 m/s

The indirect GPS signals which are reflected from the region of interest are used to take the imagery of the targets by using match filter processing technique. Thus, the reflected GPS signals are reached the GPS receiver by following an indirect path and traverse the distance as

$$D_{reflected} = D_{sr} = D_{st} + D_{tr} \qquad (4.36)$$

$$\text{Delay (indirect)} = t_{indirect} = (D_{st} + D_{tr}) + / c \qquad (\text{sec}\,onds) \qquad (4.37)$$

As the imaging is performed in a covert way, that is why, it is said that GPS signals are used for passive microwave imaging of targets.

CHAPTER 5

THE MODIFIED GPS RECEIVER

5.1 GPS Receiver

When the GPS receiver receives the GPS signals, then, it amplifies and digitizes those signals. After suitable measurements, the receiver provides the feedback for the acquisition and tracking of the signals.

The signal received by the GPS receiver is:

$$\begin{aligned} r_i(t) &= s_i(t) + n_i(t) \\ &= x_i(t) \bullet c_i(t) \bullet \sqrt{2P} \cos(2\pi f_c t + \phi) + n_i(t) \end{aligned} \tag{5.1}$$

After down-conversion and sampling, the output is given by

$$r_i(n) = x_i(n) \bullet c_i(n) \bullet \sqrt{2P} \cos(2\pi f_{IF} n + \phi) + n_i(n) \tag{5.2}$$

The carrier frequency with Doppler shift is tracked by Costas loop. The GPS receiver has the Numerically Controlled Oscillators (NCO) which produce the In-

phase (I) and Quadrature-phase (Q) data streams which are mixed with the received digitized samples [21].

The 'I' arm produces the following result:

$$x_i(n) \bullet \cos(2\pi f_{IF} n + \varphi) \bullet \cos(2\pi f_{IF} n) = \frac{1}{2} \bullet x_i(n) \bullet \cos(\varphi) + \frac{1}{2} \bullet x_i(n) \bullet \cos(4\pi f_{IF} n + \varphi) \tag{5.3}$$

Where:

φ = Phase difference between the phases of received and locally generated receiver

The 'Q' arm produces the following result:

$$x_i(n) \bullet \cos(2\pi f_{IF} n + \varphi) \bullet \sin(2\pi f_{IF} n) = \frac{1}{2} \bullet x_i(n) \bullet \sin(\varphi) + \frac{1}{2} \bullet x_i(n) \bullet \sin(4\pi f_{IF} n + \varphi) \tag{5.4}$$

Where:

φ = Phase difference between the phases of received and locally generated receiver

By low pass filtering, we get

$$I^i = \frac{1}{2} \bullet x_i(n) \bullet \cos(\varphi) \tag{5.5}$$

$$Q^i = \frac{1}{2} \bullet x_i(n) \bullet \sin(\varphi) \tag{5.6}$$

The phase error 'φ' of the local carrier phase replica is given by [21]

$$\frac{Q^i}{I^i} = \frac{\frac{1}{2} \bullet x_i(n) \bullet \sin(\varphi)}{\frac{1}{2} \bullet x_i(n) \bullet \cos(\varphi)} = \tan(\varphi) \tag{5.7}$$

$$D_{CL} = \varphi = \tan^{-1}\left(\frac{Q^i}{I^i}\right) \tag{5.8}$$

This phase error ' φ ' is feed back to the carrier phase oscillator. The above equation shows that phase error ' φ ' can be minimized when ' Q^i ' is zero and ' I^i ' is maximum.

The code tracking is a delay lock loop (DLL) known as early late tracking loop. In this technique, the base band signal which is obtained by multiplying the received signal with locally generated carrier replica are correlated with the three different replicas of the code (Early, Prompt and late) as shown in the figure 5.1.

The early and late versions are the same as the prompt code but time shifted by $\pm 1/2$ chips. The resultant values are integrated and dumped. The output of these integrations provides a numerical value which describes the amount of correlation between the incoming signals and the locally generated replicas. The correlation values of I_E, I_P and I_L are then compared and the highest value of the specific code replica shows the highest correlation.

The early late normalized envelop discriminator is

$$D_{DLL} = \frac{\sqrt{I_E^{i\,2} + Q_E^{i\,2}} - \sqrt{I_L^{i\,2} + Q_L^{i\,2}}}{\sqrt{I_E^{i\,2} + Q_E^{i\,2}} + \sqrt{I_L^{i\,2} + Q_L^{i\,2}}} \tag{5.9}$$

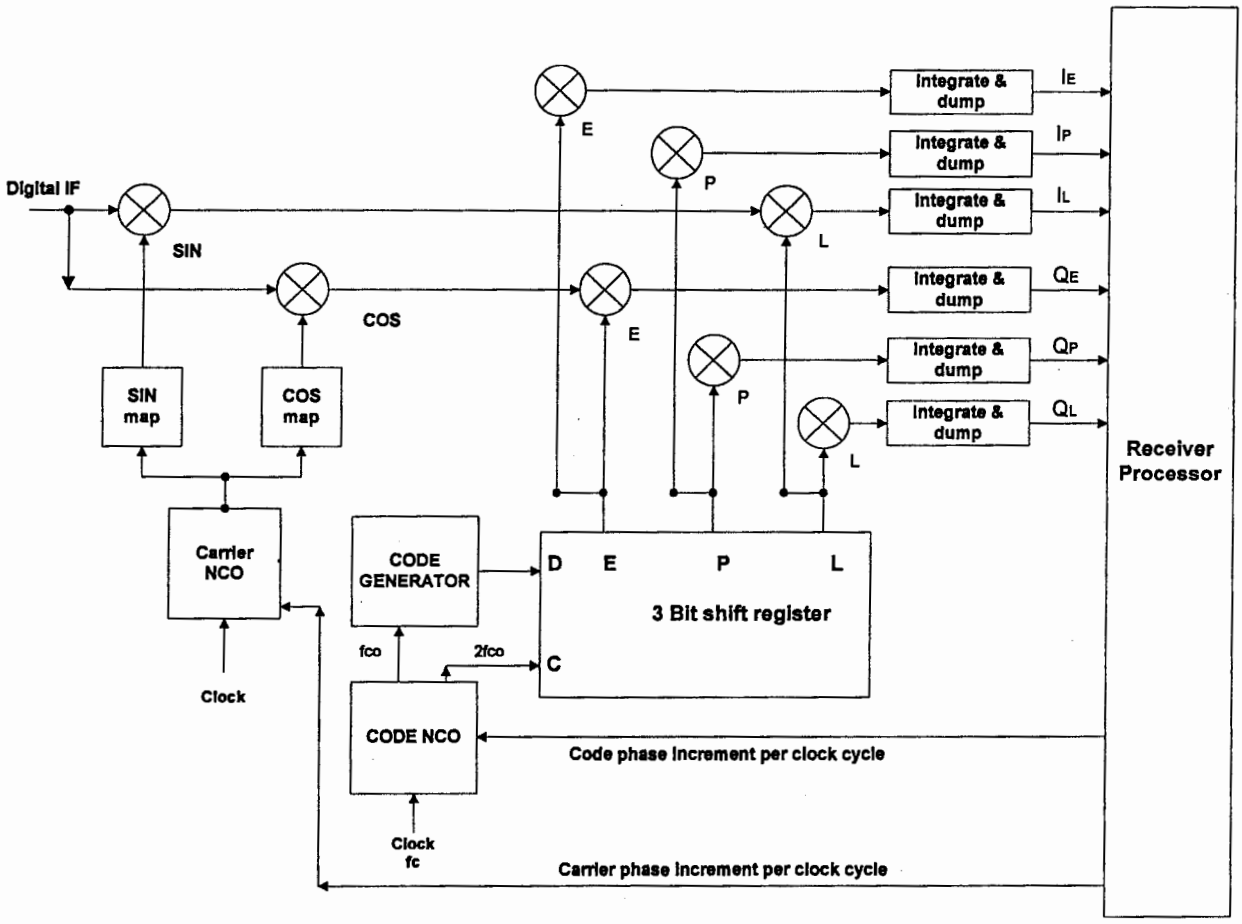

Figure 5.1: GPS receiver channel block diagram

5.2 Position Measurement

The GPS Receiver position measurement is a complex process which becomes even more complicated if different errors sources are included in the process as given below.

5.2.1 GPS Receiver Position Measurement

For measuring the correct position of a receiver, the receiver must not only receive signals from the four satellites in the view, but, it must also generate the four signals of same structure locally. By synchronizing the received and locally generated signals, the

time shift ' Δt_{s-i} ' of the four satellites can be measured as a time mark. The four time shifts ' Δt_{s-i} ' are then used to determine the exact signal travel time.

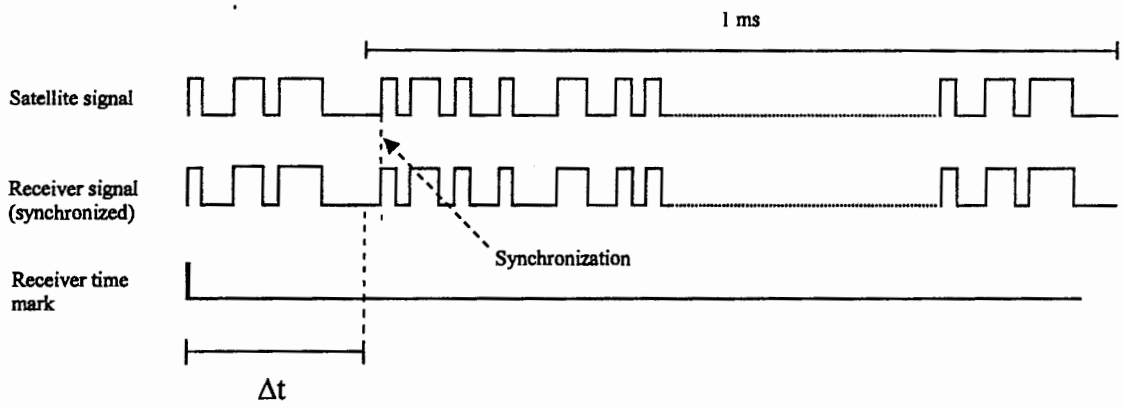

Figure 5.2: Measuring signal travel time

But, in reality the satellite and the receiver clock are not in synchronization with each other. As a result, due to this time difference of ' $\Delta t_{\circ}$ ' between the onboard time of satellite and receiver clock, a range error is occurred called pseudo range ' ρ_{pseu-i} 'given by [21][22]:

$$\rho_{pseu-i} = \Delta t_{measured} \bullet c = (\Delta t_{actual} + \Delta t_{\circ}) \bullet c \tag{5.10}$$

$$\rho_{pseu-i} = (\Delta t_{actual} \bullet c) + (\Delta t_{\circ} \bullet c) = \rho_{act-i} + \rho_{fal-i} \tag{5.11}$$

Where:

$$\Delta t_{\circ} = \Delta T_i + \Delta I_i + \Delta t_{s-i} + \Delta t_{rec}, \text{ with} \tag{5.12}$$

ΔT_i = Tropospheric Error

ΔI_i = Ionospheric Error

Δt_{rec} = Receiver clock error

Δt_{s-i} = Satellite clock correction term

$$= af_0 + af_1(t_c - t_{oc}) + af_2(t_c - t_{oc})^2 + \Delta t_{rel} - T_{gd} \qquad (5.13)$$

We know that in the Cartesian coordinate system, the actual distance ' ρ_{act-i} ' from the satellite and user is given by using the distance formula as:

$$\rho_{act-i} = \sqrt{(x_{sat-i} - x_{user}) + (y_{sat-i} - y_{user}) + (z_{sat-i} - z_{user})} \qquad (5.14)$$

Likewise pseudo range ' ρ_{pseu-i} 'given by:

$$\rho_{pseu-i} = \sqrt{(x_{sat-i} - x_{user}) + (y_{sat-i} - y_{user}) + (z_{sat-i} - z_{user})} + (\Delta t_{\circ} \bullet c) \qquad (5.15)$$

It is clear from the above equation that for finding the exact position of a GPS receiver, we will solve four unknowns $(x_{user}, y_{user}, z_{user}, \Delta t_{\circ})$. Therefore, we need four satellites to yield four equations.

The above equation 5.15 is non-linear. In order to make it linear, we use Taylor expansion given by:

$$f(\dot{x}) = f(x_{\circ}) + \frac{f'}{1!}(x_{\circ}).\Delta x + \frac{f''}{2!}(x_{\circ})^2.\Delta x + \frac{f'''}{3!}(x_{\circ})^3.\Delta x + \ldots$$

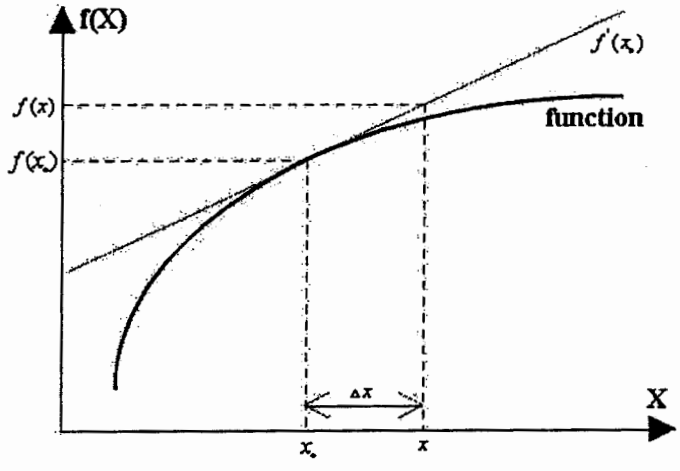

Figure 5.3: Taylor series conversion

Using the 1st order Taylor expansion, the above equation becomes

$$f(x) = f(x_\circ) + f'(x_\circ).\Delta x$$

Moreover, we will also make an initial guess of the receiver position [21]. The initial guess is at $(x_\circ, y_\circ, z_\circ)$, so,

$$\begin{aligned} x_{user} &= x_\circ + \Delta x \\ y_{user} &= y_\circ + \Delta y \\ z_{user} &= z_\circ + \Delta z \end{aligned} \tag{5.16}$$

In the above equations $\Delta x, \Delta y$ and Δz shows the difference between the initial guesses $(x_\circ, y_\circ, z_\circ)$ and the true position of the receiver $(x_{user}, y_{user}, z_{user})$ in the ECEF coordinate system. Thus we will calculate $(\Delta x, \Delta y, \Delta z)$ and update the initial guesses $(x_\circ, y_\circ, z_\circ)$ accordingly.

The actual distance '$\rho_{\circ-i}$' from the four satellites to the initial guessed position is given by [21]:

$$\rho_{\circ-i} = \sqrt{(x_{sat-i} - x_\circ) + (y_{sat-i} - y_\circ) + (z_{sat-i} - z_\circ)} \tag{5.17}$$

Applying the 1st order Taylor expansion on it, we get

$$\rho^{user}{}_{\circ-i} = \rho_{\circ-i} + \frac{\partial(\rho_{\circ-i})}{\partial x} \bullet \Delta x + \frac{\partial(\rho_{\circ-i})}{\partial y} \bullet \Delta y + \frac{\partial(\rho_{\circ-i})}{\partial z} \bullet \Delta z \tag{5.18}$$

The pseudo range from the four satellites to the initial guessed position is given by

$$\rho_{pseu-i} = \rho^{user}{}_{\circ-i} + c \bullet \Delta t_\circ \tag{5.19}$$

$$\rho_{pseu-i} = \rho_{\circ-i} + \frac{\partial(\rho_{\circ-i})}{\partial x} \bullet \Delta x + \frac{\partial(\rho_{\circ-i})}{\partial y} \bullet \Delta y + \frac{\partial(\rho_{\circ-i})}{\partial z} \bullet \Delta z + c \bullet \Delta t_\circ \tag{5.20}$$

After partial differentiation, we get

$$\rho_{pseu-i} = \rho_{o-i} + \frac{(x_o - x_{sat-i})}{\rho_{o-i}} \bullet \Delta x + \frac{(y_o - y_{sat-i})}{\rho_{o-i}} \bullet \Delta y + \frac{(z_o - z_{sat-i})}{\rho_{o-i}} \bullet \Delta z + c \bullet \Delta t_o \tag{5.21}$$

By transposing the above equation having $i = 1, 2, 3, 4$, we get

$$\begin{pmatrix} \rho_{pseu-1} - \rho_{o-1} \\ \rho_{pseu-2} - \rho_{o-2} \\ \rho_{pseu-3} - \rho_{o-3} \\ \rho_{pseu-4} - \rho_{o-4} \end{pmatrix} = \begin{pmatrix} \frac{(x_o - x_{sat-1})}{\rho_{o-1}} & \frac{(y_o - y_{sat-1})}{\rho_{o-1}} & \frac{(z_o - z_{sat-1})}{\rho_{o-1}} & c \\ \frac{(x_o - x_{sat-2})}{\rho_{o-2}} & \frac{(y_o - y_{sat-2})}{\rho_{o-2}} & \frac{(z_o - z_{sat-2})}{\rho_{o-2}} & c \\ \frac{(x_o - x_{sat-3})}{\rho_{o-3}} & \frac{(y_o - y_{sat-3})}{\rho_{o-3}} & \frac{(z_o - z_{sat-3})}{\rho_{o-3}} & c \\ \frac{(x_o - x_{sat-4})}{\rho_{o-4}} & \frac{(y_o - y_{sat-4})}{\rho_{o-4}} & \frac{(z_o - z_{sat-4})}{\rho_{o-4}} & c \end{pmatrix} \bullet \begin{pmatrix} \Delta x \\ \Delta y \\ \Delta z \\ \Delta t_o \end{pmatrix} \tag{5.22}$$

$$\begin{pmatrix} \Delta x \\ \Delta y \\ \Delta z \\ \Delta t_o \end{pmatrix} = \begin{pmatrix} \frac{(x_o - x_{sat-1})}{\rho_{o-1}} & \frac{(y_o - y_{sat-1})}{\rho_{o-1}} & \frac{(z_o - z_{sat-1})}{\rho_{o-1}} & c \\ \frac{(x_o - x_{sat-2})}{\rho_{o-2}} & \frac{(y_o - y_{sat-2})}{\rho_{o-2}} & \frac{(z_o - z_{sat-2})}{\rho_{o-2}} & c \\ \frac{(x_o - x_{sat-3})}{\rho_{o-3}} & \frac{(y_o - y_{sat-3})}{\rho_{o-3}} & \frac{(z_o - z_{sat-3})}{\rho_{o-3}} & c \\ \frac{(x_o - x_{sat-4})}{\rho_{o-4}} & \frac{(y_o - y_{sat-4})}{\rho_{o-4}} & \frac{(z_o - z_{sat-4})}{\rho_{o-4}} & c \end{pmatrix}^{-1} \bullet \begin{pmatrix} \rho_{pseu-1} - \rho_{o-1} \\ \rho_{pseu-2} - \rho_{o-2} \\ \rho_{pseu-3} - \rho_{o-3} \\ \rho_{pseu-4} - \rho_{o-4} \end{pmatrix} \tag{5.23-a}$$

$$x = A^{-1} r \tag{5.23-b}$$

If the satellites are more than 4, then, the system will be over determined. Then

$$\begin{pmatrix} \Delta x \\ \Delta y \\ \Delta z \\ \Delta t_o \end{pmatrix} = \begin{pmatrix} \frac{(x_o - x_{sat-1})}{\rho_{o-1}} & \frac{(y_o - y_{sat-1})}{\rho_{o-1}} & \frac{(z_o - z_{sat-1})}{\rho_{o-1}} & c \\ \frac{(x_o - x_{sat-2})}{\rho_{o-2}} & \frac{(y_o - y_{sat-2})}{\rho_{o-2}} & \frac{(z_o - z_{sat-2})}{\rho_{o-2}} & c \\ \cdot & \cdot & \cdot & \cdot \\ \cdot & \cdot & \cdot & \cdot \\ \cdot & \cdot & \cdot & \cdot \\ \frac{(x_o - x_{sat-n})}{\rho_{o-n}} & \frac{(y_o - y_{sat-n})}{\rho_{o-n}} & \frac{(z_o - z_{sat-n})}{\rho_{o-n}} & c \end{pmatrix}^{-1} \bullet \begin{pmatrix} \rho_{pseu-1} - \rho_{o-1} \\ \rho_{pseu-2} - \rho_{o-2} \\ \cdot \\ \cdot \\ \cdot \\ \rho_{pseu-n} - \rho_{o-n} \end{pmatrix} \tag{5.24}$$

Equivalently for equation 5.23-b, we have

$$(A^{+} \bullet A) \bullet x = A^{+} \bullet r, \qquad \text{with: } A^{+} = \text{Pseudoinverse of A}$$
$$= Q \bullet A^{T} \qquad (5.25\text{-a})$$
$$I = (A^{+} \bullet A)$$

The equation 5.25-a can be written as

$$x = Q \bullet A^{T} \bullet r \qquad (5.25\text{-b})$$

The above solution will be an iterative process in which the most recent solution will become the initial guess fro the next iteration. This process is continued until the desired accuracy (e.g. error component less than 1cm) is obtained.

From the pseudo ranges and the calculated position of the satellites, the receiver determines its own position on earth by finding out Latitude (φ), Longitude (λ), height (h) by the formulas given in the Table 2.2.

5.2.2 GPS Errors Measurement

Although, the GPS signals are affected by the several types of errors, three types of errors are discussed in detail here:

5.2.2.1 Ionospheric Klobuchar Error Model

When the GPS signals are passed through the ionosphere then they are delayed due to the presence of free ions there. These ionospheric effects can be computed and corrected on the basis of parameters of a predicted ionospheric correction model (Klobuchar model) which are broadcasted through the GPS message [22].

The Klobuchar model requires the approximate receiver's geodetic latitude (φ_r), geodetic longitude (λ_r), GPS observation time (T_{GPS}), satellite's elevation angle (E_s) and satellite's azimuth (A_s) [see also Appendix D]. Then we calculate:

- Earth-centered angle (ψ_e) as

$$\psi_e = \frac{0.0137}{(E_s + 0.11)} - 0.022 \qquad (semicircles) \qquad (5.26)$$

- Sub-ionospheric latitude (φ_I) as

$$\varphi_I = \varphi_r + \psi_e \bullet \cos(A_s) \qquad (semicircles) \qquad (5.27)$$

Where:

$$\begin{cases} \varphi_I = +0.416, & if: \varphi_I > 0.416 \\ \varphi_I = -0.416, & if: \varphi_I \le 0.416 \end{cases}$$

- Sun-ionospheric longitude (λ_I) as

$$\lambda_I = \lambda_r + \left(\psi_e \bullet \frac{\sin(A_s)}{\cos(\varphi_I)} \right) \qquad (semicircles) \qquad (5.28)$$

- Geo-magnetic latitude (φ_m) of the sub-ionospheric location while seeing GPS satellite as:

$$\varphi_m = \varphi_I + 0.064 \bullet \cos(\lambda_I - 1.617) \qquad (semicircles) \qquad (5.29)$$

- Local time (t_{local}) at the sub-ionospheric point as

$$t_{local} = 4.32 \bullet 10^4 \lambda_I + T_{GPS} \qquad (seconds) \qquad (5.30)$$

Where:

$$\begin{cases} t_{local} = t_{local} - 86400, & if: t_{local} \ge 86400 \\ t_{local} = t_{local} + 86400, & if: t_{local} < 86400 \end{cases}$$

- Slant time factor (F) for converting slant time delay as

$$F = 1 + 16(0.53 - E_s)^3 \tag{5.31}$$

- Period (P) as

$$P = \begin{pmatrix} \sum_{i=1}^{3} \beta_i \varphi_m^i, & if: P \geq 72,000 \\ 72,000, & if: P < 72,000 \end{pmatrix} \quad (\text{sec}\, onds) \tag{5.32}$$

- Phase (x) as

$$x = \frac{2\pi(t_{local} - 50400)}{P} \quad (radians) \tag{5.33}$$

- Amplitude (Q) as

$$Q = \begin{pmatrix} \sum_{i=1}^{3} \alpha_i \varphi_m^i, & if: Q \geq 0 \\ 0, & if: Q < 0 \end{pmatrix} \quad (\text{sec}\, onds) \tag{5.34}$$

- Ionospheric time delay (ΔI) as

$$\Delta I = \begin{bmatrix} F \bullet (5 \bullet 10^{-9}), & if: |x| \geq 1.57 \\ F \bullet \left\{ (5 \bullet 10^{-9}) + Q \bullet \left(1 - \frac{x^2}{2} + \frac{x^4}{24} \right) \right\}, & if: |x| < 1.57 \end{bmatrix} (\text{sec}\, onds) \tag{5.35}$$

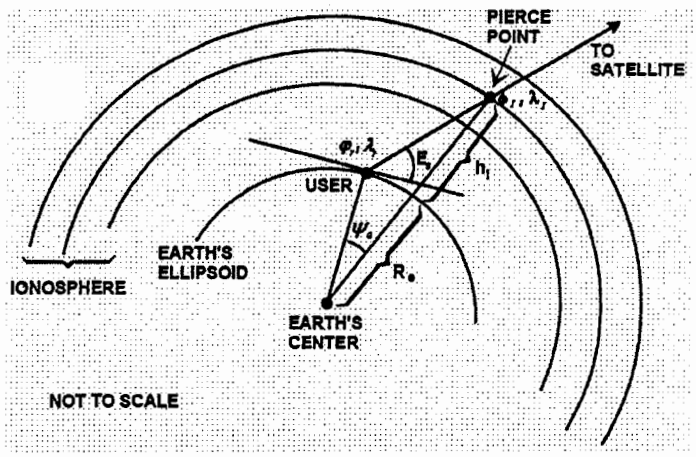

Figure 5.4: Ionospheric Model

5.2.2.2 Tropospheric Hopfield Error Model

The lowest portion of the earth's atmosphere is called troposphere where the weather phenomenon takes place. This layer contains about 99% of the water vapors and contributes 75% of the atmospheric mass. Hopfield measured the tropospheric delay on the basis of "Dry" and "Wet" atmosphere as [22]:

- Dry tropospheric delay (T_d) is

$$T_d = \left(\frac{1.55208 \bullet 10^{-4} \bullet P_{amb} \bullet (40136 + 148.72 \bullet T_{amb})}{T_{amb} + 273.16} \right) (\text{sec}\, onds) \qquad (5.36)$$

Where:

T_{amb} = Ambient Temperature

P_{amb} = Ambient air Pressure

P_{vap} = Air vapor pressure

- Wet tropospheric delay (T_w) is

$$T_w = \left(-\frac{(0.282 \bullet P_{vap})}{(T_{amb} + 273.16)} + \frac{(8307.2 \bullet P_{vap})}{(T_{amb} + 273.16)^2} \right) \quad (\text{sec}\, onds) \qquad (5.37)$$

- The tropospheric delay (ΔT) is

$$\Delta T = \left(\frac{T_d}{\sin(\sqrt{E_s^2 + 1.9403 \bullet 10^{-3}})} + \frac{T_w}{\sin(\sqrt{E_s^2 + 0.6854 \bullet 10^{-3}})} \right) (meter) \qquad (5.38)$$

5.2.2.3 Satellite Clock Error

The satellite clock error is given by [23]:

$$\Delta t_{s-i} = af_0 + af_1(t_c - t_{oc}) + af_2(t_c - t_{oc})^2 + \Delta t_{rel} - T_{gd} \qquad (5.39)$$

Where, 'af_0, af_1' and 'af_2' are the correction coefficients known as phase error, frequency error and rate of change of frequency error (in ephemeris data), 'T_{gd}' is the effect of satellite group delay (in ephemeris data), 't_{oc}' is the reference time for the clock correction (in ephemeris data) and 'Δt_{rel}' is the relativistic correction term which corrects the slower motion of the clock at the perigee and the faster motion of the clock at the apogee [23] given by:

$$\Delta t_{rel} = F \bullet e_s \bullet \sqrt{a_s} \bullet \sin(E_k) \tag{5.40}$$

Where:

$F = -4.442807633 \bullet 10^{-10}\ \text{sec}/(meter)^{1/2}$

E_k = Eccentric anomaly of the satellite orbit

a_s = Semi major axis of the satellite orbit

5.2.3 Receiver Position Measurement Algorithm

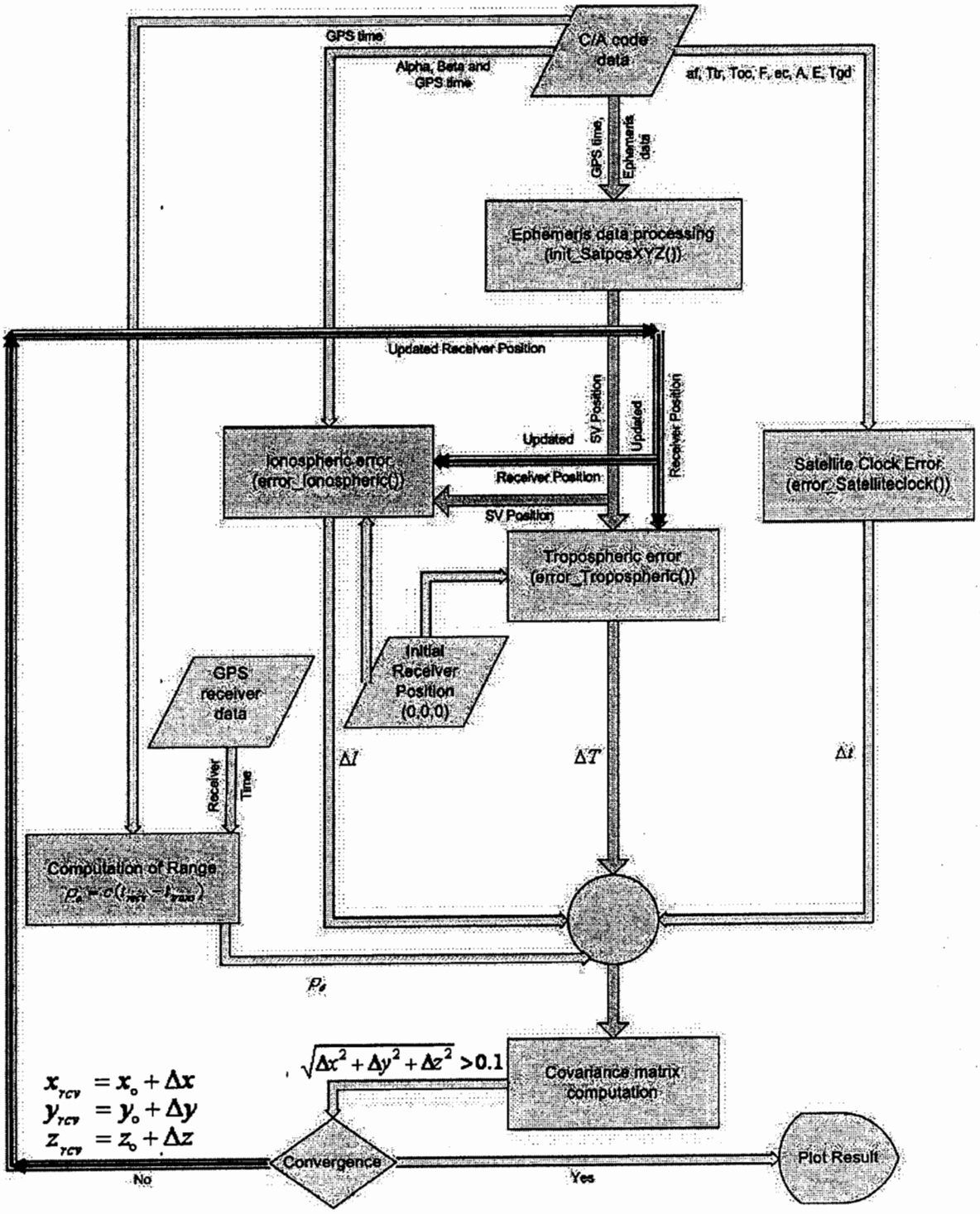

Figure 5.5: Receiver position measurement block diagram

As depicted in the figure 5.5, the program starts by setting the initial position of the receiver at (0, 0, 0). The positional error in the receiver position (i.e. measure of deviation from the true position of receiver when the receiver position is initialized as (0, 0, 0)) is then minimized iteratively using the covariance matrix solution. The ionospheric, tropospheric and satellite clocks errors are also considered during the calculations for getting the more accurate results. When the normalized error becomes less than 0.1, then, the loop breaks and the final position of receiver (4022500,322200,5026000) is obtained.

5.3 Target Imaging System (TIS)

The TIS that will materialize the simulation will have all the features of conventional GPS receivers used for the navigation process and some additional features essential for the target imaging.

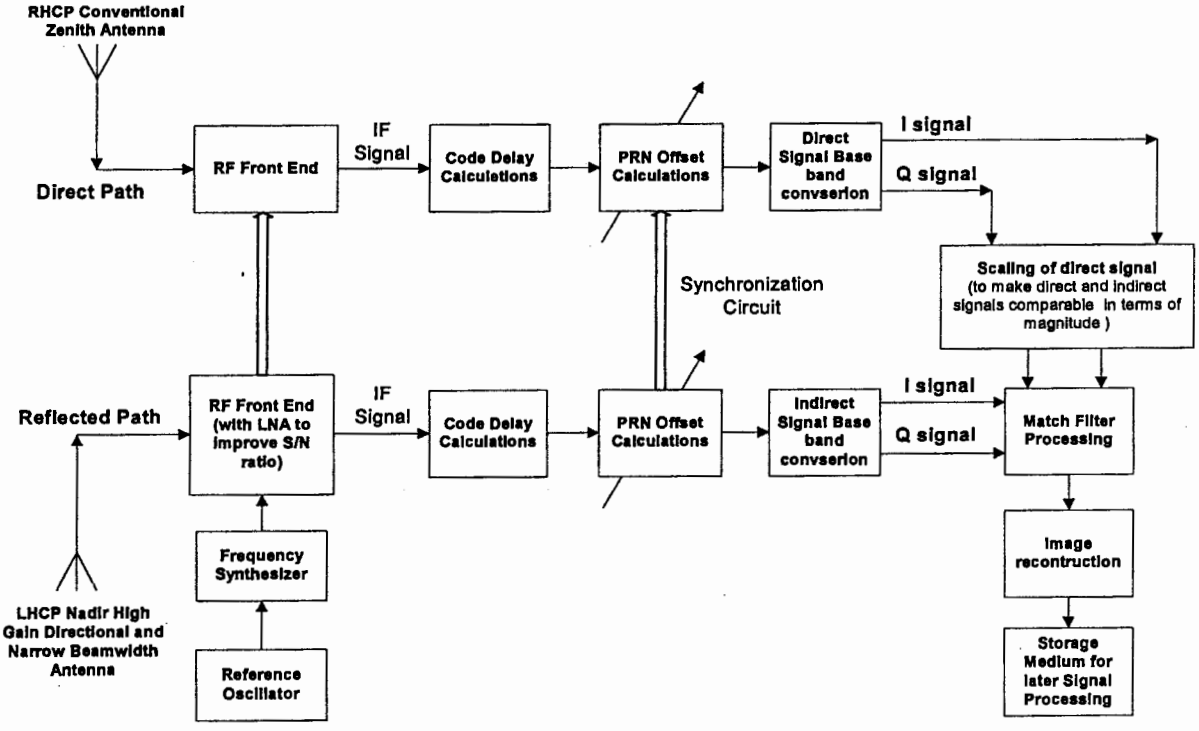

Figure 5.6: Target Imaging System (TIS) block diagram

The direct signals obtained through the Right Handed Circularly Polarized antenna (RHCP) are converted to I and Q components as follows:

$$I_{direct} = d(t) \bullet \sin \omega_{\circ} t \tag{5.41}$$

$$Q_{direct} = d(t) \bullet \cos \omega_{\circ} t \tag{5.42}$$

Where

$d(t)$ = Data signal

$\omega_{\circ}$ = Carrier frequency (radians / sec) having Doppler frequency shift

The direct signals are then scaled down in order to make them comparable to the indirect signals in amplitude. This process is done so that the indirect signal must not lose in the tails of the auto-correlation function of the direct signals. Hence, it is necessary to have some suitable method of attenuation of the direct signals or some cancellation technique for the main beam is required. Moreover, the PRN offset calculations circuit must be designed effectively so that the direct and the indirect signals must be synchronized to each other to perform the necessary measurements.

The indirect signals obtained through the Left Handed Circularly Polarized antenna (LHCP) are very weak and buried in noise. Hence, a highly efficient low noise preamplifier is essential to amplify these signals with an assurance that SNR ratio will be acceptable enough to make the necessary calculations. The indirect signals are then converted into I and Q components and then compared to the direct signals through the matched filter processing technique for getting the image of the target. The data must be stored in the memory of TIS for performing the later signal processing and analysis.

As, the direct and the indirect signals follow the different paths, so, there is a difference of phase between them which can be calculated as

$$\Phi = (\omega \bullet \text{path difference})/c \qquad \text{(radians)} \qquad (5.43)$$

The 'I' and 'Q' components of the reflected signals are given by

$$I_{reflected} = \alpha d(t) \bullet \sin(\omega_{\circ} t + \Phi) \qquad (5.44)$$

$$Q_{reflected} = \alpha d(t) \bullet \cos(\omega_{\circ} t + \Phi) \qquad (5.45)$$

Where

$d(t)$ = Data signal

$\omega_{\circ}$ = Carrier frequency (radians / sec) having Doppler frequency shift

α = Attenuation factor

In order to simulate a practical system, noise is simulated and added to the direct and reflected signals. The MATLAB function RANDN(1) is used to generate pseudo-random numbers chosen from a normal distribution with mean zero, variance one and standard deviation one. It is multiplied to factor of 20, which is equal to about 16 dB of noise altogether.

In order to simplify the simulation, we assume that the receiver has some method of locking on to the correct phase of the indirect signal and therefore 'Φ' is assumed to be zero.

5.3.1 Display of Image

The search area for imaging the targets is traversed using the two arrays of size 101. Each individual element/pixel of the region of interest has size of 20 meters. As the size of the target is $20m$ therefore, each target is represented by the pixel size of $20m \times 20m$ and overall area of the region of interest is $2000m$ x $2000m$. The candidate position can

be any where in the matrix above. The position (4024000, 324000, 5021000) is fixed to be in the middle of the search area as shown in the figure 5.7.

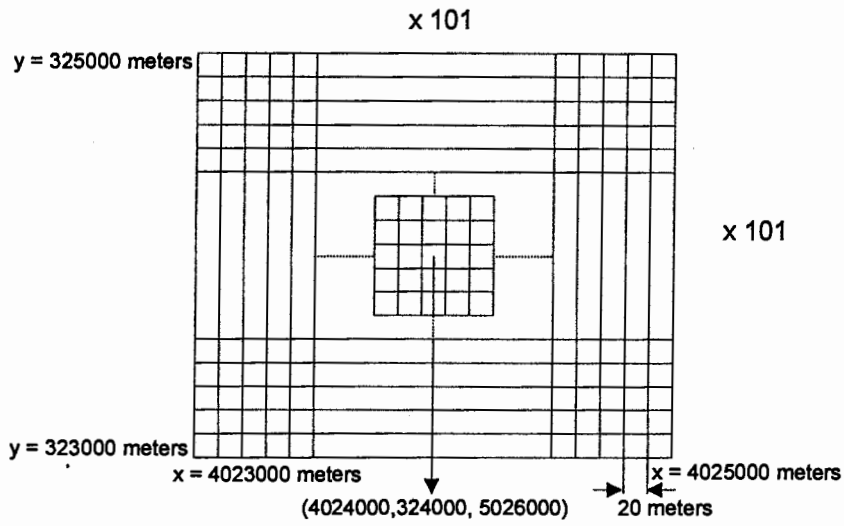

Figure 5.7: Candidate position for the target

5.3.2 Image Reconstruction using Matched Filter Processing

Although, the auto-correlation function of the linear FM signals demonstrates a narrow pulse property, but, when the output pulse is passed through the match filter, then, it becomes even narrower. Hence, the overall system resolution is increased. In the MATLAB environment this is performed by multiplying two codes bit by bit and then adding them up. This process is carried out for each sample or epoch and the relevant value is stored in the 101 x 101 matrix as shown in the figure 5.7 above. The two signals used in matched filter processing in our simulation are the input signal that consists of the direct and reflected signals coming from all satellites in view and the test signal that is received only from the reference satellite.

But first of all we have to calculate the delay and offset PRN (delayed PRN) for the test signal. These parameters are determined by calculating the distance between

reference satellite to candidate position and receiver to candidate position. The delay is calculated in a manner similar as in section 4.5.3. Here, we obtain only one PRN sequence for the Reference SV and the delays are calculated not for a particular target position, but for all candidate positions in the area of interest, so the distance calculations are performed not for a fixed target position but for the expected target positions. Finally the test signal is collapsed to base band by multiplying the instantaneous value of the sequence by the sine of L1 frequency in radians to the negative of delay calculated above.

Both signals are multiplied and added at each epoch or sample and a different value of correlation is obtained for each instant in time. The value is stored in the 101 x 101 matrix by suitable MATLAB commands. The matrix is scanned for each sample in time, rendering the procedure equivalent to a matched filter process. In fact it multiplies the signal and delayed versions of the signal and adds them for all epochs, this is similar to integrating over the sampling period. The location of target will have maximum value or correlation. The values for the base-band in-phase (I) and quadrature phase (Q) components are converted to equivalent magnitude by the following simple equation.

$$\text{Equivalent Magnitude} = \sqrt{I^2 + Q^2} \tag{5.46}$$

Using the above mentioned information, we construct the grey scale image which is consisted of mixtures of black, white and shades of grey colors. When there is a maximum correlation then data is displayed as black in the pixel or square and in case of minimum correlation, the pixel or square is displayed as white and we conclude that there is no target. Thus the image produced directly pin points the target at the desired coordinate in the candidate position. The MATLAB function IMAGE is used in order to culminate the task of image generation.

5.3.3 TIS Block Diagram

The simplified and detailed block diagrams of TIS are given below.

5.3.3.1 Simplified block Diagram of TIS

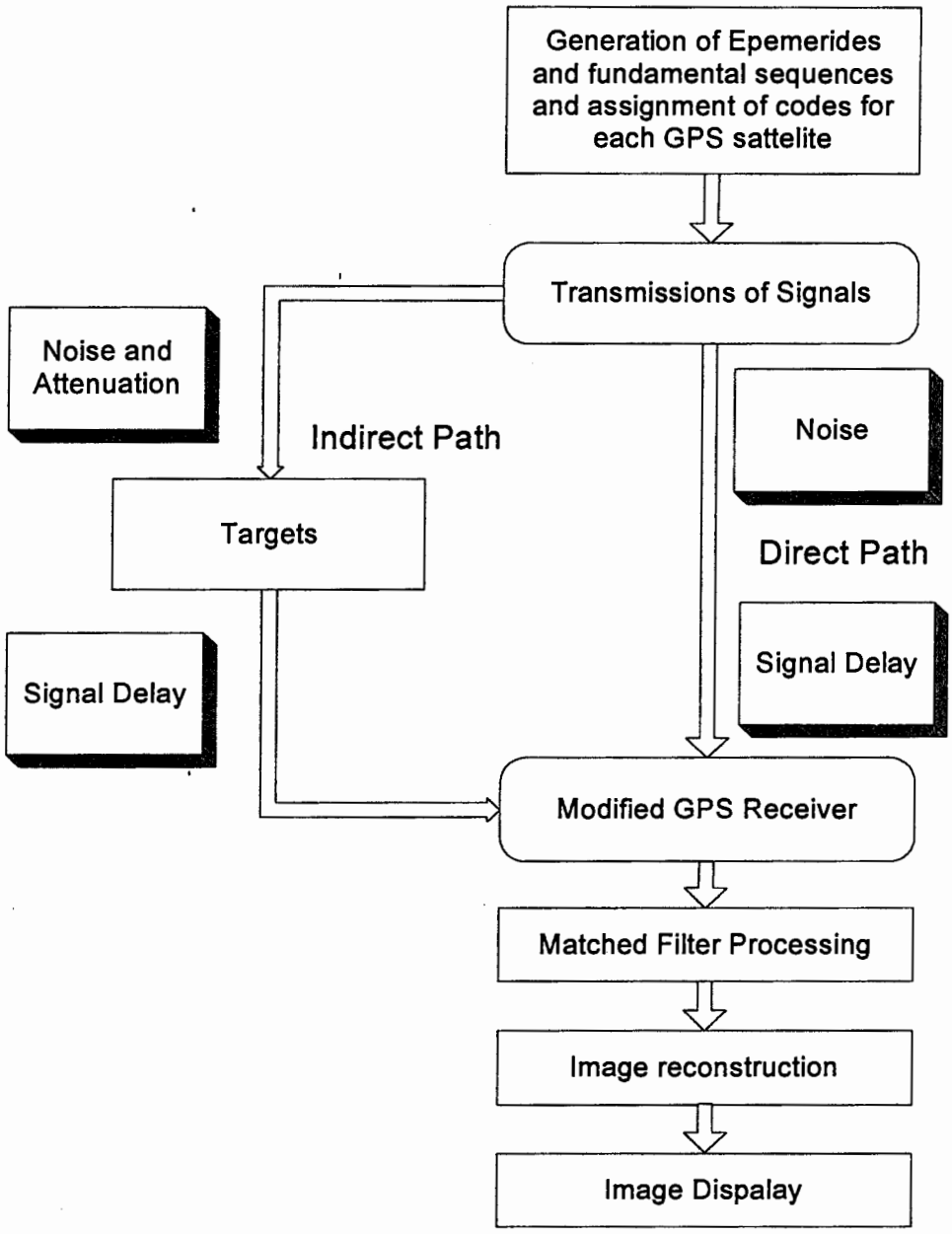

Figure 5.8: TIS (Simplified block diagram)

5.3.3.2 Detailed Block Diagram of TIS

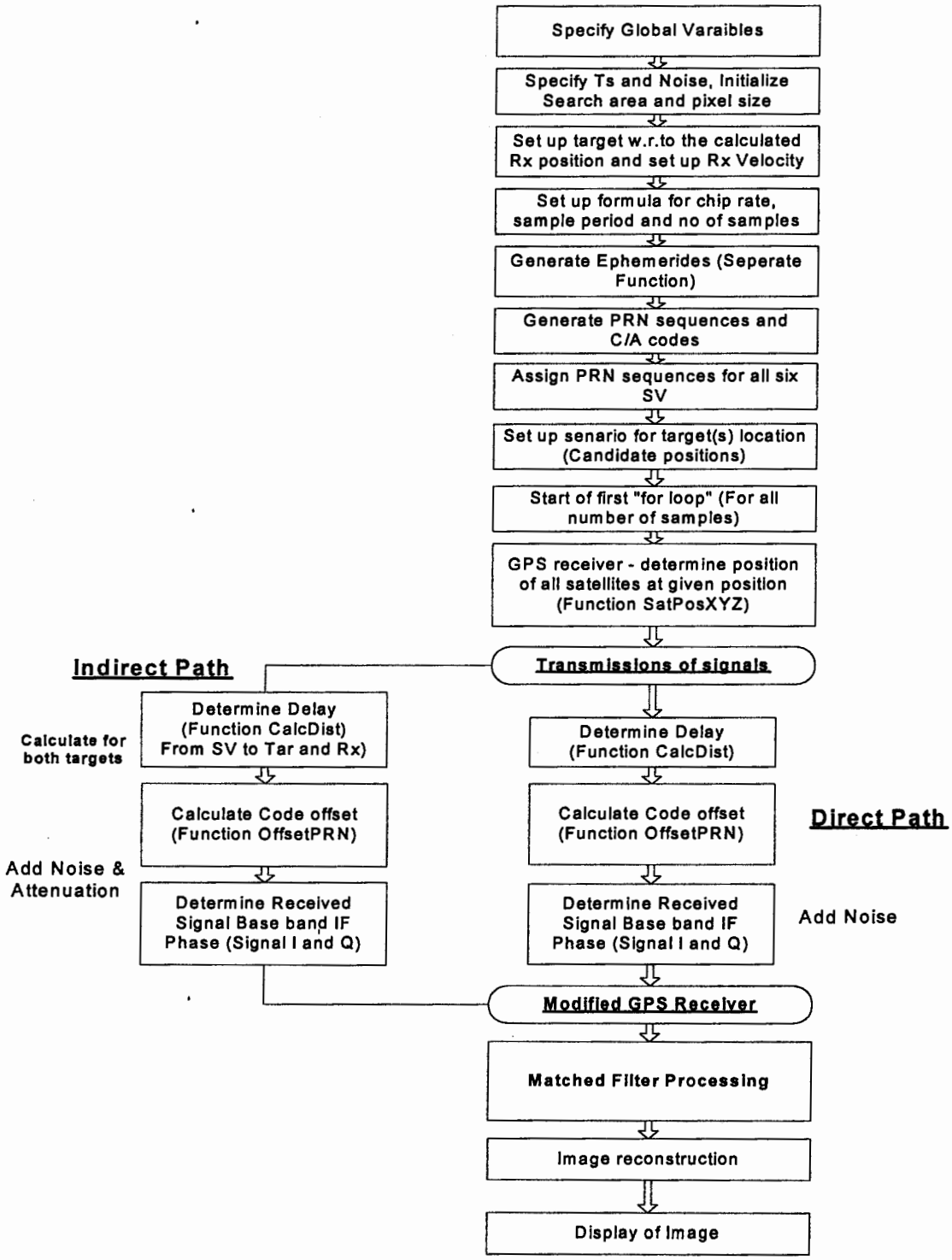

Figure 5.9: TIS (Detailed block diagram)

As depicted in the figure 5.8 & 5.9, the program starts with specifying the global variables, sampling time, noise, search area and pixel size. The region of interest for locating the targets has an area of 2000m x 2000m with the pixel size of 20m x 20m. A three dimensional array is used to traverse the area of interest; one each for the x, y and z axes. The position (4024000, 324000, 5021000) lies in the middle of search area. Two targets are fixed at the position of (4023800, 324000, 5026000) and (4024200, 324000, 5026000) respectively in the ECEF coordinate system. The receiver position is calculated to be (4022500, 322200, 5026000) on the basis of ephemeris data and the receiver is moved with a velocity of (300, 0, 0) m/s or speed of 1080 km/hour and images the targets using the SAR concept, where

Receiver Synthetic Aperture (RSA) = (Satellite Speed) x (Integration Time)

Total number of satellites used for the purpose are six having SV No 1, 7, 9, 14, 16, 22. The SV No 14 has been considered as the reference SV. The PRN sequences are generated for the six satellites on the basis of the ephemeris data of satellites. When the receiver moves with a velocity of (300, 0, 0) m/s, then, it calculates the delay of the direct and indirect signals for each sample, taken at a new location, every time. The direct and indirect signals are then processed through the matched filter processing technique. Finally, the images of the targets are reconstructed according to the region of interest and displayed.

CHAPTER 6

SIMULATION AND RESULTS

6.1 Overview of Simulation

This chapter presents the results of the work presented in the previous chapters. It describes the block diagram and the detailed code flow chart of the simulation. The simulation is done in the Matlab version 8.0. Moreover, the simulation is divided into two phases. In the first phase, the position of the receiver is calculated on the bases of the ephemeris data which is calculated to be (4022500, 322200, 5021000). In the next phase, the static targets are added on the positions (4023800, 324000, 5026000) and (4024200, 324000, 5026000) and the receiver is moved with a velocity of 300 m/sec for imaging the targets position using the principle of SAR.

6.2 Receiver Position Measurement

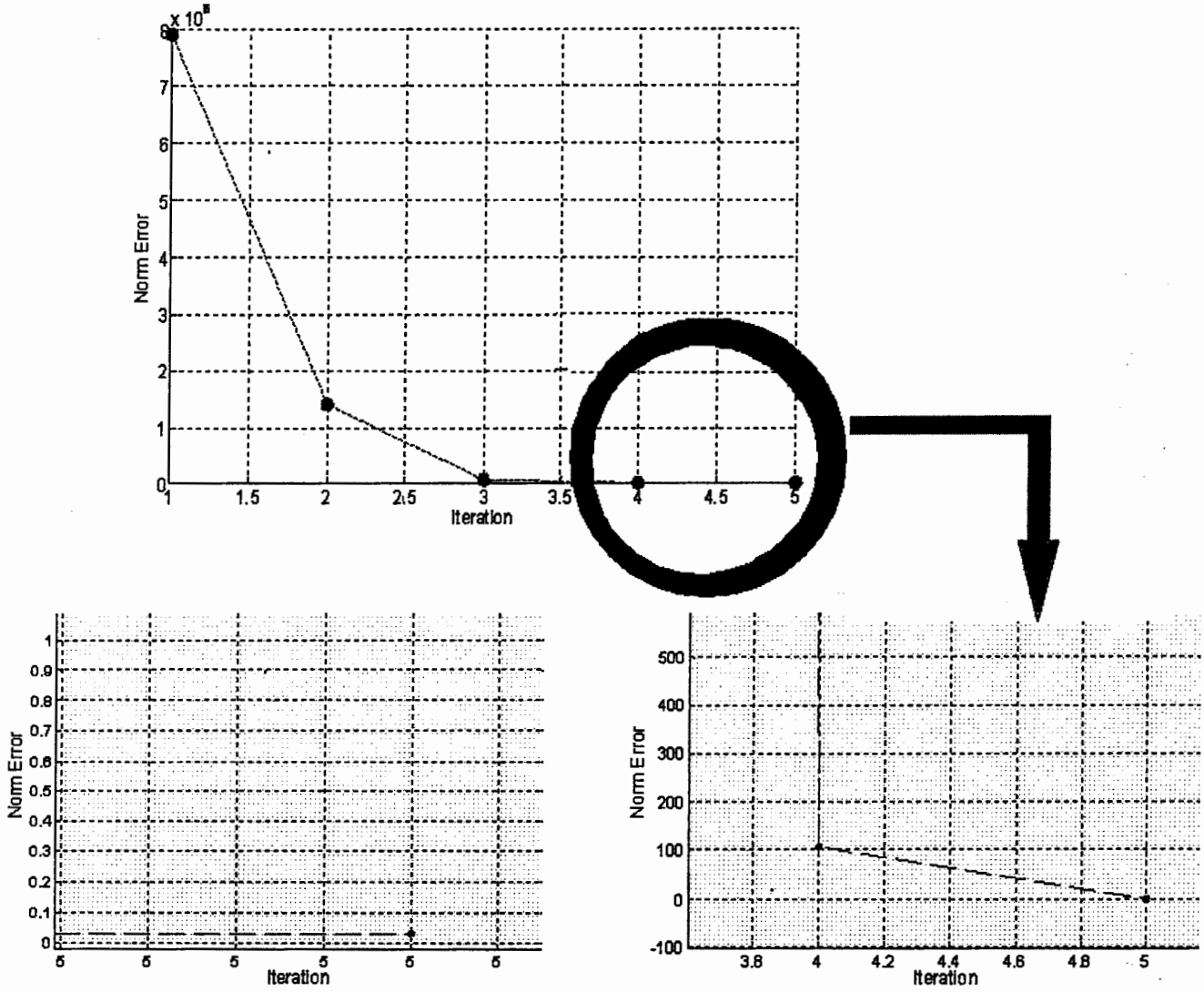

Figure 6.1: (a) GPS receiver norm/positional error solution (in meters)

(b) Zoomed value of norm error (in meters) from iteration 4 to 5 (rightmost figure)

(c) Norm error ($\sqrt{\Delta x^2 + \Delta y^2 + \Delta z^2}$) final value less than 0.1 (leftmost figure)

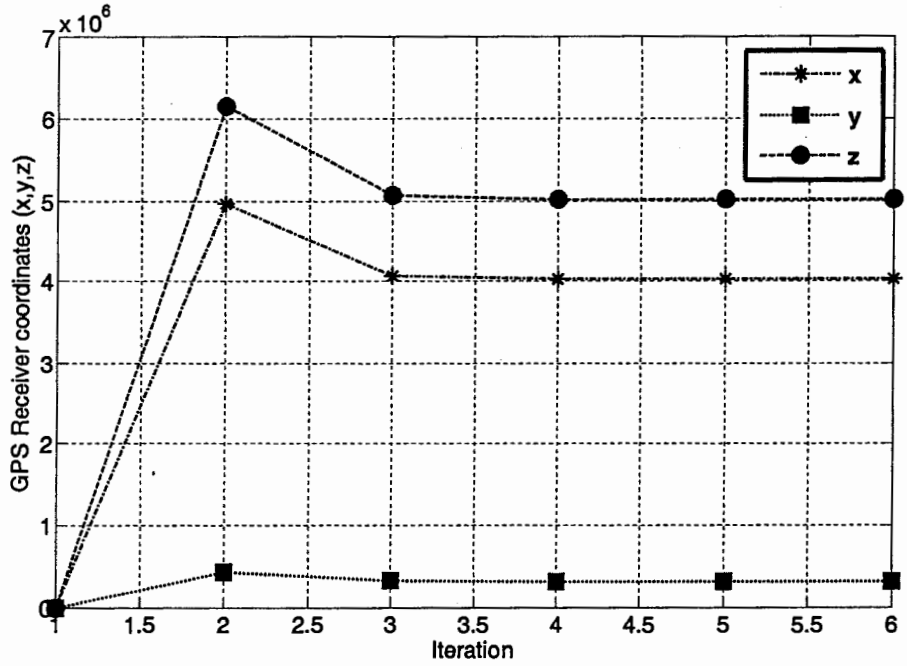

Figure 6.2: GPS receiver position measurement

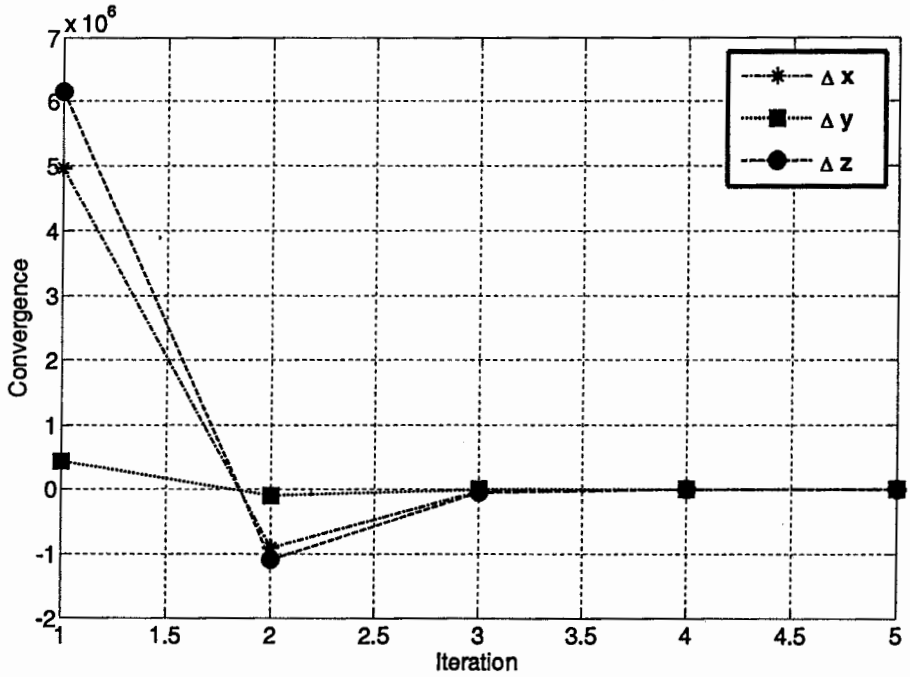

Figure 6.3: GPS receiver covariance solution

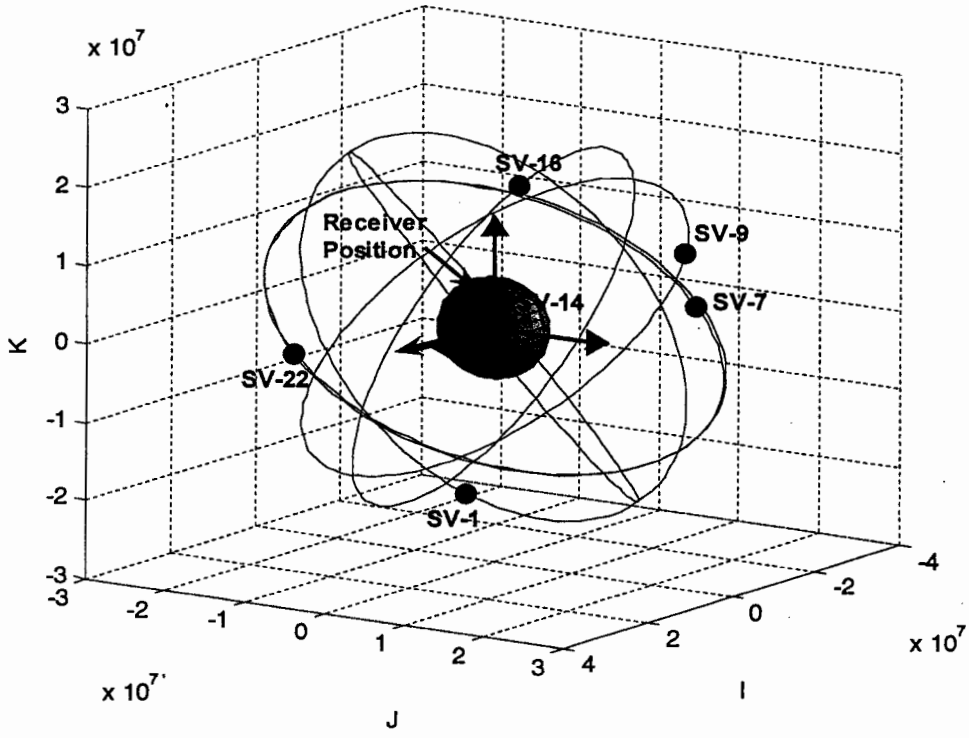

Figure 6.4: GPS receiver final position

6.3 Target Imaging

For imaging the targets, various simplifications and assumptions are performed to facilitate the simulation process. The target is assumed to be a fixed point scatterer which reflects all the signals towards the receiver and so has a reflection coefficient of one. It is also assumed that the receiver has some means to lock to the correct phase of the carrier signal. A convenient value of attenuation is assumed on the consideration that the signal strength will be improved during the correlation process.

The MATLAB simulation was performed under different circumstances and scenarios by varying the parameters. The cases with results are given below.

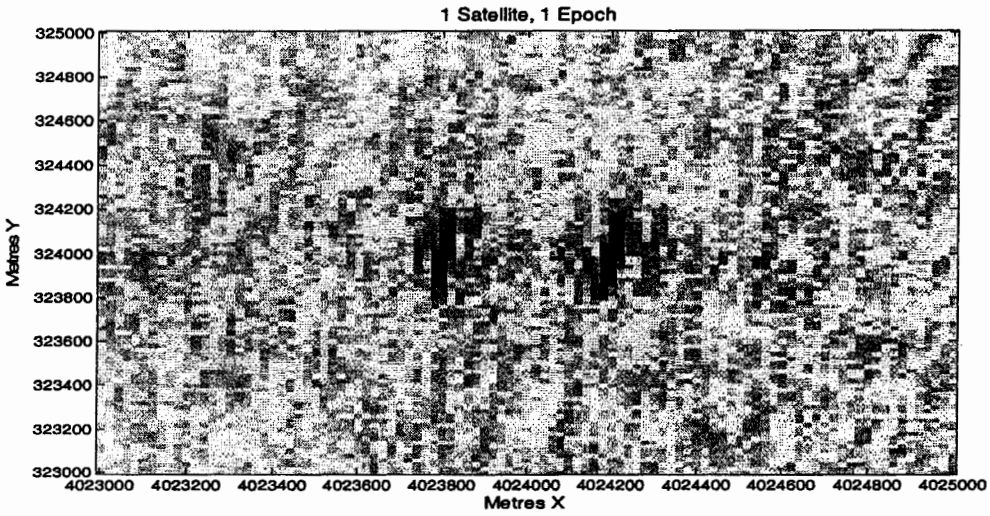

Figure 6.6: Integration time 0.1 seconds with 16 db noise

When the integration time is reduced further to 0.01 seconds (RSA = (300) **X** (0.01) = 3m), then, the simulation takes much less time, but, the cost is very low resolution due to decrease of Radar Synthetic Aperture (RSA) from 30m (for integration time 0.1) to 3m (for integration time 0.01). Moreover, with the introduction of noise, the targets are no longer resolved in the later case (integration time 0.01 seconds). Therefore, for getting the acceptable results, it is essential to perform the simulation over an integration time of at least 0.1 seconds or above, when the over sampling value is 5.

Case No 2: Integration Time 0.2 Seconds

The simulation is carried out by setting the integration time of 0.2 seconds (RSA = (300) **X** (0.2) = 60m) and other parameters as shown in the table 6.2. Although, the processing time is increased but the targets are recognizable with the better spatial resolution than case 1 because Radar Synthetic Aperture (RSA) has been doubled as shown in the figure 6.7 and 6.8.

Table 6.2: Set of parameters for case no. 2

Sr. No	Description	Values
1.	Integration time (Ts)	0.2 seconds
2.	Attenuation Factor	0.5
3.	Noise (in db)	0 (figure 6.7) and 16 (figure 6.8)
4.	Over –sampling rate	5
5.	No of samples	1.0230×10^6
6.	SV Involved	1, 7, 9, 14, 16, 22
7.	Reference SV	14

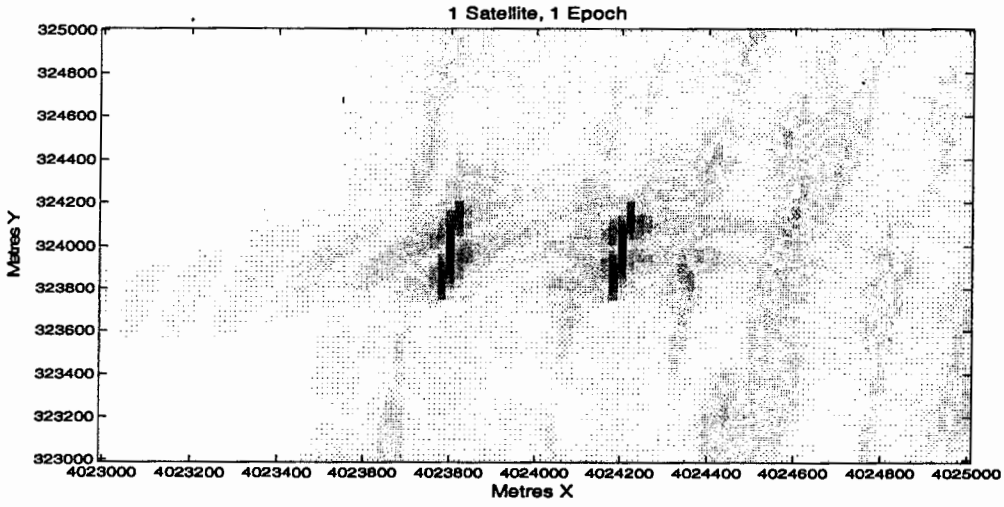

Figure 6.7: Integration time 0.2 seconds with no noise

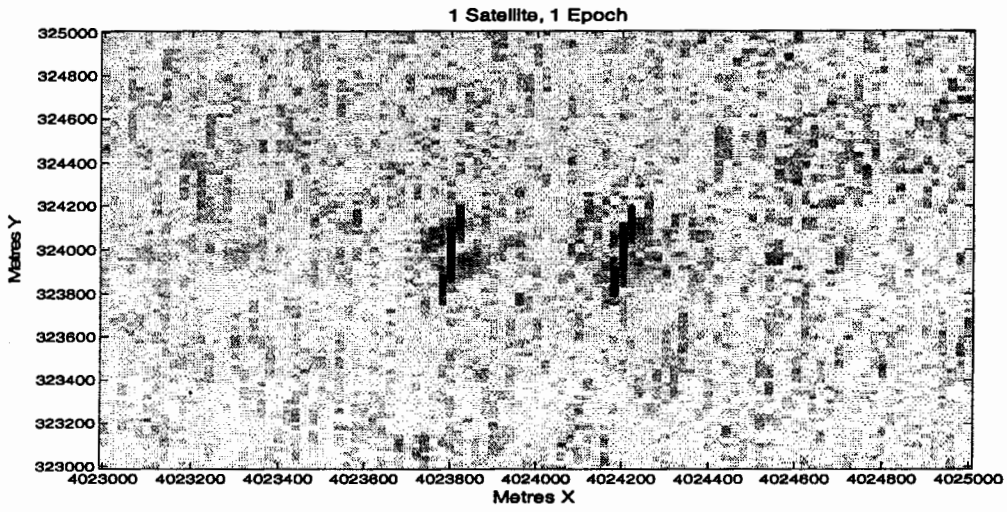

Figure 6.8: Integration time 0.2 seconds with 16 db noise

Moreover, it is also concluded that the longer the integration time, the more will be the number of samples and the less will be the susceptibility to noise. It is because increase in the no of samples averages out the noise which results in the creation of images of better quality.

Case No 3: Integration Time 0.1 Seconds with Movable Targets

In this simulation, the integration time of 0.1 seconds is used and the targets are moved with a speed of 10 m/s (36 km/hours), 20 m/s (72 km/hours) and 50 m/s (180 km/hours) and 100 m/s (360 km/hours) away from each other as shown in the figure 6.9, 6.10, 6.11 and 6.12 respectively.

It is observed that when the targets are moved with the velocity of 10 m/s (figure 6.9) and 20 m/s (figure 6.10) then, the results are almost like the case 1.

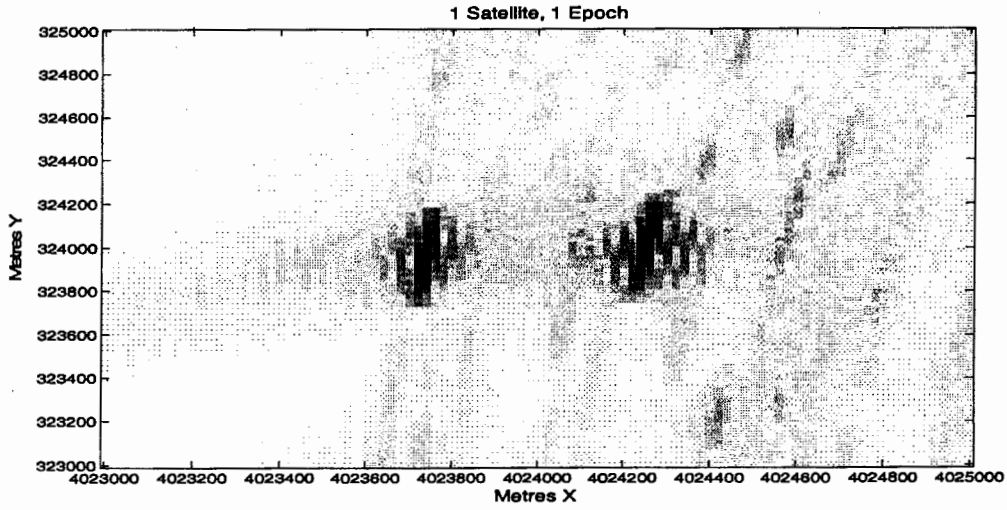

Figure 6.9: Integration time 0.1 seconds and target moving with 10 m/s

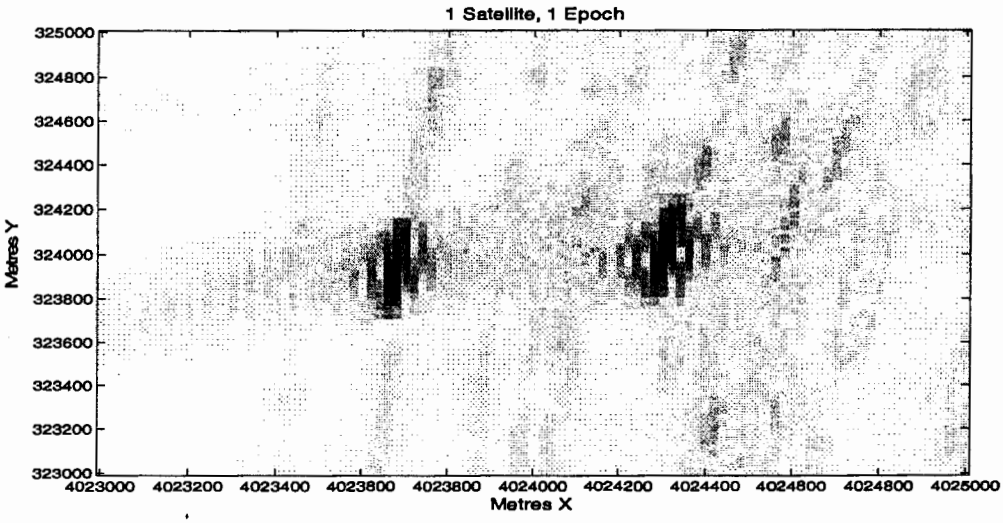

Figure 6.10: Integration time 0.1 seconds and target moving with 20 m/s

When the targets are moved with the velocity of 50 m/s and 100 m/s, then, the resultant figures (6.11 and 6.12 respectively) clearly show that the background noise increases with the increase in the target velocity.

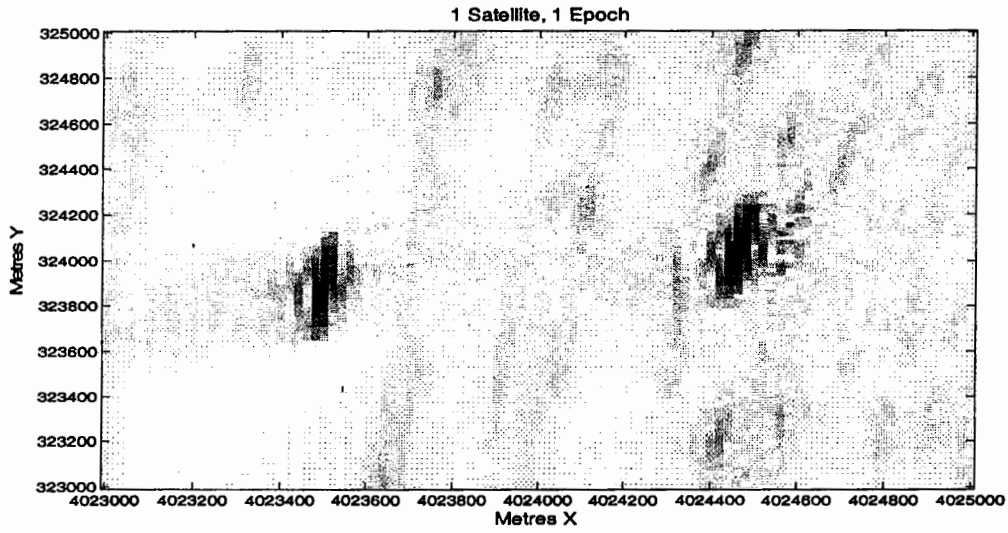

Figure 6.11: Integration time 0.1 seconds and target moving with 50 m/s

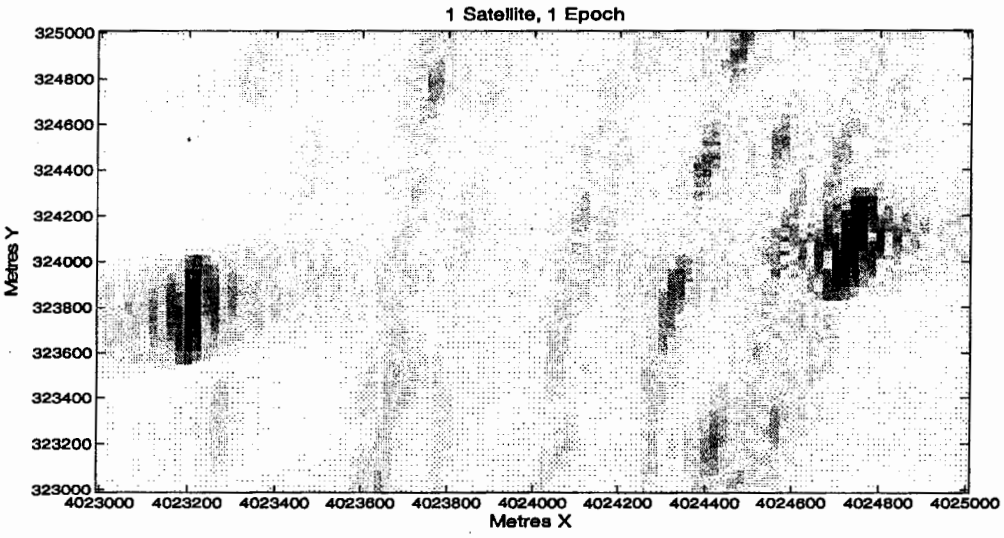

Figure 6.12: Integration time 0.1 seconds and target moving with 100 m/s

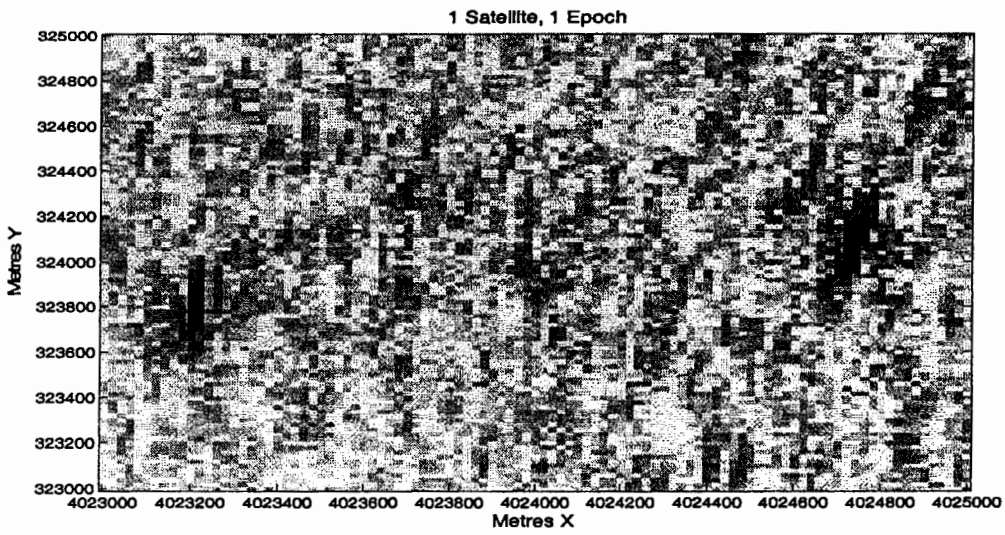

Figure 6.13: Integration time 0.1 seconds (with noise) & target moving with 100m/s

The results of the figures of Case 3 indicate that it is possible to resolve the stationary targets, ships or slow moving terrestrial targets and high speed aero planes with this technique. It can be noticed that as target velocity increases the image resolution also enhances (ISAR principle), but, the resultant image suffers from degradation due to background noise.

Case No 4: Integration Time 0.1 Seconds with Receiver Moving with Increased Velocity

The simulation is done under the integration time of 0.1 & in the absence of noise (figure 6.14) and presence of noise (figure 6.15). The receiver velocity is increased to [600, 0, 0] m/sec (RSA = (600) **X** (0.1) = 60m). The simulation results show that higher resolution images will be obtained; if, for a fixed interval of time, the imaging receiver speed is increased which is according to the SAR principle.

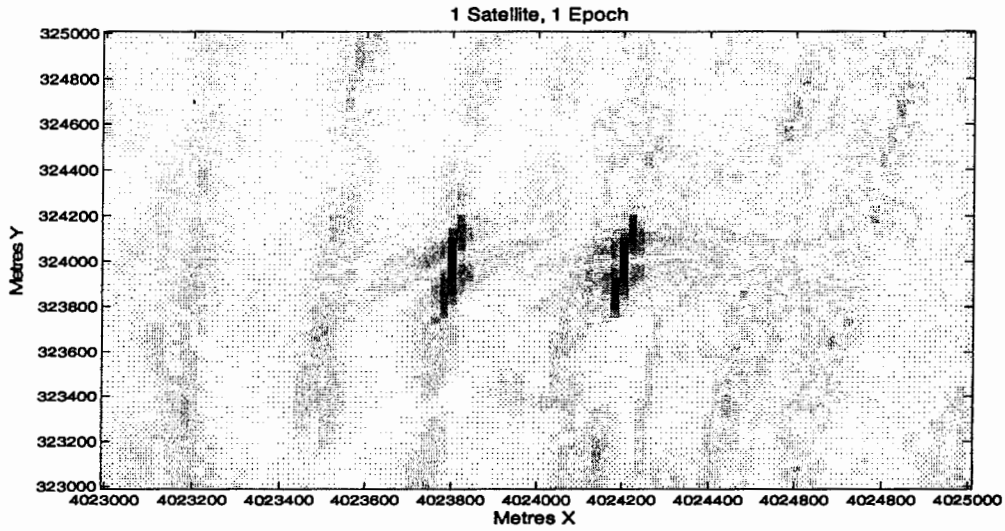

Figure 6.14: Integration time 0.1 seconds and receiver moving with 600 m/sec

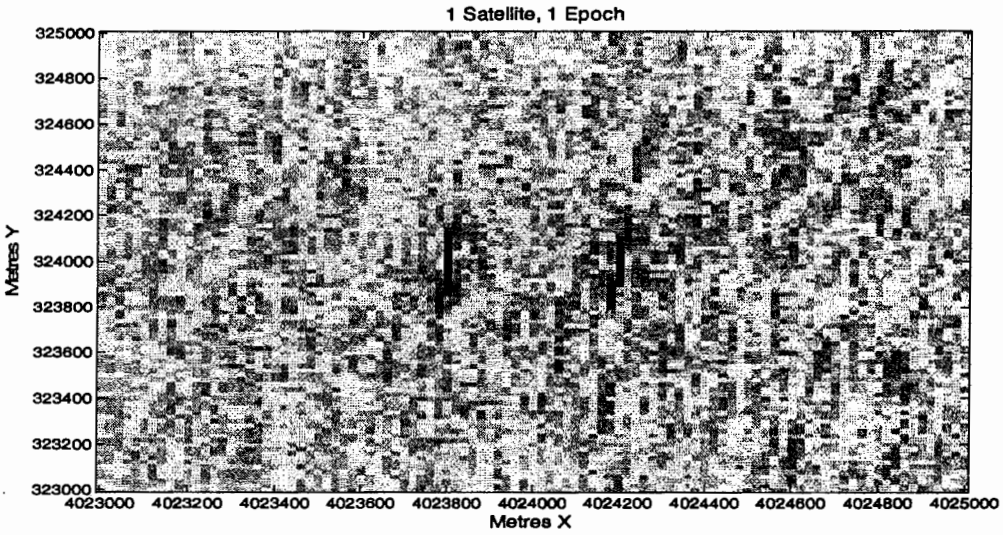

Figure 6.15: Integration time 0.1 seconds (with noise) and receiver moving with 600m/sec

Although, the target resolution of both the case 4 and case 2 is almost same because they have the same value of the Radar Synthetic Aperture (RSA = 60m), but, the case 4 images have more background noise than case 2. It is because; greater numbers of

samples of case 2 averages out the background noise to better extent than case 4 and as a consequence, overall better images are produced for case 2 than case 4.

Case No 5: Receiver Deviating from the Planned Route

The receiver was made to deviate +/- 10 m/sec from its original course in the y and z dimensions i.e. $(300, y \pm 10, z \pm 10)$. The targets are little bit blurred and surprisingly noise in the background is reduced little bit.

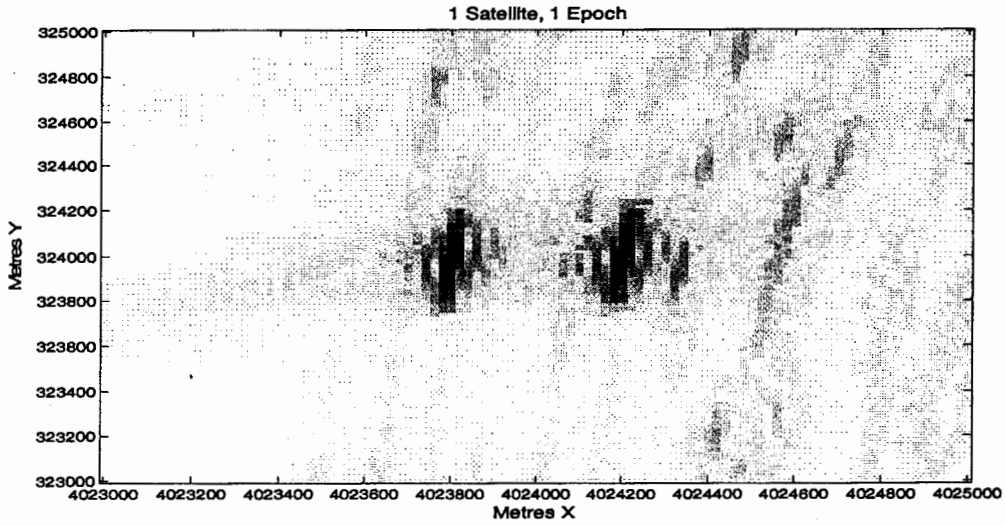

Figure 6.16: Integration time 0.1 seconds and receiver deviating from the planned route

The above result shows that if the receiver is moved in the 3D, then, filtering of noise is performed and, consequently, the images of the better quality will be obtained.

Case No 6: Attenuation of Direct and Reflected Signals

There are two sub cases in this case. In the first case, the reflected signals are attenuated to such an extent which results in the invisibility of the targets. In the second case, the weakest attenuated value of the reflected signal is made constant and the direct signals are attenuated to recover the targets.

Case No 6.1: Attenuation of Reflected Signals

In case 6.1, the reflected signals are made weaker by increasing the level of attenuation of the reflected signals in accordance with table 6.3.

Table 6.3: Set of parameters for case no. 6.1

Sr. No	Description	Values
1.	Integration time (Ts)	0.1 seconds
2.	Attenuation values of reflected signals	0.3 (figure 6.17 & 6.18), 0.1 (figure 6.19 & 6.20), 0.05 (figure 6.21), 0.01 (figure 6.22)
3.	Over –sampling rate	5
4.	No of samples	5.1150×10^5
5.	SV Involved	1, 7, 9, 14, 16, 22
6.	Reference SV	14

When the reflected signals are attenuated to a value of 0.3 then the blurriness is increased, but, the targets can be resolved easily & even in the presence of noise (figure 6.18).

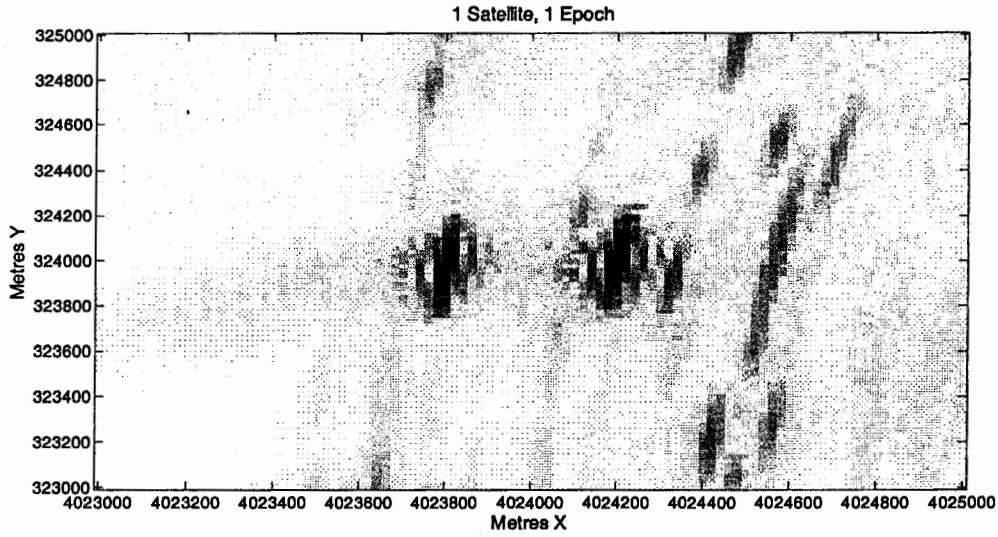

Figure 6.17: Attenuation of 0.3 for reflected signal

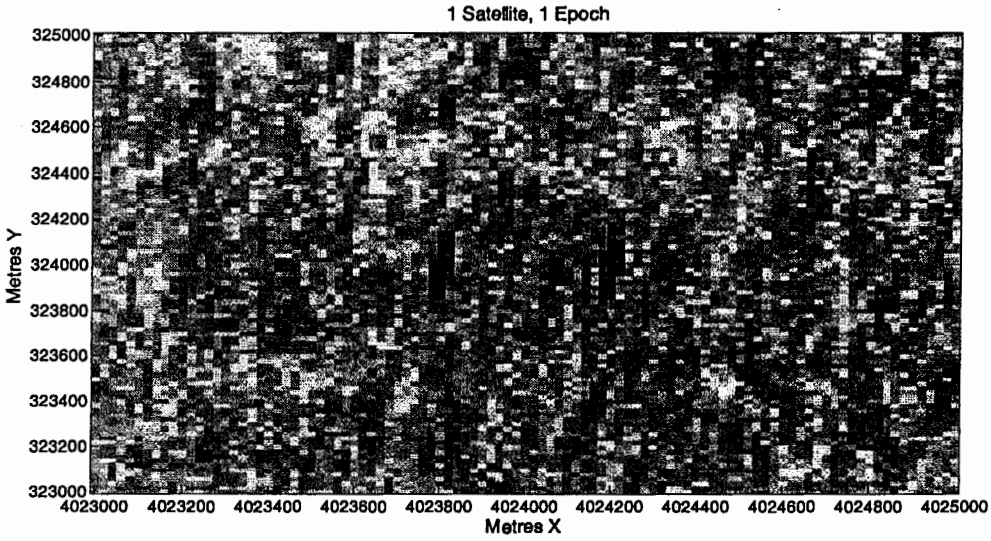

Figure 6.18: Attenuation of 0.3 for reflected signal with 16 db noise

When the reflected signals are attenuated to a value of 0.1, then, although the targets can be distinguish in the absence of noise as shown in the figure 6.19, but, they are no more visible in the presence of noise as shown in the figure 6.20.

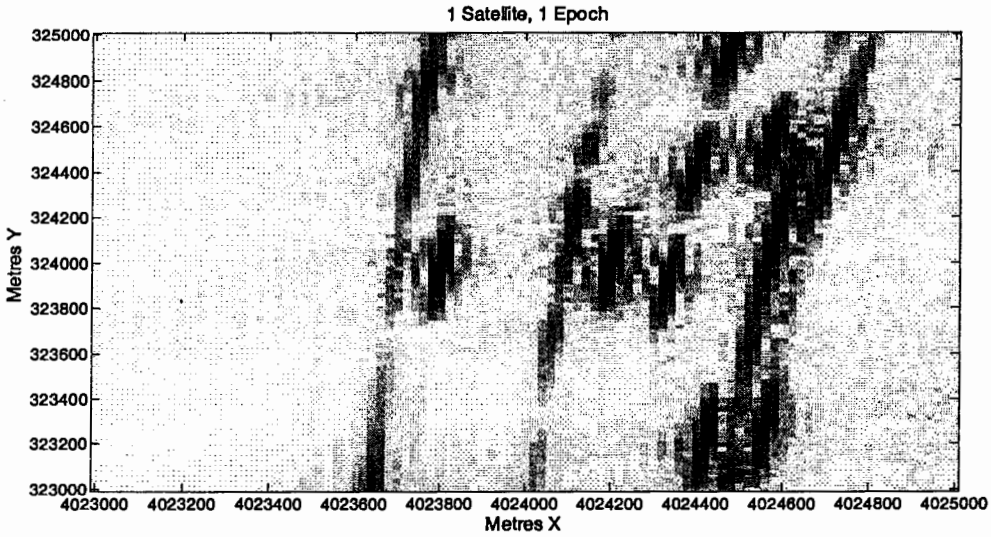

Figure 6.19: Attenuation of 0.1 for reflected signal

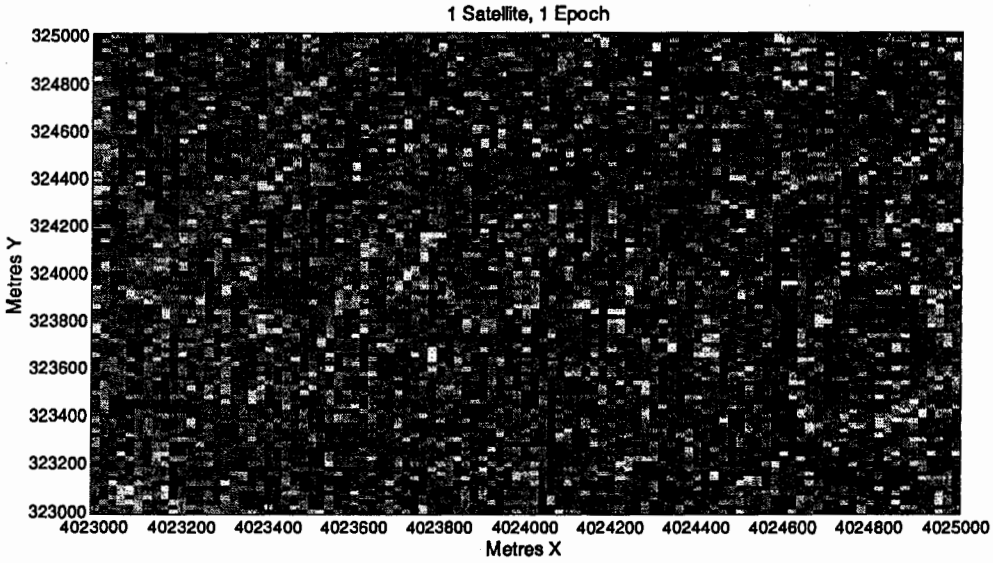

Figure 6.20: Attenuation of 0.1 for reflected signal with 16 db noise

When the attenuation of reflected signals is further reduced i.e. 0.05, then, the visibility of targets is further decreased as shown in the figure 6.21. Moreover, the targets are no more visible (even in the absence of noise) when the reflected signals have the attenuation value of 0.01 as shown in the figure 6.22.

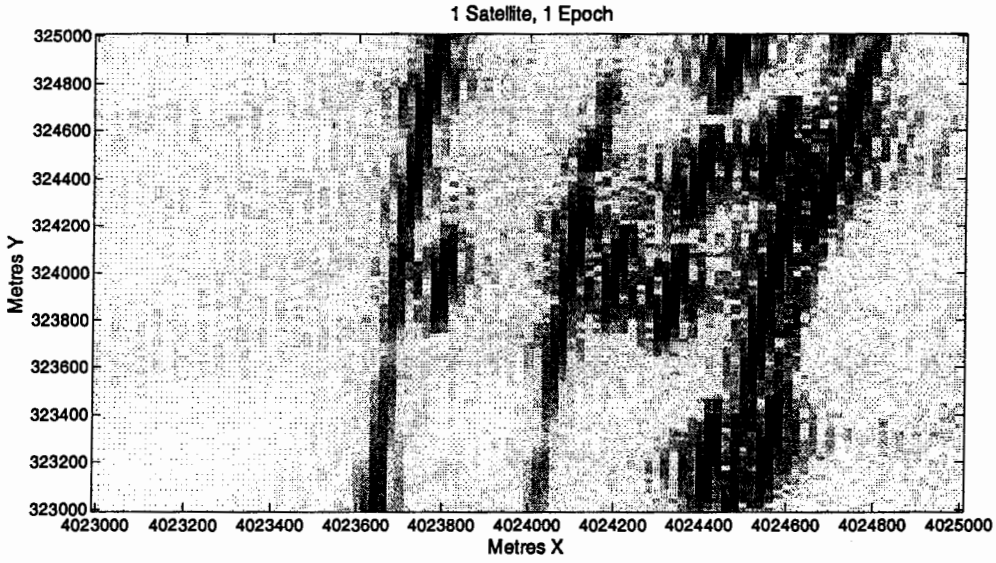

Figure 6.21: Attenuation of 0.05 for reflected signals

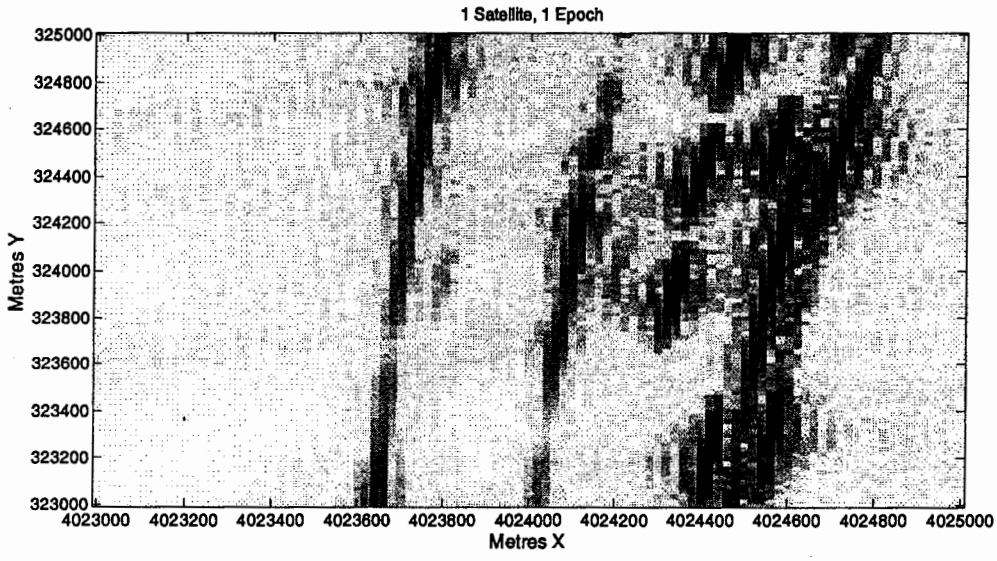

Figure 6.22: Attenuation of 0.01 for reflected signals

The results of the figure 6.21 and figure 6.22 are due to the fact that the weaker reflected signals are lost in the tails of the auto correlation function of direct signals and, therefore, cannot be recovered, no matter how longer they are integrated.

Case No 6.2: Attenuation of Direct Signals

In case 6.2, the direct signals are made weaker by increasing the level of attenuation of the direct signals in accordance with table 6.4. It is observed that when the direct signals are attenuated to a value of 0.5, then, the targets show some visibility as shown in the figure 6.23.

Table 6.4: Set of parameters for case no. 6.2

Sr. No	Description	Values
1.	Integration time (Ts)	0.1 seconds
2.	Attenuation values of direct signals (reflected signals attenuation value 0.01)	0.5 (figure 6.23), 0.3 (figure 6.24), 0.1 (figure 6.25), 0.05 (figure 6.26) and 0.03 (figure 6.23)
3.	Over –sampling rate	5
4.	No of samples	5.1150×10^5
5.	SV Involved	1, 7, 9, 14, 16, 22
6.	Reference SV	14

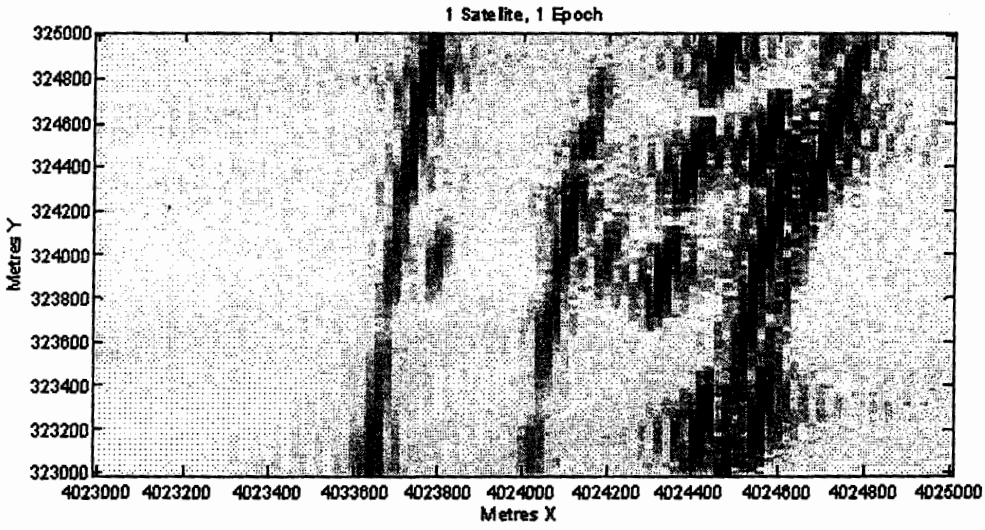

Figure 6.23: Direct signals attenuation 0.5 & reflected signals attenuation 0.01 (no noise)

The visibility of targets further increases when the direct signals are attenuated to a value of 0.3 (as shown in the figure of 6.24) and 0.1 (as shown in the figure of 6.25). Although, the targets are reasonably visible in the figure 6.25, but, the background noise is also convincingly larger which can be a troublesome factor in target detection in the real time systems.

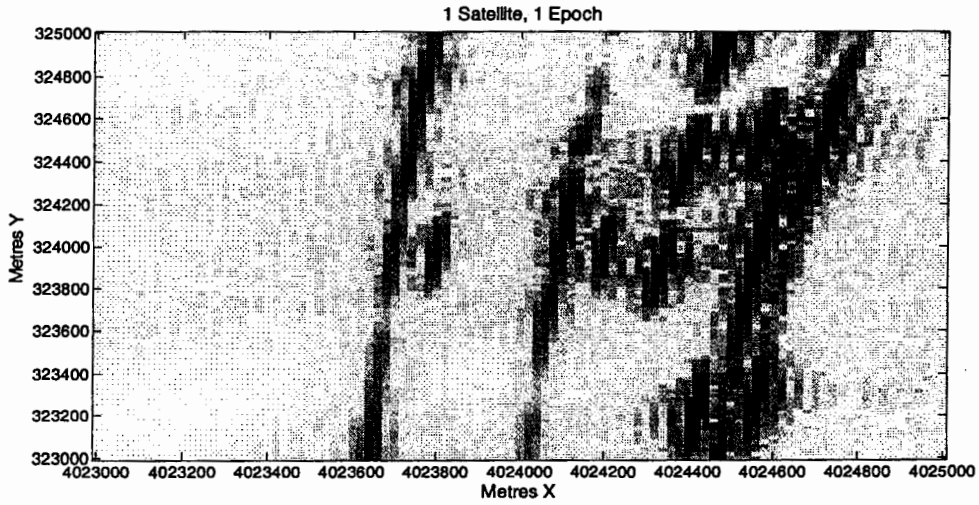

Figure 6.24: Integration time 0.1 seconds with direct signals attenuation 0.3 and reflected signals attenuation 0.01 (no noise)

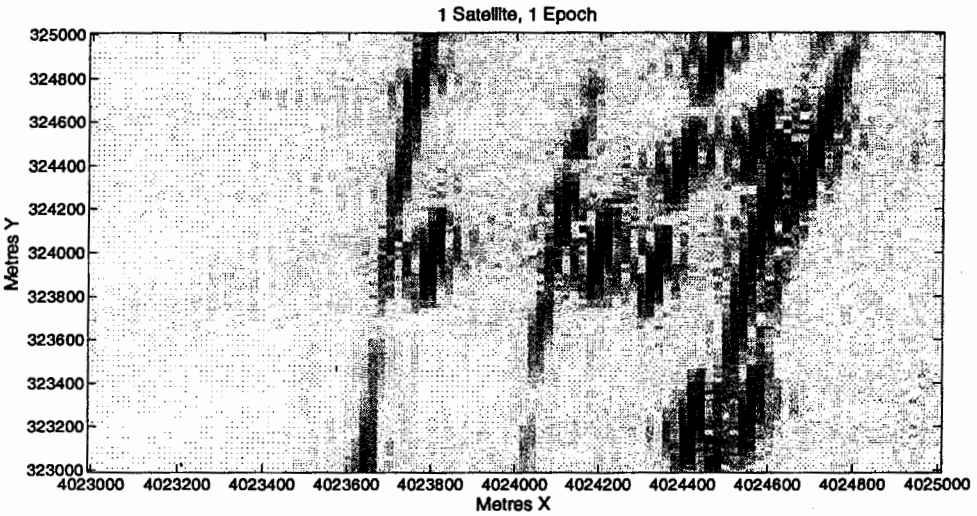

Figure 6.25: Integration time 0.1 seconds with direct signals attenuation 0.1 and reflected signals attenuation 0.01 (no noise)

The visibility of the targets increases by attenuating the direct signals more and more. It is experiential that when the direct signals are attenuated to a value of 0.05, then, the targets are clearly visibility as shown in the figure 6.26.

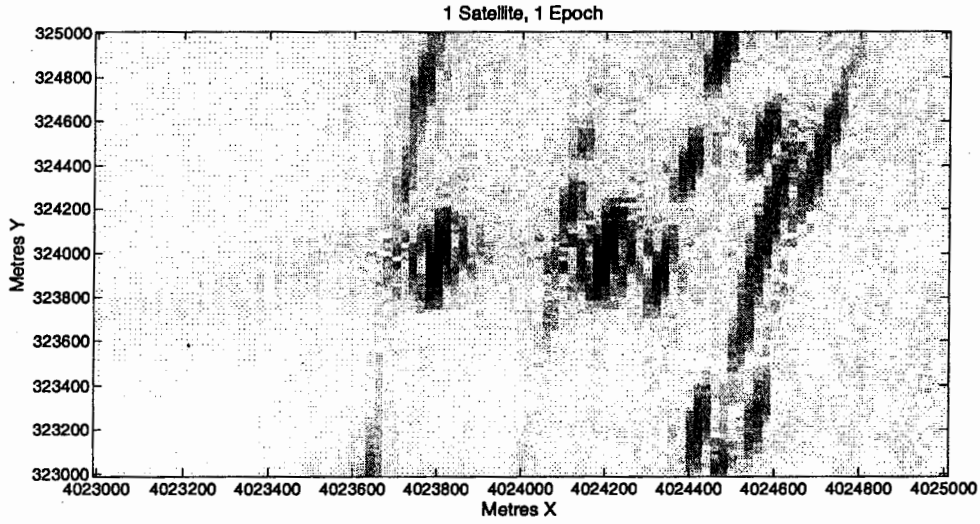

Figure 6.26: Integration time 0.1 seconds with direct signals attenuation 0.05 and reflected signals attenuation 0.01 (no noise)

When the attenuation value is set to 0.03, then, the targets are more clearly visible as shown in the figure 6.27. The reason is that the direct signals are now comparable to the reflected signal and so the reflected signals are no longer lost in the tails of auto correlation function of direct signals. Moreover, when the noise is introduced, then, the targets are no more visible as shown in the figure 6.28.

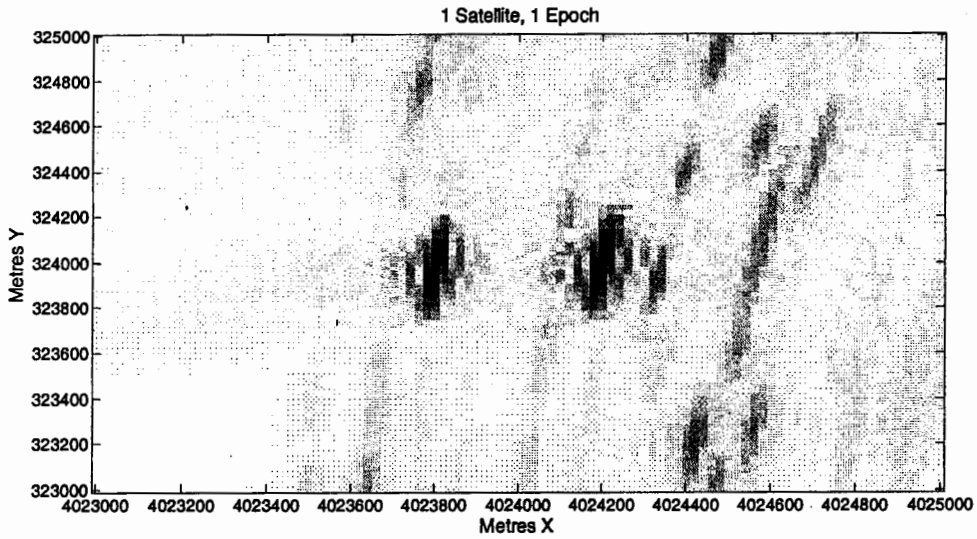

Figure 6.27: Integration time 0.1 seconds with direct signals attenuation 0.03 and reflected signals attenuation 0.01 (no noise)

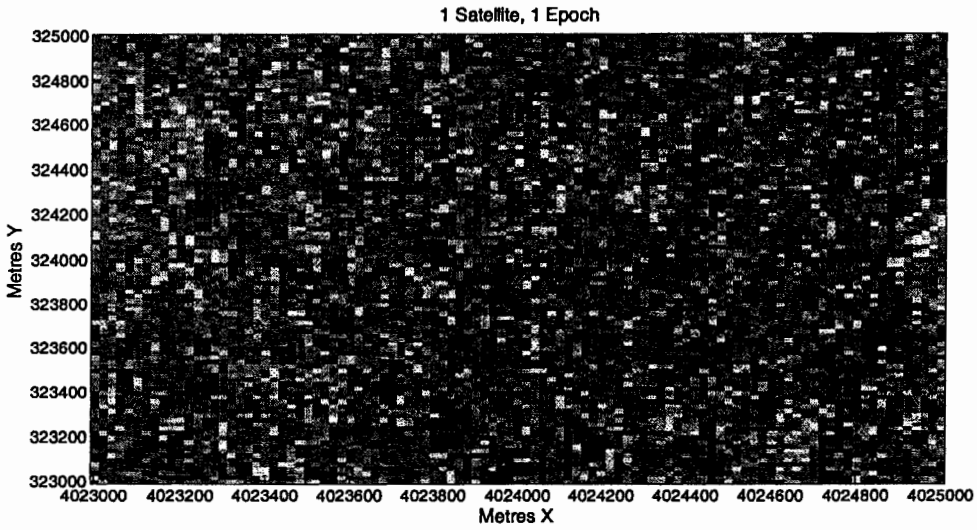

Figure 6.28: Integration time 0.1 seconds with direct signals attenuation 0.03 and reflected signals attenuation 0.01 (with noise)

When the integration time is increased to 0.2 seconds, then the targets are still not resolved in the presence of noise as shown in the figure 6.29. Thus it is imperative to keep the noise as minimum as possible for satisfactory results. One of the methods is by employing high efficiency low noise amplifiers at the receivers input stages. Extraction of

useful data from low power reflected signal in presence of noise remains the biggest challenge in the remote sensing environment.

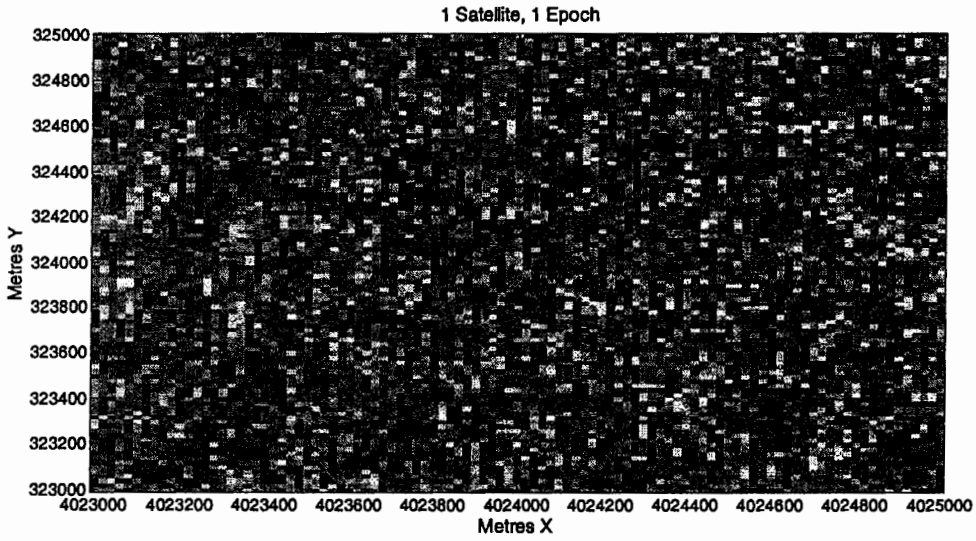

Figure 6.29: Integration time 0.2 seconds with direct signals attenuation 0.03 and reflected signals attenuation 0.01(with noise)

Case No 7: Integration Time 21600 Seconds

In this case, the simulation is carried out by setting the integration time of 21600 seconds (RSA = (300) **X** (21600) = 6480000m) and other parameters as shown in the table 6.5. The integration time of 21600 seconds (equivalent to 6 hours) is chosen because it is the maximum visibility time of a satellite to receiver. Although, the processing time is increased but the targets are recognizable with the better spatial resolution as compared to case 1 (as shown in the figure 6.30 and 6.31). Moreover, as shown in the table 6.5, the total no of samples in this case are 5.115×10^5 which are equal to the no of samples of case 1.

Table 6.5: Set of parameters for case no. 7

Sr. No	Description	Values
1.	Integration time (Ts)	21600 seconds
2.	Attenuation Factor	0.5
3.	Noise	0 (figure 6.9) and 16 (figure 6.10)
4.	Over –sampling rate	$2.314814815 \times 10^{-5}$
5.	No of samples	5.115×10^{5}
6.	SV Involved	1, 7, 9, 14, 16, 22
7.	Reference SV	14

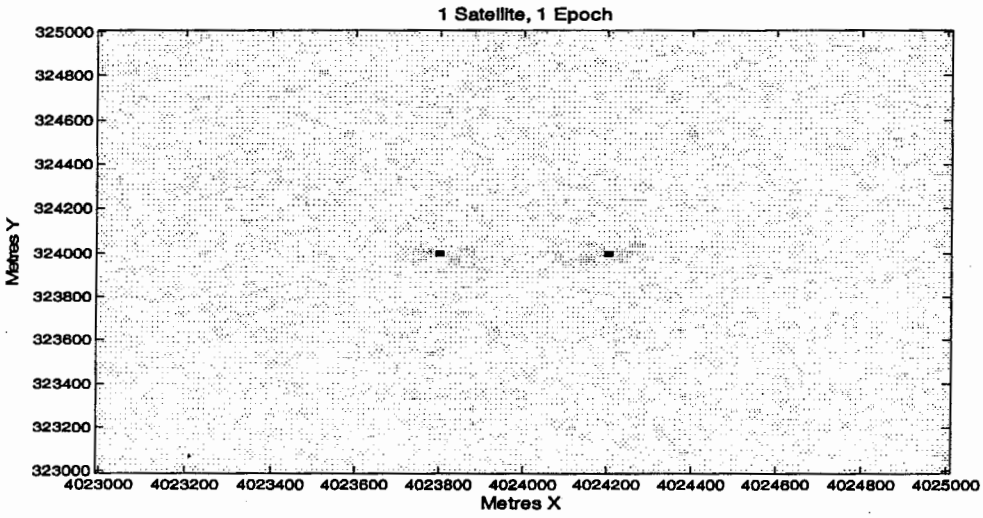

Figure 6.30: Integration time 21600 seconds with no noise

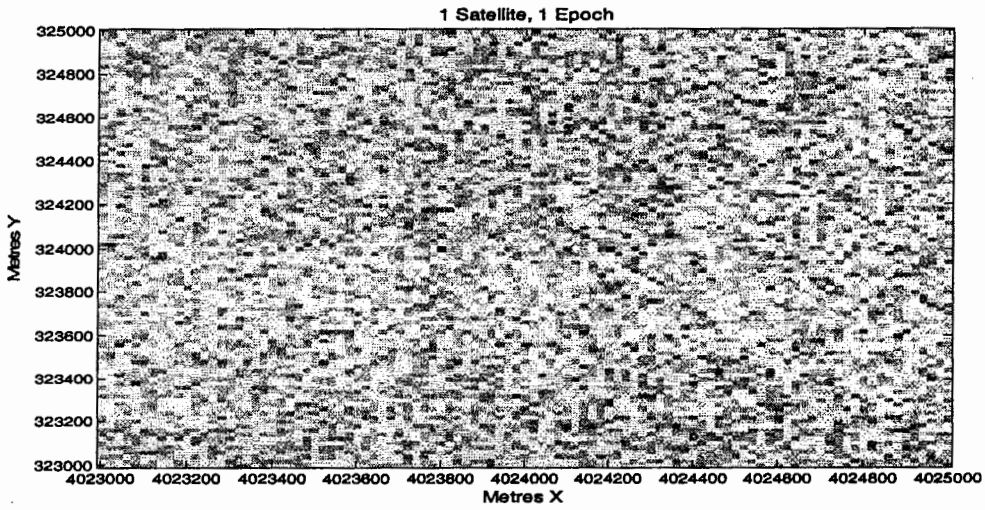

Figure 6.31: Integration time 21600 seconds with 16 db noise

The results verify that the resolution has improved considerably. The targets are more clearly visible. A look at the results obtained reveal that the resolution is perfect with both targets visible as one distinct pixels length each with no distortion as shown in figure 6.30. One of the numerous possible applications with this type of set up are atmospheric remote sensing for weather forecasting, monitoring of landslides, long- term seismic studies and many other commercial applications.

As a next step the over sampling is further increased, increasing the numbers of samples. As expected, the resolution is perfect with both targets visible as one distinct pixels length each and no distortion as shown in the figure 6.32. The noise in the background is nearly cancelled out due to the longer integration time and large number of samples. The resolution was perfect with both targets visible as one pixel length each and no distortion. The simulation can no doubt be termed as having achieved an idea result.

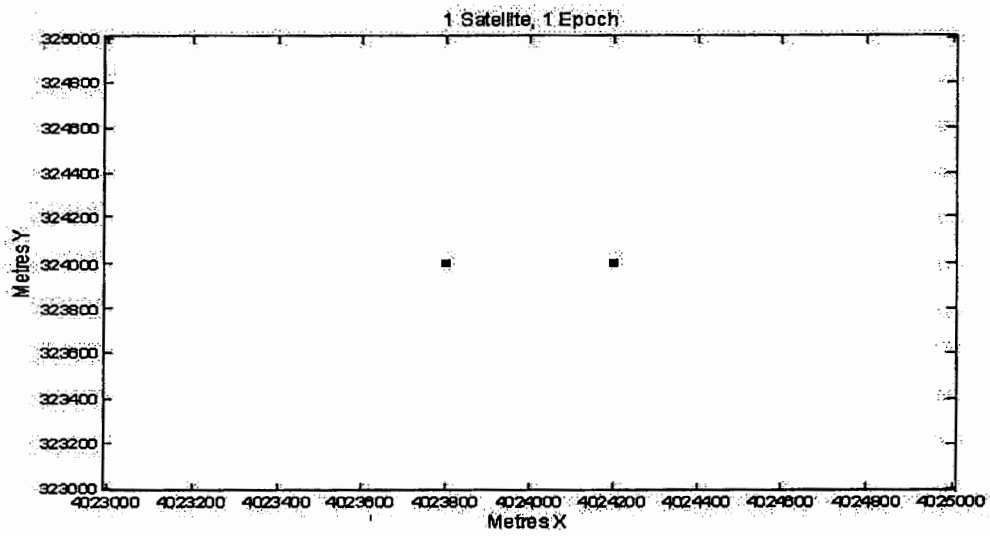

Figure 6.32: Integration time 21100 seconds with increased over sampling

CHAPTER 7

CONCLUSIONS AND RECOMMENDATIONS

The project has achieved its objectives set forth in the project feasibility report. The simulation results clearly wrap up that it is possible to locate the targets with good spatial resolution in the region of interest using the reflected GPS signals.

In line with the project feasibility report the code was tested under various conditions simulating various practical scenarios. Movement was induced in the receiver and the effect of noise, attenuation and interference on direct and reflected signal was also analyzed more carefully and in a detailed manner. The modified GPS receiver that may be utilized to materialize the simulation was discussed and a block diagram has been generated in this respect. Thus the project has fulfilled all of the objectives set forth in the project feasibility report.

Many interesting results have been observed during the simulation process and are as follows:

(a) Increase in the observation time results in larger number of samples. It results in the better simulation results and improved resolution due to the cancellation of the noise.

(b) The technique is effective for the stationary, slow moving and fast moving targets.

(c) The technique also verifies SAR principles by producing images of high resolution, when the receiver speed is increased.

(d) The simulation result shows that if the receiver is moved in the 3D, then, filtering of noise is performed and, consequently, the images of the better quality will be obtained.

(e) An important finding was that when attenuation in the direct signal is comparable to the attenuation of indirect signal (0.03 of original value in case of direct signal and 0.01 in case of reflected signal) then the targets reappear and the reflected signal is no longer lost in the tails of the auto correlation function.

(f) Unexpectedly, when the integration time was increased in part (e) above in the presence of noise, then the targets could not be resolved. Reminding us that extraction of useful data from low power reflected signal in presence of noise remains the biggest challenge in the remote sensing environment under the contemporary circumstances.

(g) But, however due to the time constraints and broadness of the topic, many aspects could not explored in detail and left for future research. Some of them are summarized in the next few paragraphs.

The speed of execution of the MATLAB program is very costly in terms of processing time and memory because the MATLAB program takes about 8 hours for execution on Pentium IV processor (1.6 GHz) with an integration time of 0.1 seconds and 12 hours for execution with an integration time of 0.2 seconds. The execution time can be improved to some extent by using the compiled code and the integer calculations in place

of double precision real calculations. It is imperative to reduce the execution time for deploying this system for the real time usage.

The proposed modified receiver can be studied in a more detailed manner. If possible a working "proof of concept" development model of the system can be assembled and tested under practical situation.

The reflected GPS signals are very weak. So, the extraction of reflected GPS signals in the presence of noise is the biggest issue in remote sensing in the real time environment and is a topic of worth importance for future.

The GPS is an emerging technology. The next generation of GPS satellites systems (GPS III) are on the one hand, not distorting the GPS signals and on the other hand, are transmitting the C/A code at a third and a fourth L-band frequency with more power and provide improved accuracy. Hence, it will enhance GPS-based remote sensing well in future. Moreover, the satellite systems developed by European Union and Russia will add new signals of opportunity in the future. Therefore, future of this topic seems to be quite promising.

REFERENCES

[1] Ahmed Al-Rabbany, "Introduction to GPS, The Global Positioning System" Artech House Publishers

[2] http://www.esrl.noaa.gov/psd/psd3/multi/remote/

[3] E D Kaplan, C J Hegarty, "Understanding GPS Principles and Application", Second Edition, Artech House Publishers, 2006

[4] M. Usman, D. W. Armitage, "A Remote Imaging System Based on Reflected GPS Signals" Proceedings of ICAST 2006 Conference, 2-3 September 2006, Islamabad, Pakistan.

[5, old 21] M. Usman, D. W. Armitage, "Details of an Imaging System Based on Reflected GPS Signals and Utilizing SAR Techniques"- *Journal of Global Positioning Systems*, Vol. 8, No. 1, 2009

[6] H. D. Griffiths, "Bistatic and Multistatic Radar"- Journal of Global Positioning Systems, <www2.theiet.org/oncomms/pn/radar/Griffiths%20Shrivenham.pdf>

[7] Yonghong Li, Chris Rizos, Eugene Donskoi, John Homer, Bijan Mojarrabi "Terrain Imaging using a SAR System based on Reflected GPS Signals" Wuhan University Journal of Natural Sciences, Volume 8, Number 2 / June, 2003, 659-664

[8] http://spaceflight.nasa.gov/realdata/elements/

[9] http://en.wikipedia.org/wiki/Global_Positioning_System

[10] http://adn.agi.com/SatelliteOutageCalendar/SOFCalendar.aspx

[11] Public Release Version of "Navstar GPS User Equipment Introduction"

[13] NAVCEN: GPS SPS Signal Specifications, 2nd Edition, 1995, http://www.navcen.uscg.gov/pubs/gps/sigspec/gpssps1.pdf

[14] Timothy Pratt, Charles Bostian, Jeremy Allnutt, "Satellite Communications" Second Edition, John Wiley & Sons, Inc.

[15] R. Michael Buehrer, "Code Division Multiple Access (CDMA)" Morgan and Claypool Publishers

[16] Vijay K. Garg, "Wireless Communication and Networking" Morgan Kaufmann Publishers

[17] John A. Richards, "Remote Sensing with Imaging Radar" Springer Publishers.

[18] Bernard Sklar, "Digital Communication fundamentals and application" Prentice Hall International edition.

[19] John G.Proakis, "Digital Communications", Fourth edition.

[20] Steven W. Smith PhD, "The Scientist and Engineer's Guide to Digital Signal Processing" Chapter: 17, www.dspguide.com/

[21] Borre, K., Akos, D.M., Bertelsen, N., Rinder, P., Jensen, S.H., "A Software-Defined GPS and Galileo Receiver: A Single Frequency Appproach", Springer Publishers

[22] Guochang Xu, "GPS: Theory, Algorithms and Applications" Springer Publishers

[23] James Bao, Yen Tsui, "Fundamentals of Global Positioning System Receivers: A Software Approach" Second Edition, John Wiley & Sons, Inc.

APPENDICES

APPENDIX A

GEOID AND ELLIPSOID

Geoid is used as reference model for measuring the height of a point on earth as shown in the figure A.1[1]. It is a theoretical body whose surface intersects the gravitational field lines everywhere at right angles. The height of an object above the reference ellipsoid can be calculated as:

$$h = H + N$$

Where:

h = Ellipsoidal Height from GPS

H = Orthometric Height (measures through spirit leveling)

N = Geoid Height (from reference ellipsoids)

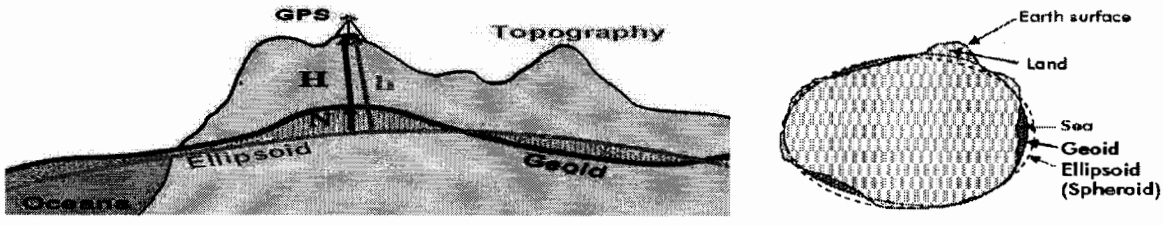

Figure A.1: Relationship between geoid and ellipsoid

[1] http://principles.ou.edu/earth_figure_gravity/geoid/geoid-ellipsoidal-orthometric_height.jpg

APPENDIX B

MAXIMUM LENGTH SEQUENCES AND GOLD CODES

Maximum Length Sequences are the random sequence of 0's $(2^{m-1}-1)$ and 1's (2^{m-1}) with good autocorrelation & poor cross correlation properties. They have a flat frequency spectrum like white noise, but, unlike white noise they are deterministic & repeatable with periods 'N'.

$$\text{MLS Length} = N_{MLS} = 2^m - 1, \qquad m = \textit{length of shift register}$$

MLS generators have linear feedback shift register for sequences generation as shown in the figure B.1[1].

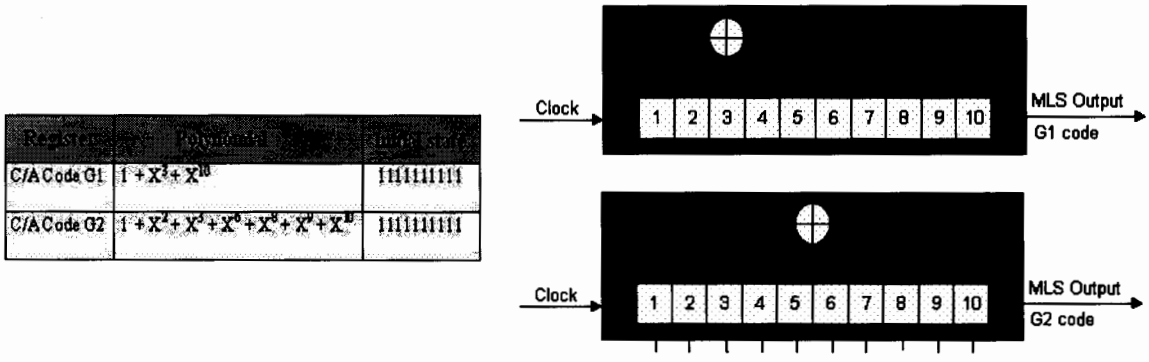

Figure B.1: Generation of MLS sequences

[1] James Bao, Yen Tsui, "Fundamentals of Global Positioning System Receivers: A Software Approach" Second Edition, John Wiley & Sons, Inc, 2005, Chapter 5, pp.75

The Gold Codes have good cross correlation properties with values and are made from 2 m- sequences of length n with periodic cross correlation function having values of $\{-1, -t(m), t(m)-2\}$, where't (m)' is the cross correlation peak given by

$$t(m) = \begin{Bmatrix} 2^{(m+1/2)}+1, & \text{for odd m} \\ 2^{(m+2/2)}+1, & \text{for even m} \end{Bmatrix}$$

The detailed block diagram of the Gold Codes is given by figure B.2[1] as shown below:

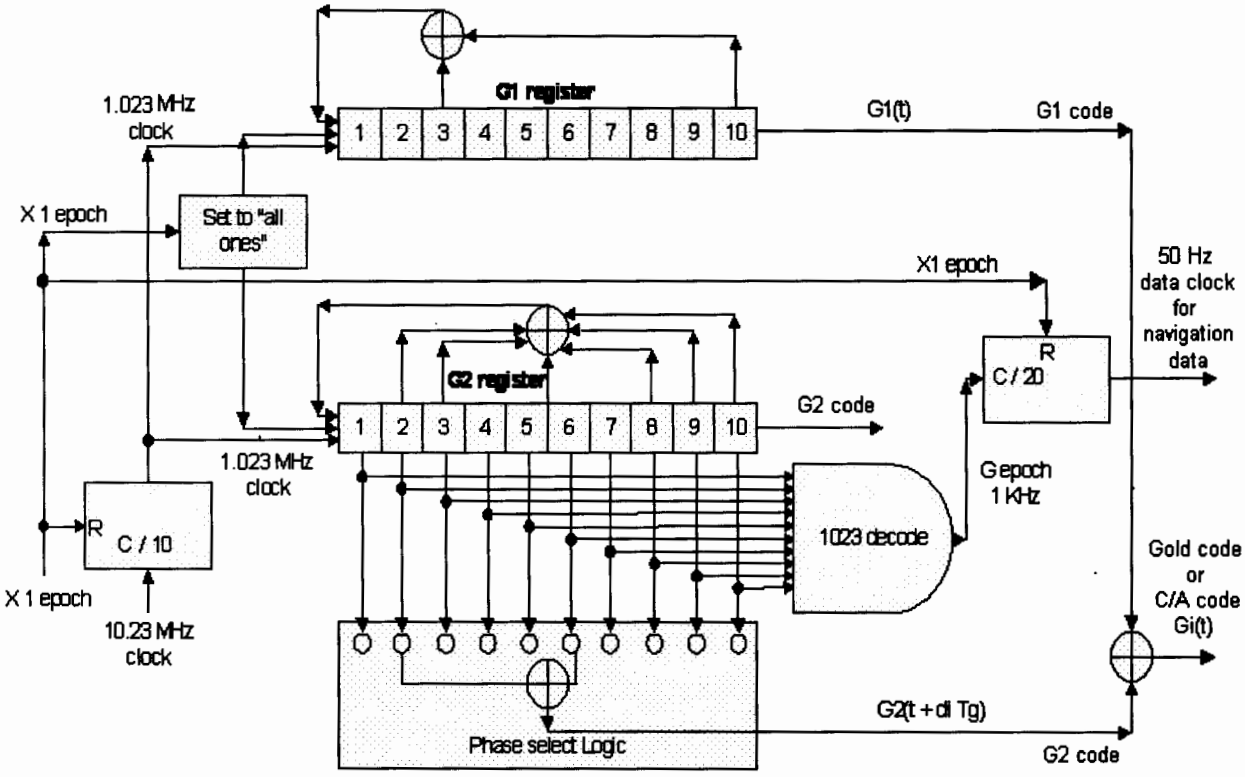

Figure B.2: Detailed diagram of Gold codes generator

[1] E D Kaplan, C J Hegarty, "Understanding GPS Principles and Application", Second Edition, Artech House Publishers, 2006, Chapter 4, pp.130

APPENDIX C

DIAGRAMMATIC REPRESENTATION OF THE EPHEMERIS DATA PARAMETERS

The term *anomaly* (instead of *angle*), which means irregularity, is used by astronomers describing planetary positions. The term originates from the fact that the observed locations of a planet often showed small deviations from the predicted data.

The mean anomaly 'M' is the angular distance from perihelion which a (fictitious) planet would have if it moved on the circle of radius 'a' with a constant angular velocity and with the same orbital period 'T' as the real planet moving on the ellipse. By definition, 'M' increases linearly (uniformly) with time. The value of 'M' at a given time is easily found when the eccentricity e and the eccentric anomaly 'E' are known. The problem is to find 'E' (from which the position of the planet can be computed) when 'M' and e are known. The true anomaly (symbol 'v') is the angular distance of the planet from the perihelion of the planet, as seen from the Sun. For a circular orbit, the mean anomaly and the true anomaly are the same[1] as shown in the figure C.1.

[1] http://www.jgiesen.de/kepler/kepler.html

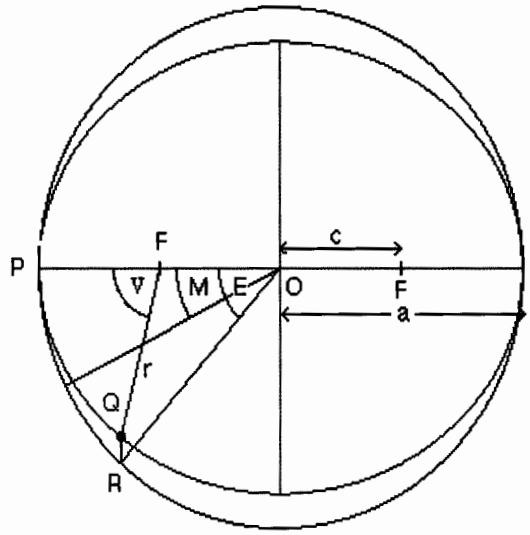

Figure C.1: Diagrammatic representation of the orbital anomalies (E,M,V)[1]

The Ephemeris Data parameters given on page 32-35 of chapter 3 can be better understand with the help of figure C.2 given below:

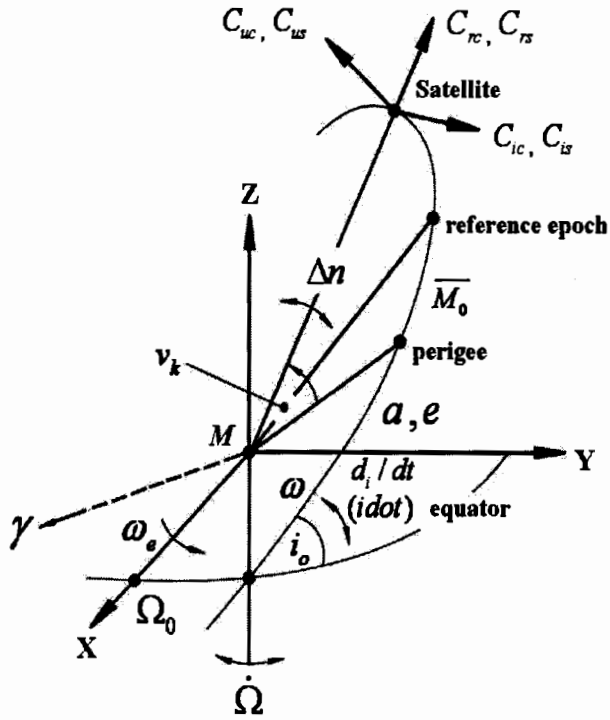

Figure C.2: Diagrammatic representation of ephemeris data parameters

[1] http://www.jgiesen.de/kepler/kepler.html

APPENDIX D

ELEVATION AND AZIMUTH ANGLES CALCULATION FROM ENU COORDINATES

The ionospheric klobuchar error model calculates the elevation and azimuth by firstly converting the GPS coordinates (latitude, longitude, height) to ENU (east, north, up)[1] as follows:

$$\begin{bmatrix} e \\ n \\ u \end{bmatrix} = \begin{bmatrix} -\sin(\lambda) & \cos(\lambda) & 0 \\ -\sin(\phi)\bullet\cos(\lambda) & -\sin(\phi)\bullet\sin(\lambda) & \cos(\phi) \\ \cos(\phi)\bullet\cos(\lambda) & \cos(\phi)\bullet\sin(\lambda) & \sin(\phi) \end{bmatrix} \begin{bmatrix} (x_{sat-i} - x_{user}) \\ (y_{sat-i} - y_{user}) \\ (z_{sat-i} - z_{user}) \end{bmatrix}$$

The elevation angle can be calculated as:

$$E_s = \sin^{-1}\left(\frac{u}{\sqrt{e^2 + n^2 + u^2}}\right)$$

The azimuth angle can be calculated as:

$$A_s = a\tan 2\left(\frac{e}{\sqrt{e^2 + n^2 + u^2}}, \frac{n}{\sqrt{e^2 + n^2 + u^2}}\right)$$

[1] http://dspace.dsto.defence.gov.au/dspace/bitstream/1947/3538/1/DSTO-TN-0432.pdf, pp.3